NOVEL AMBIENT IONIZATION SAMPLING METHODOLOGIES WITH MASS SPECTROMETRY

by

Michael C. Godwin, B.S.

A thesis submitted to the Graduate Council of
Texas State University in partial fulfillment
of the requirements for the degree of
Master of Science
with a Major in Chemistry
May 2020

Committee Members:

William D. Hoffmann, Chair

Jennifer Irvin

Gary Beall

FAIR USE AND AUTHOR'S PERMISSION STATEMENT

Fair Use

Duplication Permission

DEDICATION

I would like to dedicate my thesis to my loving wife, Emily Godwin, my parents Michael T. Godwin, and Mark and Chris Grissom. Without all of your love and financial support, I would not be able to complete my extensive education. A special thanks to my wife Emily for being my study-buddy, therapist, proof-reader, and overall amazing human being. At times where I felt the full effect of imposter syndrome, she was always there to reassure and restore my confidence in myself.

ACKNOWLEDGEMENTS

I would like to give a special thanks to all of the Texas State University faculty for providing me with tools and education to become an independent chemist. I would like to give my gratitude and a special salute to William D. Hoffmann, for recognizing my potential as an analytical chemist and paving the way to help me succeed. The mentorship he gave me throughout my graduate studies has been nothing but superior, and he has equipped me to objectively think about how to rationalize complex problems that exist in nature and biological systems. He made me truly understand the physical properties of taking measurements, data interpretation, and instrumentation. Amongst other things, he has also become a great friend and has always been there to listen and bolster my confidence in my abilities in analytical science. I would also like to thank my other committee members, Jenifer Irvin, and Gary Beall for their mentorship and support throughout my studies. Thank you, Ben Martin, for providing me with 4 years of preliminary research experience when I was a chemistry minor, which ultimately led me to choose a second major and my path as a career chemist. If he hadn't taken a chance on me in my undergraduate studies, I would not be where I am today.

TABLE OF CONTENTS

Page

LIST OF TABLES

Table **Page**

LIST OF FIGURES

Figure **Page**

ABSTRACT

Expanding on the current paradigm of ambient ionization, herein is reported the use of a metal surface for metal spray ionization and the use of online derivatization to separate isomass compounds. A metal surface has several advantages over some of the newer ambient ionization sampling methodologies in the fact that it is reusable, relatively inexpensive, has a fixed geometry, does not require wicking to initiate a spray, and can be functionalized with many coatings depending on the metal used.

A bare copper surface was used as a spray initiator and the sensitivity, limits of detection and quantitation were compared to a copper surface that was functionalized with a superhydrophobic coating on singly and doubly charged peptides. These surfaces were tested with a 30°, 60°, and 90° tip with a channel extending from the proximal tip of the surface, where 0.5 µL of analyte was loaded prior to each spray event. Overall the superhydrophobic surface displayed greater sensitivity, lower limits of detection and quantitation compared to the bare copper surface, and the 30° tip resulted in the highest sensitivity. There were several limitations to using a copper surface as a spray initiator, in that over time, it seems that the copper underneath the superhydrophobic coating oxidized due to the applied external voltage. Reliable calibration curves could not be obtained with nonpolar analytes, such as lipids. This is likely due to the attractive forces

between the superhydrophobic coating and the analyte, which caused the analyte to adhere to the surface instead of being ejected.

To combat many of the limitations of the superhydrophobic surface, gold was electroplated onto a copper surface. Gold is inert and will not oxidize over time, and also has some very unique properties in creating a very strong bond with thiols, which can only be destroyed under very harsh oxidizing conditions. This surface can be reused, and re-functionalized with different thiols to give the desired surface properties. Depending on the functional groups the thiol contains, (hydrophobic/philic) properties can be further enhanced on the surface with other coatings to give greater sensitivity depending on the polarity of the analyte. A stepwise procedure was employed to create an omniphobic surface. Omniphobic surfaces maintain a static contact angle and have repellency to all oils and liquids. This provides an opportunity to make reliable and reproducible calibration curves with nonpolar analytes that could not be established with superhydrophobic surfaces. Sensitivity, limits of detection (LOD) and limits of quantitation (LOQ) of the omniphobic surface were compared to that of a heated electrospray ionization source, and overall the results obtained using an omniphobic metallic surface were similar, and sometimes better than those using electrospray.

An atmospheric solids analysis probe (ASAP) was used to rapidly differentiate isomass drugs such as Δ^9-tetrahydrocannabinol (THC) from

cannabidiol (CBD), and hydromorphone from morphine. These pairs cannot be distinguished on the basis of tandem mass spectra via collision induced dissociation (CID) because their fragmentation patters are so similar. This presents a unique problem to law enforcement and forensic analysts. These compounds however have different number of exchangeable hydrogens, so known mixtures of these compounds were derivatized with *N*,O-Bis(trimethylsilyl)trifluoroacetamide (BSTFA) through direct infusion in order to shift the *m/z* envelope.

1. INTRODUCTION

Mass spectrometry (MS) is a powerful tool in analytical chemistry used to detect the mass to charge ratio (*m/z)* of an ionized molecule. Two of the most common types of mass spectrometry are gas chromatography mass spectrometry (GC-MS) and liquid chromatography (LC-MS).

LC-MS uses a stationary and mobile phase to separate an analyte from a complex mixture, where the analytes of the mixture are dissolved in the mobile phase and are partitioned into the stationary phase. There are two types of chromatography used in LC-MS experiments, reverse-phase and normal phase chromatography. In normal phase a hydrophilic or polar stationary phase is used, where molecules that are polar in nature will preferentially adsorb to the surface, and the non-polar molecules in the mixture will be washed off the column along with the mobile non polar solvent. Typically, reverse-phase chromatography is the most common type of chromatography used in LC-MS experiments, where a hydrophobic or nonpolar stationary phase is used. Nonpolar analytes are adsorbed onto the surface through intermolecular forces, and polar analytes are not retained on the column are washed off along with eluant. There are several drawbacks to this design, in that sample analysis can take several to tens of minutes. If the speed of analysis is too high, (i.e. the solvent flow in mL/min) could cause coelution of the analyte of interest and provide inaccurate results.[1] These inaccuracies that arise from coelution of the analytes are usually in the

form of artificially inflated peaks, making quantitation a cumbersome task if proper chromatography is not used.[1]

In GC-MS, an analyte must be capable of being volatized into the gas form in order to be analyzed. This requires the sample and the solvent it is dissolved in to be heated in the injection port of the GC, where they both become subsequently vaporized and dissolved into a carrier gas and are adsorbed onto the column.[2] The column is housed inside an oven, where a temperature gradient allows the molecules with weaker intermolecular forces and a lower vapor pressure to become vaporized and start to elute down the non-polar column (usually HP-5), carried by some inert gas such as helium, N_2, H_2, or argon.[3] The vaporized analyte is separated as a result of being partitioned between the gaseous phase and the solid stationary phase in the column. Gas chromatography has several limitations however, and they mainly lie in the length of time for analysis, and what kind of analytes can be seen with GC. Because it requires the molecule to be converted into a gas, there is a possibility the analyte can be thermally degraded and is not representative of the sample in its native state. Such is the case with the carboxylic acid of Δ^9-tetrahydrocannaibinol acid

(THCA), where upon GC analysis undergoes decarboxylation and is converted to (THC).[4–6]

Both GC and LC suffer from many of the same drawbacks which include, analysis time, sample pretreatment, and derivatization. Coincidently, these processes also require a trained scientist to operate these instruments.

Atmospheric pressure ionization (API) mass spectrometry sampling such as atmospheric pressure chemical ionization (APCI) and electrospray chemical ionization (ESI) have become the major work horses in routine analyte verification due to their ease of use, and short analysis time (i.e. seconds to minutes). In both APCI and ESI, an analyte can be seen in positive or negative mode, in which a positively charged ion (i.e. H^+, Na^+) is adducted to the analyte or an electron, which can then be detected by the MS.[7]

In APCI an analyte or mixture is dissolved in a solvent, in which the mixture is vaporized typically around 250-300°C and a high voltage is applied to a Corona discharge needle which creates an electric field between the discharge needle and the inlet of the mass spectrometer. The high-density electric field ionizes and excites the nebulizing gas N_2, which undergoes a series of proton transfer reaction that protonates the water clusters naturally present in the atmosphere and in the mobile phase.[8] These protonated water clusters undergo a proton transfer to the analyte, which becomes declustered from the surrounding water molecules in the vacuum of the MS. Because of the nature of

proton transfer reactions with analyte in APCI, the ions that are created with APCI are only singly charged molecules and proton-bound dimers.

Electrospray ionization, first developed by John Fenn, ions are pre-formed in solution, and the solution is pushed through a small orifice (typically several micrometers), that is held at electric potential of several kV, which distorts the solution into a Taylor cone.[9,7] The Taylor cone emits a fine mist of droplets that are positively or negatively charged from the excess of weak acid or weak base in solution, which rapidly evaporate the solvent, which can be assisted by additional heating. The charge density of the aerosol builds up until the surface tension is exceeded by coulombic repulsion, known as the Raleigh limit. At this point further evaporation of these droplets produces highly charged product droplets via jet fission. These subsequent process continue to occur until the final aerosol produces multiply charged ions that are pulled into the vacuum drag of the mass spectrometer.[9] The formation of multiply charged species in ESI, allows large analytes, like biologicals, which might be several thousand Daltons and by adducting several protons to them. bring down them *m/z* range (2k-5k) to something that is detectable with the MS.[9,10]

The utility of ambient ionization in the past decade has provided a greater understanding in the field of forensics[11,12], proteomics[13–15], lipidomics[16–18], drug discovery[19–22], and many more.[23] Ambient ionization also provides the capability to observe analytes in their native state, that cannot be provided through sample pretreatment. These great strides in ambient ionization in the last decade have been so advantageous to our own understanding of biological processes and the

like, new ambient ionization techniques have emerged and can be classified into two categories because of the way the ions are generated are inherently different: spray of the analyte, and desorption of the analyte.

Spray-based ambient ionization sources use a high voltage applied to a conductive material. This induces an electrospray-like event where analytes of the same polarity (either positive or negative) as the applied voltage are ejected from the surface for analysis. Examples of spray-initiated analytes include: paper spray (PS)[24] ionization, thread spray ionization[25], coated blade spray (CBS)[26,27], glass spray (GS)[28], and polymer spray.[29]

Introduced by Graham Cook's group in 2010[24], PS has quickly been adopted in a variety of applications.[30] PS is carried out using a section of filter paper as a sample holder. The sample is applied to the filter paper and allowed to dry. After the sample is applied to the filter paper, a solvent system is applied to wet the filter paper and a high voltage is applied. The net result is an ESI like spray emanating from the proximal tip of the filter paper section. PS has been applied to a variety of systems including peptides[31], proteins[32,33], pharmaceuticals[34–37], and whole blood.[34–37] The broad variety of sample types to which PS has been applied highlights the utility of the technique. In some very complex matrices, including whole blood, with little to no sample preparation, therapeutic drugs including pazopanib, tamoxifen, imatinib, and irinotecan have been individually characterized to determine the limits of detection.[37] In addition, Wysocki's group has investigated the nature of non-covalent protein complexes by ion mobility-mass spectrometry (IM-MS).[33] When compared to

nanoelectrospray ionization (nESI), Wysocki's group found that the spectra were qualitatively similar, but PS suffered from a lack of desolvation. Interestingly, the authors found, on the basis of collision cross section calculations, evidence that the native structure of the protein complexes may be preserved in PS.[33] Ouyang's group has shown by covalently coating silica to the filter paper, paper spray has also been used to bypass chromatographic techniques such as column chromatography in whole blood samples, in order to separate amitryptyline using various solvents to elute the analyte, while also suppressing matrix effects.[38]

Thread spray ionization was recently developed in 2018 by the Badu-Tawiah group, where they used a thread with an applied DC voltage to induce a spray event capable of analyzing the interior peppers for capsaicinoid content with minimal destruction of the fruit.[25] The authors found that capsaicinoids content for various pepper had a strong correlation to the Scoville Heat Unit index, which is a measure of the perceived level of heat derived from the pepper. This quantitative technique was achieved through direct sampling of the thread without the use of any chromatographic separation.

Coated blade spray (CBS) was developed in Janusz Pawliszyn's lab uses stainless-steel coated with a C-18 polyacrylonitrile in lieu of a C-18 column to bypass chromatographic separation. The stainless-steel coated blade is used as a solid phase micro extraction (SPME) device that can enhance the signal of an analyte from a complex matrix without removing the matrix itself.[26] The blade is sharpened to a point angled less than 90 ° and a high potential (3.5 kV) is

applied to the blade in front of the inlet to the mass spectrometer. This facilitates a desorption event, where the high potential electric field that induces a charge onto the analyte, causing ionization. This configuration is unique because the coated blade can act as an extraction device and an ion source. Depending on the solvents used in the cleaning step and the polarity of the analyte, undesired components in the sample matrix can be washed off the coated blade. Washing the blade acts as a preconcentration step of the analyte as far as increasing signal and can overcome signal suppression that arises from the sample matrix. In other work done by the Pawliszyn group, they were able to independently quantitate multiple targets from a small sample volume from a dried biofluid without wetting or other preconditioning steps.[27]

Recent experiments by Richard Zare's group of Stanford University demonstrated the ability to generate a stable ESI like spray from a solid glass surface.[28] This solid surface eliminates the wicking necessary to carry out a PS measurement and may increase the speed with which measurements may be taken. GS has been used to monitor polymerization reactions in real time. This methodology has been further extended to look at the development of ions from solid polymer surfaces.[29]

Ambient ionization sources where the analyte is desorbed off of a surface, which include: direct analysis in real time (DART)[39], desorption electrospray ionization (DESI)[40], low temperature plasma (LTP)[41], and atmospheric solids analysis probe (ASAP).[42–46] These ionization sources offer low limits of detection (LOD), and limits of quantitation (LOQ) similar to those conventional ESI and

APCI. The high sensitivity and quantitation capabilities of these desorption ionization sources has become amenable to a broad variety of analytes including: steroids[47], direct sampling of tissues from plants[48], small molecule drugs[44], biologicals[46], secondary organic aerosols[43], pesticide and food contaminants[42], and low molecular weight synthetic polymers.[45]

First published in 2004, DESI uses a high-velocity stream of charged solvent droplets directed at a surface containing analytes.[49] The analytes are desorbed from the surface and subsequently ionized by the charged droplet stream. DESI has been applied to samples of forensic interest including fingerprints and drugs. Additionally, chemical imaging has been of significant interest in the DESI community. By rastering the DESI source across a sample surface, spatially resolved chemical imaging is achieved so that analytes may be located across a surface. To this end, fingerprints have been analyzed so that individuals can be distinguished from one another and traces of illicit substances can be found within these fingerprints.[50,51] In addition to the imaging capabilities, DESI has been used to detect counterfeit pharmaceuticals.[52,53]

DART is an ambient ionization source that relies on an electrostatic discharge in a high-temperature stream of an inert gas.[54] Analytes are desorbed from a surface and subsequently ionized. Similar to other ambient ionization sources, DART requires no, or very little, sample preparation[55] leading to rapid analysis of illicit drugs[56–59], pharmaceuticals[52], lipids, and explosives[60,61] among others.[39] The relatively soft nature of ionization is similar in affect to ESI or APCI

in that there is little fragmentation observed and the major ions observed are protonated molecules.

The focus of this work is investigating the generation of ions directly from a metal surface in an ESI-like spray event. Termed metal spray ionization, an aliquot of a solution containing the analyte is applied directly to a copper surface. After application of the sample, a high voltage is applied, and a spray is initiated. In the work reported here we investigate the ability detect singly and multiply charged peptides in order to facilitate easier sampling with biologicals, along with lipids. The ability to detect food additives, small pharmaceuticals, illicit drugs, cosmetics, and pesticides is also investigated. In addition, the ability to quantitate those analytes is demonstrated as well.

Later work will discuss the use of desorbing an analyte off of a surface without any preconcentration or dilution procedures are avoided by utilizing ASAP in order to detect and quantitate isomass drugs from a mixture. This was performed with the use of a derivatizing agent that is commonly used for GC analysis in order to make compounds with a low vapor pressure more volatile and increase their thermal stability.

2. METAL SPRAY IONIZATION FROM A BARE COPPER SURFACE

Initial work was focused on optimizing features of paper spray, by using a metal surface to generate ions. The term used for this methodology throughout the paper is referred to as “metal spray ionization” or “metal spray”. In this first set of experiments, copper metal was used as the ionization source. Copper has a unique advantage over using a piece of filter/chromatography paper, because the surface is reusable, easy to clean, and can be functionalized by oxidizing copper to copper (II) oxide. By applying as little of 0.5 µL of solution to the tip of a copper surface, a +(4.0-4.3 kV) bias is applied to the surface and a spray event is initiated, similar to that observed with nESI or PS experiments. The initial data for this work was collected in full-scan mode using an extracted-ion-chronogram (XIC) and the ratio of peak intensity of the analyte to the peak intensity of the internal standard were plotted as a function of analyte concentration. As a proof of concept, biological peptides were analyzed and quantified. Initially, two peptides were studied: bradykinin and leucine-enkephalin. These peptides have been studied by a variety of mass spectrometric methods and their behavior has been well characterized.[62–65] Calibration curves were created with both peptides and their sensitivity, LOD, and LOQ were all evaluated separately and compared to commercial heated electrospray ionization (HESI) source.

Before any quantitation could be performed and compared to HESI, several variables needed to be optimized, in order to obtain a stable intensity spray from the analyte. Primarily, the distance from the inlet of the MS to the tip of the copper surface, and the voltage applied to the copper surface. A stage

platform was purchased from ThorLabs, which allowed X, Y, and Z manipulation of the copper surface. Copper surfaces were fabricated to the dimensions of 23 mm x 10 mm with a 90° tip. The edges of the copper surface were beveled to 45° to eliminate spurious discharge events that would deflect the ionized analyte away from the inlet of the MS. Presumably this would affect the signal intensity, making quantitation much more difficult. Voltage applied to ion optics and to the copper surface was optimized using 25 μM substance P with a (HESI) using direct infusion, by varying the voltage until the maximum absolute signal intensity was achieved.

Spectra collected with HESI source, were visually compared with those collected via metal spray to verify that there was not a change in the charge state of the analyte induced by the ionization source. After it was verified that the spectra produced by both ion sources were similar, experiments were performed to evaluate the ability to quantitate analytes directly from the surface. Bradykinin and Leucine-enkephalin were chosen because they have been characterized with a long track record of mass spectral methods, and their behavior is well understood.[62–65] Bradykinin is a hormone peptide that signals distress for many vascular and renal functions.[64,66] Activation of the kinin system causes the release of bradykinin to the arteries which is a vasodilator in order to regulate high blood pressure, inflammation, and allergic reactions.[66] Leucine-enkephalin is an interesting neuropeptide that functions as a neurotransmitter and modulator that inhibits neurotransmitters responsible for the perception of pain, and acts as an agonist on several opioid receptors.[63,65] Substance P is another neuropeptide

and is noted for its widespread abundance and circulation throughout the body, and its ability to induce inflammation.[67] Elevated levels of substance P are commonly associated with gastrointestinal diseases such as IBS, and found in the respiratory system of asthmatic patients.[67] Substance P was used as an internal standard (I.S.) to account for any signal fluctuations that may arise from uneven spray events between samples, or instrumental drift. It is worth mentioning that the most abundant *m/z* is 674 which corresponds to the doubly charged analyte. These neuropeptides mediate a diverse range of physiological and pathological processes, which has made them attractive targets for therapeutic validation. The ability to quantitate these peptides with a different ionization technique, shows the ubiquity/utility of the method, and the ease of sampling could expedite the adoption of this system.

Materials

Bradykinin acetate salt ≥98% HPLC was obtained from Sigma Aldrich. 1,2-Dioleoyl-sn-glycero-3-phosphocholine lyophilized powder was obtained by Sigma. Substance P acetate salt ≥ 95% HPLC powder obtained from Sigma. [leu5]-enkephalin from AnaSpec Inc. High purity formic acid, chloroform, methanol HPLC- Ultra LC-MS, and water HPLC were all obtained from VWR. 1 ft x 1 ft x 1 mm thick copper sheet from McMaster Carr. Time of flight (TOF) power supply R. M. Jordan Company Inc. A Thermo-Scientific Velos Pro was used for these experiments equipped with a dual linear ion trap with a high-pressure ion trap for high fragmentation efficiency, in tandem with a low-pressure ion trap for high resolution. Qual browser software was used for analysis.

Methods

Copper was cut to the desired dimension mentioned previously. A 5 mm channel 0.5 mm deep extending from the tip of the surface was cut using a Philips screwdriver. Power supply used to supply the voltage to the tip was a TOF power supply by R. M. Jordan Company Inc. Voltage supplied to the tip of the surface was+ 4.3 kV. The tip of the copper surface is between 2-5 mm from the inlet of the mass spectrometer and for optimal field stability the height of the copper surface is between 2-3 mm above the inlet, see Figure 1 below.

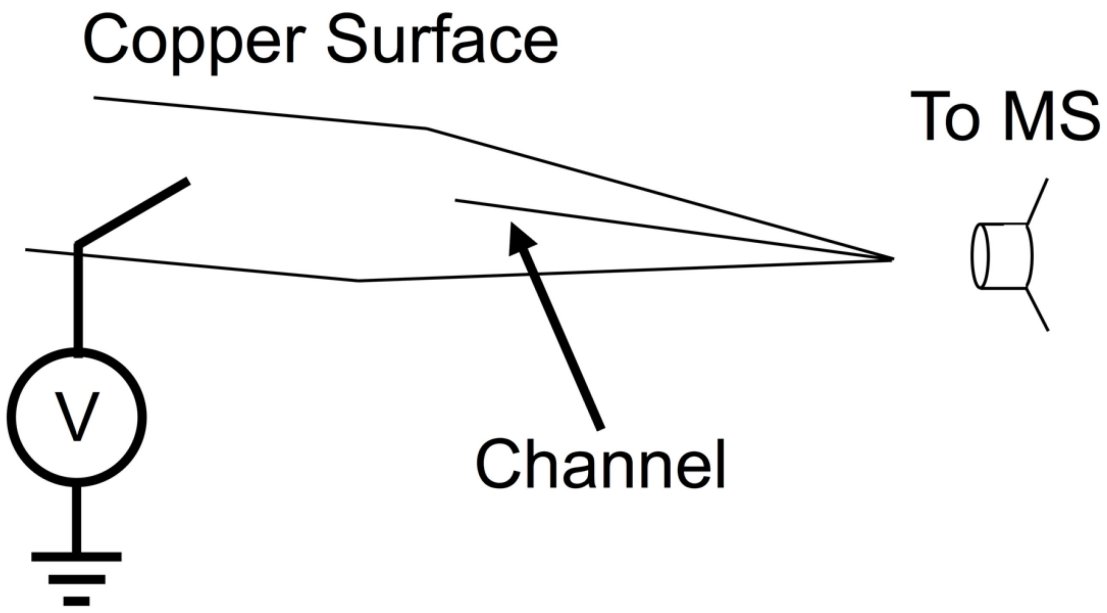

Figure 1. Schematic of the metal spray setup.

Prior to each experiment the copper surface was washed with methanol and dried. An alligator clip was placed on the surface roughly 5 mm from the channel and a 10 μL solution of methanol/water with 0.1% formic acid was

applied when the power was off. Solutions of 25, 12.5, 6.25, 3.125 μM bradykinin were produced using serial dilution. The solvent system and the blank consisted of 50:50 methanol/water with 0.1% formic acid. The final solutions were fortified with 100 μL of a 25 μM solution of substance P as the internal standard.

Solutions were analyzed in order from low to high concentration applying 0.5 μL of sample when the power supply was turned off, and each sample was run in triplicate. The 0.5 μL sample was applied to the tip of the copper surface and pulled across the 5 mm channel away from the inlet of the MS, in order to fill the channel with solution. After the sample was applied and the instrument is scanning, a +4.3kV bias was applied and a spray event was observed. After each spray event the surface was cleaned with a cotton swab to get rid of any residual solution. Calibration curves were created using the ratio of peak areas obtained after each spay event using Qual Browser software. The ratio of analyte area to internal standard was averaged for each concentration and the averaged ratios were plotted for the calibration curves using an n = 3. The standard deviations for each concentration was calculated using these averaged ratios as well.

Results and Discussion

Figure 2 below, shows the full mass spectra of a 25 μM bradykinin solution using substance P as an internal standard, measured with HESI and metal spray.

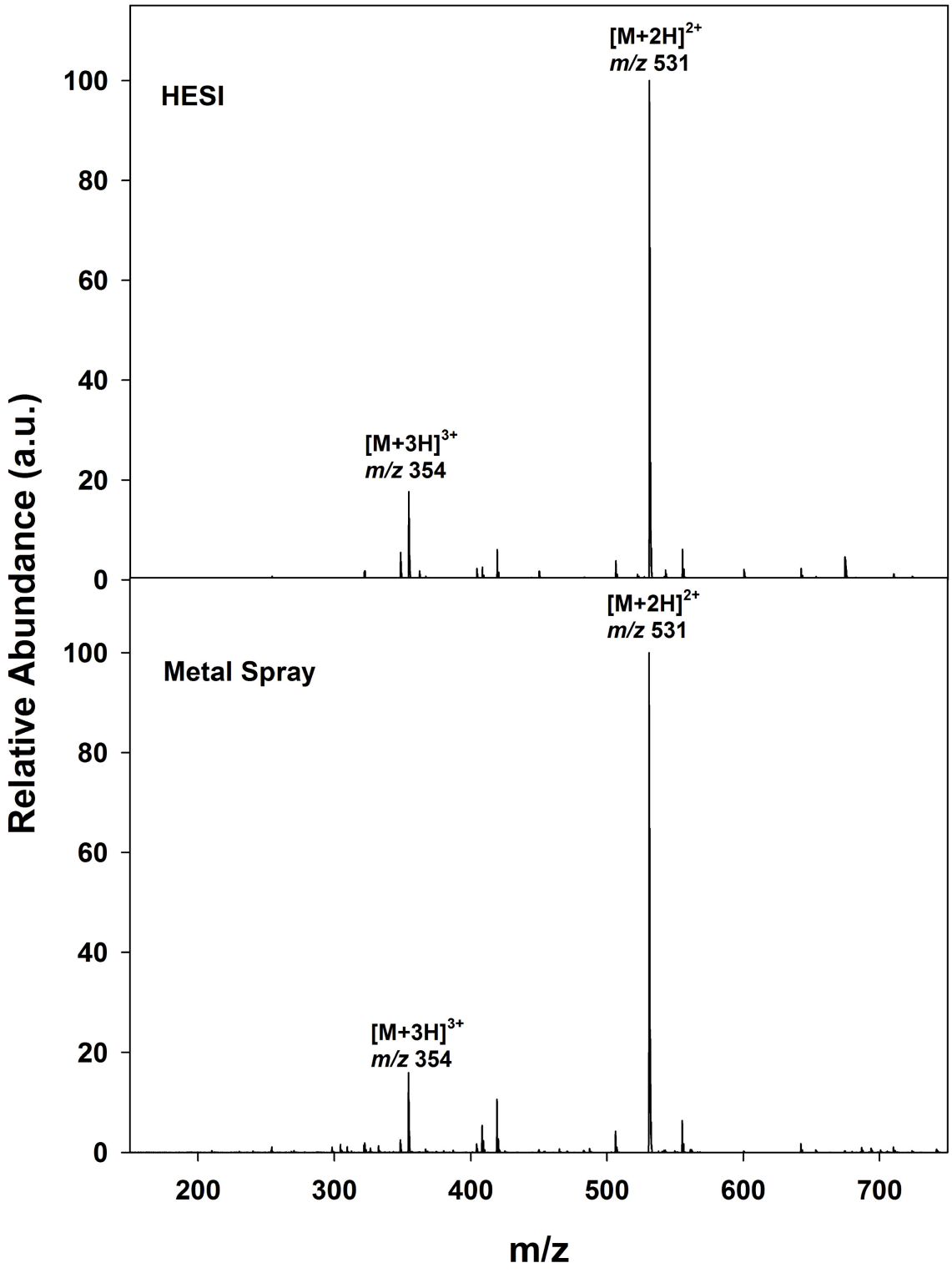

Figure 2. Mass spectral comparison of the doubly and triply charged bradykinin with HESI (top) and metal spray (bottom).

In Figure 2 it is apparent that the two spectra mirror are nearly identical, with minor differences in the background noise. In both spectra the base peak was doubly charged bradykinin at *m/z* 531, which was also reported in a PS experiment. It has been observed by Ouyang's group at Purdue that the 2+ charge state of bradykinin is often accompanied by a sodium adduct.[32] This, however, was not the case most likely due to sample preparation, as the solutions were prepared in polypropylene microcentrifuge vials, thus minimizing the possibility of sodium leaching from a glass vial.

Once visual confirmation that the spectrum produced by metal spray for bradykinin was representative of the spectrum produced by HESI, calibration curves were constructed using serial dilutions of bradykinin using HESI and metal spray, Figure 3 below.

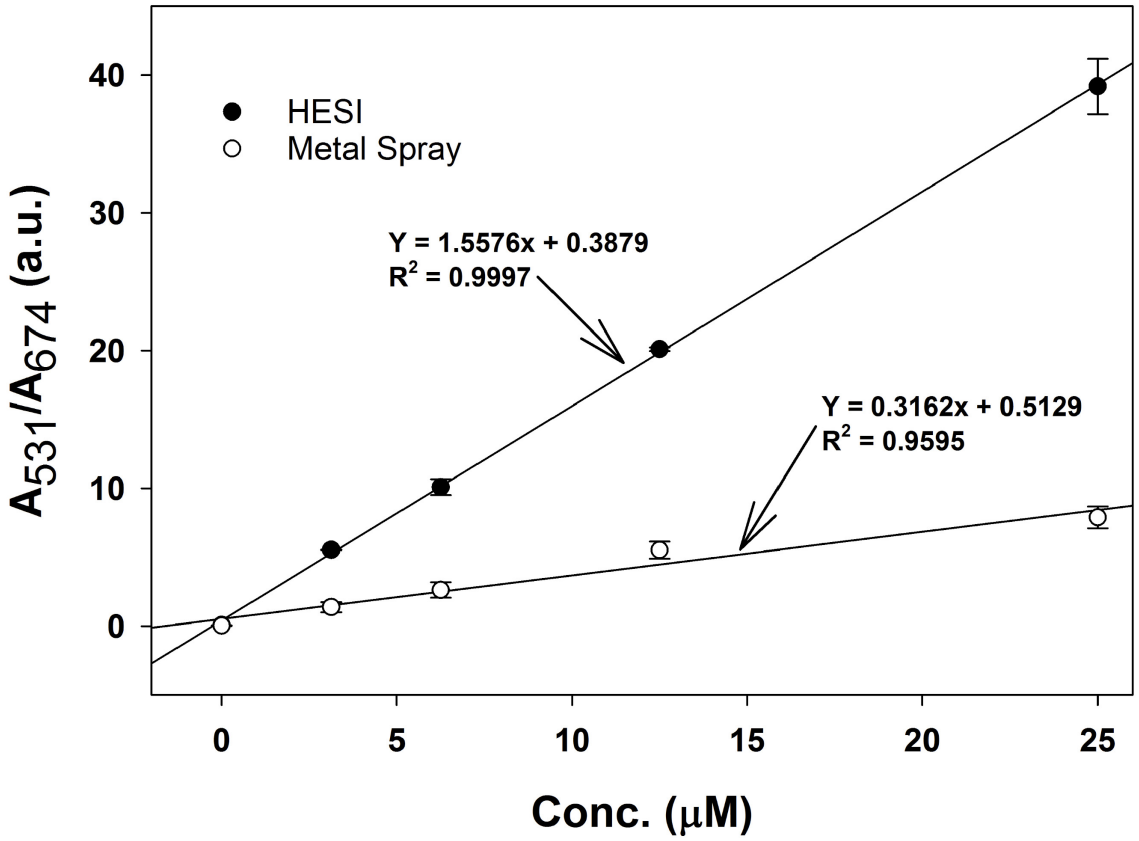

Figure 3. Calibration curves for the $[M+2H]^{2+}$ bradykinin serial dilutions spiked with substance P as an IS using HESI and metals spray.

In Figure 3, HESI exhibits almost 5 times greater sensitivity compared to metal spray, when examining the slopes of the two curves. HESI also produced a higher R^2, value, which indicates a more linear response to the analyte concentration. The LOD/LOQ for the bradykinin serial dilutions using HESI were 6.50 ng/mL and 21.6 ng/mL respectively. The LOD/LOQ for the bradykinin serial dilutions using metal spray were 38.5 and 128 ng/mL respectively. This is substantially similar to results from a PS quantitation experiment using therapeutic drugs from dried blood spots, where a very linear relationship was observed.[68] It is worth mentioning however, that though similar calibration curves

were reported for PS experiment, PS had a higher correlation coefficient compared to metal spray.[68]

To further evaluate the utility and quantification capabilities of metal spray, another peptide, Leucine-enkephalin (YGGFL) was investigated that has a singly charged base peak $[M+H]^+$ at *m/z* 556. This was to ensure that the spectrum produced with HESI and metal spray, could also be used to observe singly charged peptides.

Figure 4 shows the full mass spectra of a 25 μM solution of Leucine-enkephalin, using substance P as an internal standard. In Figure 4, it is worth mentioning that after subtracting the background there is very little, chemical noise in the metal spray spectrum. Comparing the two spectra, the base peak at *m/z* 556 for the singly charged YGGFL is the same for ESI and metal spray. These results illustrated that metal spray ionization is suitable for comparison and quantitation of doubly and singly charged peptides.

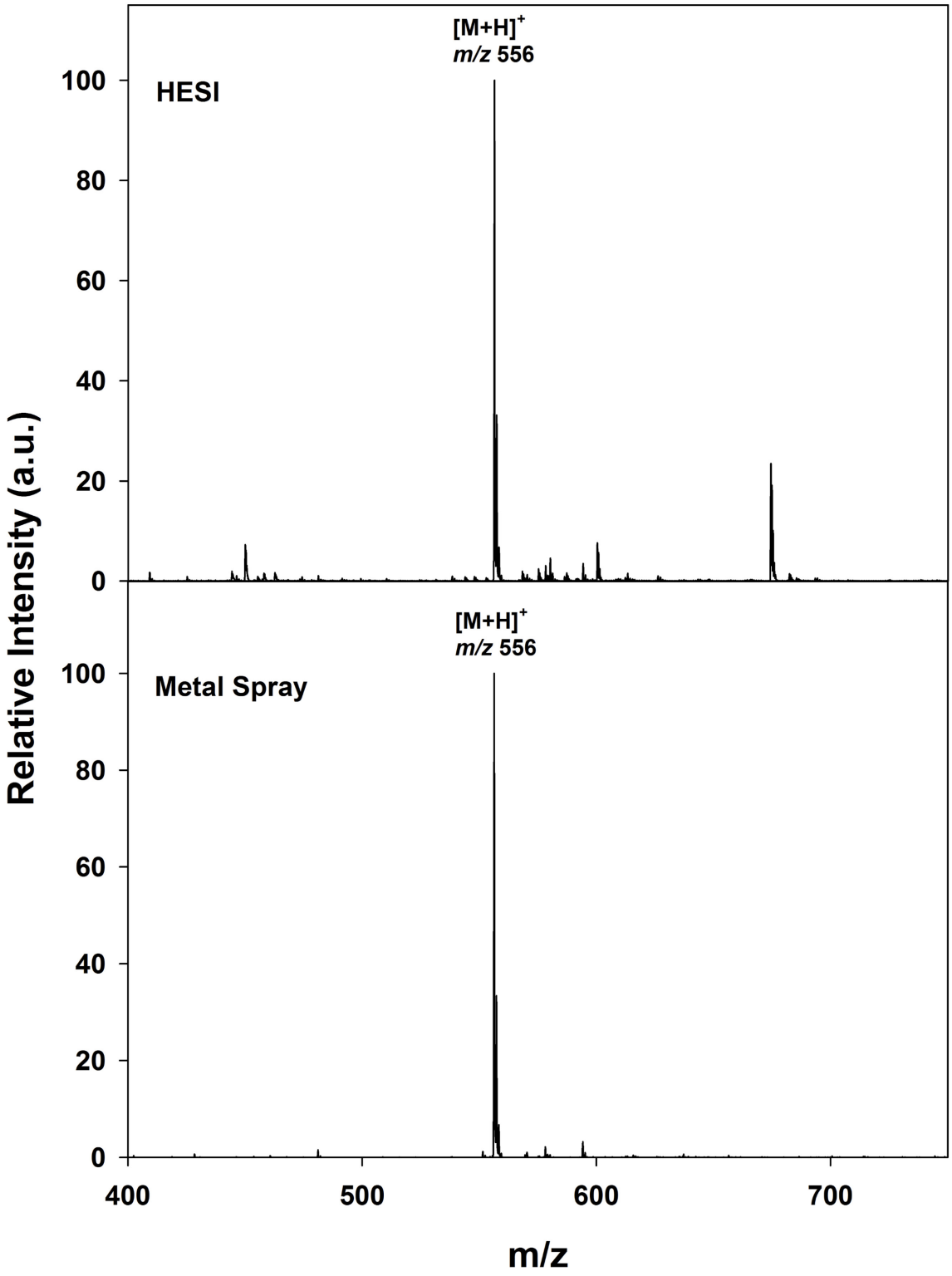

Figure 4. Mass spectral comparison of the singly charged YGGFL with HESI (top) and metal spray (bottom).

As seen in Figure 5 below, metal spray displayed a higher sensitivity to the singly charged Leucine-enkephalin, compared to HESI. The correlation coefficient for HESI was only slightly more linear than metal spray, but at this time there were still a lot of thing to be optimized with this sampling methodology.

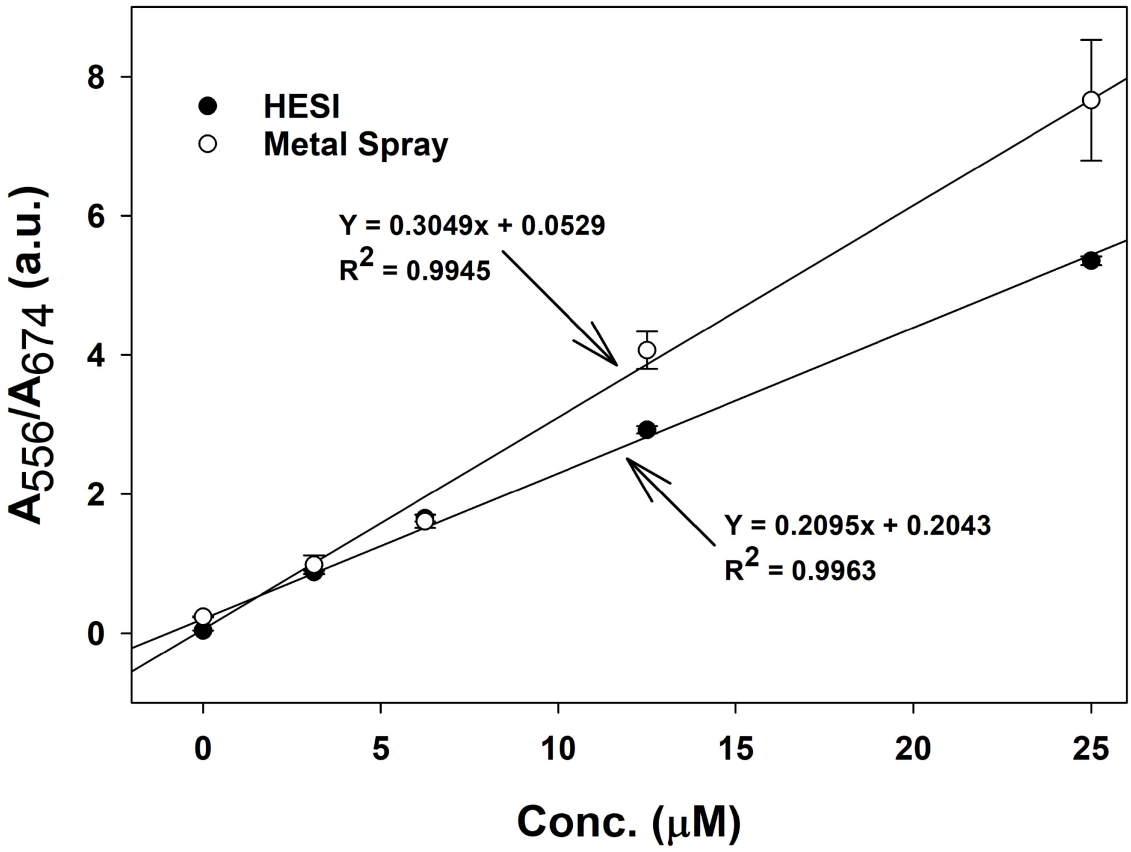

Figure 5. Calibration curves for the $[M+H]^+$ YGGFL serial dilutions spiked with substance P as an IS using HESI and metal spray.

The larger error bars on the calibration curve for metal spray in Figure 5 above, indicate that there is higher uncertainty in the confidence intervals surrounding the slope of the calibration curves. The LOD/LOQ for HESI was 4.75 and 15.9 ng/mL respectively. The LOD/LOQ for metal spray was 46.1 and 154

ng/mL respectively. Although HESI has lower sensitivity compared to metal spray (as evidenced by the slope of the calibration curve), the LOD and LOQ were approximately an order of magnitude lower for HESI than metal spray. The difference in these values likely originate from the fact that with using an n = 3, the standard deviation from the blank was ten times greater using metal spray compared to HESI. At this point it is not understood if this is an artifact of the mechanism by which the ions are produced, or if more optimization on this system is needed.

Conclusion

Conductive metals will carry a charge, regardless if there is any solvent present. By applying a voltage after the sample solution has been applied, it is theorized that the high voltage induces a charge that accumulates at the tip of the copper surface. The build-up of charge cause analytes with the same charge to be ejected from the surface in the form of charged droplets. These charged droplets then become desolvated, leaving behind the bare ions that are then detected by the MS. Metal spray ionization and PS share a few qualities in common that highly encourage the adoption of these ionization methods, they do not require sheath gas or syringe pumps, which decrease the cost of analysis and provide economical viability. The major advantage metal spray has over PS is that these copper surfaces are reusable, creating a potential benefit through the reduction of consumables.

Overall, metal-spray ionization produced spectra that were the same as those produced with HESI, with less background noise contribution. This is partly

due to the amount of material that is being sampled. Because these two spectra are substantially similar, this leads me to believe that the ions are generated in an ESI-like fashion, with the major exception that the ions are being generated from the surface, rather the flow solution in ESI. The ability to quantitate singly and doubly charged peptides of Leucine-enkephalin and bradykinin spiked with substance P as an internal standard proved that the linearity in the calibration curves were exemplary. In the case of YGGFL, even proved to be more sensitive than HESI. Future work on metal spray will be concerted at detecting illicit drugs, pharmaceuticals within their therapeutic range, pesticides, insecticides, and food adulterants/additives.

3. METAL SPRAY IONIZATION USING A SUPERHYDROPHOBIC SURFACE

To further expand the utility of metal spray, modifying the surface of copper might be able to achieve ESI-like limits of detection and quantitation, so that adoption of this methodology is practical to a spectrometrist. The most common oxidation state of copper is Cu^{2+}. By oxidizing copper to CuO, one can make use of the terminal oxygens in copper (II) oxide to covalently attach different functional groups and change the range of polarity of the surface (hydrophobic/hydrophilic/omniphobic), as well as the contact angle for different solvents. Similar work has been done using whole blood samples on hydrophobic paper in PS experiments.[69] In contrast to PS, metal spray does not require the surface to be wetted, thus avoiding the potential loss of the analyte. [1–3] Metal spray also avoids changes in signal intensity arising from deviations in surface geometry that may occur from manually cutting filter paper, or variations in the cellulose polymer network as used in PS. This method does not require the use of nitrogen gas, syringe pump, or capillary tubing, which can be a main source of contamination. Ultimately copper was chosen for this experiment because it is conductive, cheap, the surface can be cleaned, and is reusable, making all these features green when it comes down to preforming per sample analysis.

This work focused on generating ions directly from a copper metal surface. As little as 0.5 μL of sample solution was applied to the metal surface, a high voltage was applied, and a spray event was initiated. These experiments further expand the utility of PS by using surfaces that are reusable and can be modified with different surface properties (i.e.

hydrophobic/hydrophilic/omniphobic), to increase sensitivity to the analyte. Similar work has been done using whole blood samples on hydrophobic paper in PS experiment, where they were able to initiate a spray event through electrostatic-spray ionization.

Superhydrophobic and omniphobic surfaces have become quite popular in the realm of material science due to their applications in self-cleaning[71], sacrificial coatings for microelectromechanical device systems (MEMS)[72], thermal diodes, and anti-icing/fog[73], antibacterial surfaces[74], and corrosion resistant materials.[73,75,76] Superhydrophobic material is one that provides a static contact angle greater than 150° with a sliding angle lower than 10°, and is usually referenced to water.[71,76,77]

Common superhydrophobic surfaces are made using halogenated silanes with fluorinated aliphatic chains.[72,75,76,78] These superhydrophobic surfaces may be coated via vapor deposition[72], plasma, spin coating[79], or covalently bonded to the surface of the copper through the oxygen in copper oxide that is formed through a hydrolysis and condensation reaction performed in solution.[72] The procedure used for making the superhydrophobic surfaces in this experiment was a modified from a paper by Miljkovic et al., where they used vapor-deposition to create their surface.[75]

Materials

HPLC LC-MS grade methanol, concentrated hydrochloric acid, and water were purchased from VWR, along with high purity formic acid. [Leu5]-Enkephalin (YGGFL) powder purchased from AnaSpec Inc. HPCL powdered substance P

acetate ≥ 95%, and Bradykinin acetate salt ≥ 98% powder were both purchased from Sigma. 97% trichloro(1H, 1H, 2H, 2H-perflourooctyl)-silane was purchased from Aldrich. A 1’ x 1 ‘ x 1 mm thick copper shim from McMaster Carr. Stage components for the x, y, z adjustment was purchased from ThorLabs. Voltage was applied to the copper spray initiators (both bare and modified) using a time of flight (TOF) power supply from R. M. Jordan Company Inc. Mass spectra were collected with a Thermo-Scientific Velos Pro and Qual browser software was used for data analysis.

Methods

Copper was cut to 23 mm x 10 mm with a 90, 60 and 30° tip. The edges were sanded down to a 45° angle and a 5 mm channel 0.5 mm deep extending from the tip of the surface was cut using a 0.5 mm x 3 mm x 75 mm Philips screwdriver. 4.3 kV was applied to the surface to initiate the sprat events. The tip of the copper surface was between 2-5 mm from the inlet of the mass spectrometer angled at approximately 30°, and for optimal field stability the height of the copper surface is between 2-3 mm above the inlet

The superhydrophobic copper surfaces in these experiments were made by cutting the desired dimensions (23 mm x 10 mm with a 90, 60 and 30° tip), and the edges were sanded down to a 45° angle with a 5 mm channel 0.5 mm deep extending from the tip of the surface. The channel was cut using 0.5 mm x 3 mm Philips screwdriver. Surfaces were sonicated for 10 minutes in an acetone/methanol/isopropyl mixture, and then triple rinsed with deionized water. The surfaces are then placed in a 2.0 M HCl solution for 10 minutes to remove

any residual copper oxide film on the surface. Surfaces were then triple rinsed with deionized water and dried using nitrogen gas. Surfaces were submerged into a 95°C basic solution composed of $NaClO_2$, NaOH, $Na_3PO_4 \bullet 12H_2O$ and deionized water (3.75:5:10:100 wt%) until the surfaces turned black from the formation of copper (II) oxide. The surface were then rinsed with 95% ethanol and placed into a 5 mmol trichloro(1H, 1H, 2H, 2H-perflourooctyl)-silane in 95% ethanol for 24 hours, see Figure 6 below.

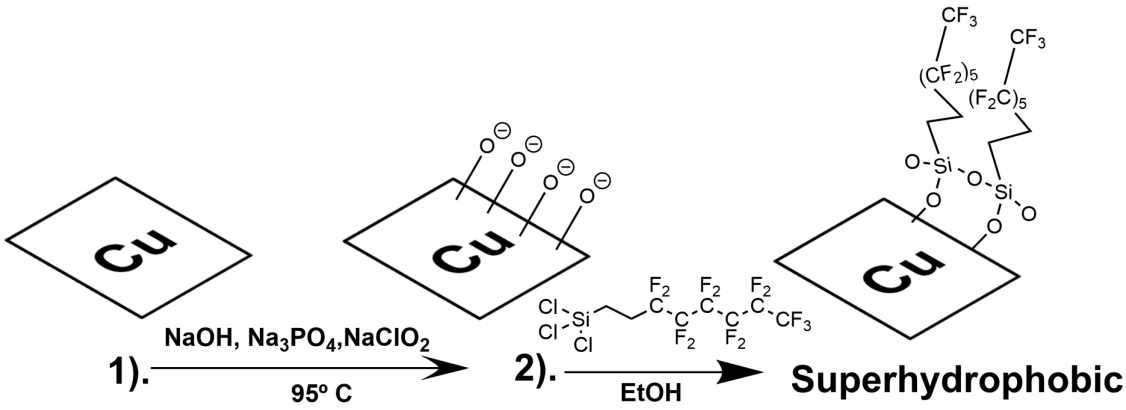

Figure 6. Synthesis of the superhydrophobic coating

This procedure for coating surfaces was adopted and modified from a paper by Wang et al, in which vapor deposition was performed.[75] Samples were applied using 0.5 µL at a time in concentrations of 0, 3.125, 6.25, 12.5, and 25 µM, in order from low to high concentration followed by the application of +4.3 kV.

Results and Discussion

Expanding on the utility of superhydrophobic surfaces and increasing the sensitivity of metal spray, these experiments report the use of superhydrophobic modified copper surfaces as spray initiators for metal spray, detecting singly and doubly protonated peptides.

When comparing two copper surfaces and their efficiency at ionizing different classes of analytes, it is necessary to look at how sensitive each surface is with the same analyte as well as different analytes of the same class (i.e. different peptides). For this purpose, different peptides, bradykinin and leucine-enkephalin were chosen. These two peptides have a long track record of use in analytical chemistry, and their fragmentation patterns are well understood.[62–65] Bradykinin is a neuropeptide composed of 9 amino acids, which is responsible for the regulation of blood pressure, inflammation, and cell growth.[64,80] The neutral form of Bradykinin has the molecular formula of $C_{50}H_{73}N_{15}O_{11}$ with a molar mass of 1059.56 g/mol. Leucine-enkephalin is another neuropeptide composed of 5 amino acids, which acts as neuromodulator antagonist on the μ-opioid receptors responsible for inhibiting the signaling transmission of pain.[63,65] Leucine-enkephalin has a molecular formula of $C_{28}H_{37}N_5O_7$ with a molar mass of 555.27 g/mol. Under the experimental conditions used herein, the leucine-enkephalin resulted in a singly charged analyte whereas bradykinin predominantly produced a doubly charged peak, thus allowing the study of the relative sensitivities for singly and doubly charged analytes from bare and

modified copper surface. The sensitivity, LOD and LOQ were analyzed for unmodified and silane-modified copper surfaces.

In order to validate that there was a discernable difference in these surfaces, and chemistry performed in solution, worked accordingly. Contact angle measurements were taken Figure 7 below, on bare copper and silane-modified surfaces using 50:50 methanol:water (V:V), with their respective 95% confidence intervals plotted as error bars.

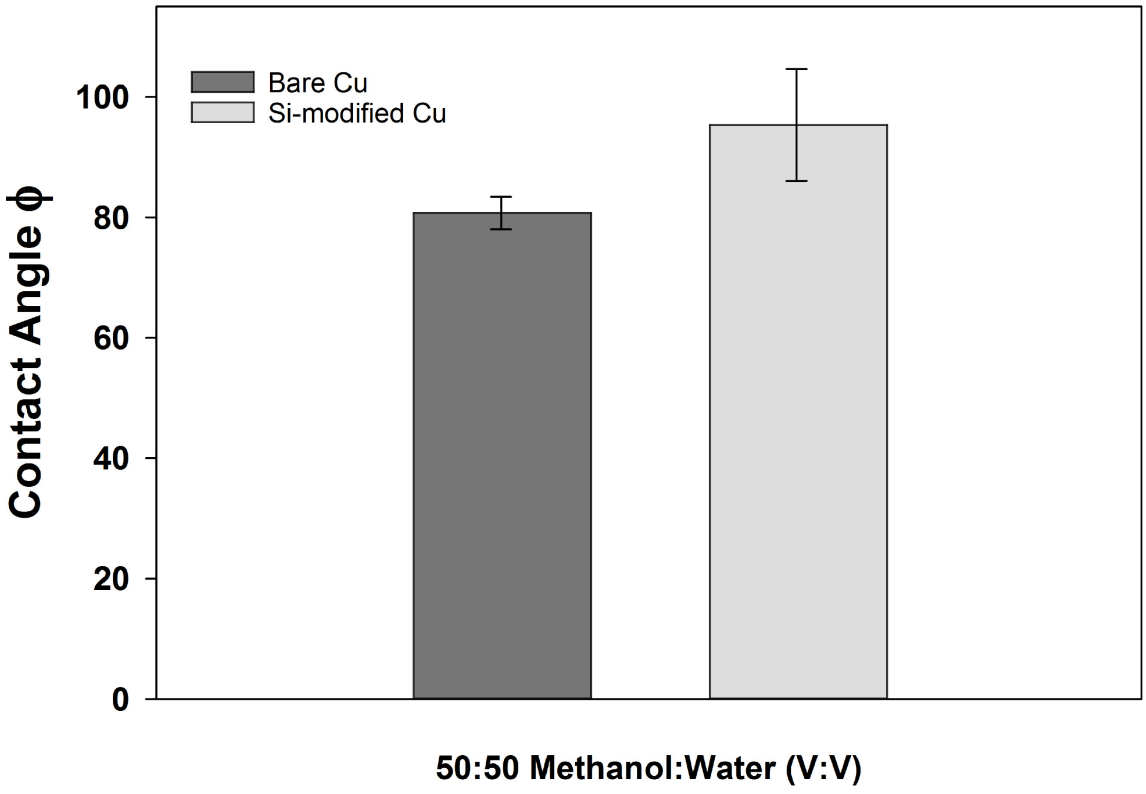

Figure 7. Contact angle measurements using 20 µL of 50:50 methanol:water (V:V) on a bare copper surface and a Si-modified surface, (n=10).

For the analysis of bradykinin on different surfaces and comparing bradykinin to YGGFL, it is necessary to point out that the most abundant peak

seen with bradykinin is the doubly charged at *m/z* 531 and the most abundant peak seen with YGGFL is singly charged at *m/z* 556. This was also observed in past experiments using an ESI probe. Analysis was performed using Qual Browser software. The ratios of areas of each ion-extracted chromatogram for each analyte and internal standard were plotted. As the intensity increases with the concentration of the analyte, so does the peak area. To account for any instrumental drift from one analyte to another, the peptide substance P was used as an internal standard in both solutions.

A representative chronogram of the spray event is shown in Figure 8 where a 0.5 µL application of bradykinin resulted in a 0.11-minute spray consisting of 33 mass spectral scans. These spray events lasted approximately 7 seconds for a 0.5 µL application, and these times were observed to extend to approximately 30 seconds if 1 µL was applied. After each spray event, the surface was cleaned with methanol and a cotton swab to remove any residual solution.

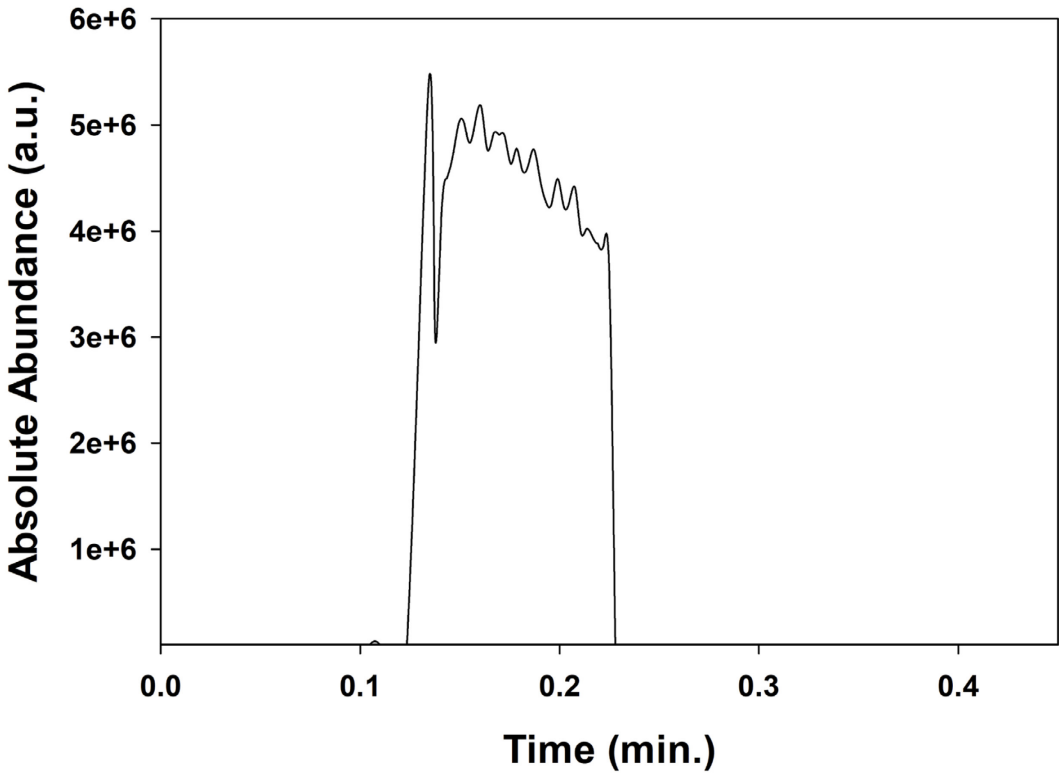

Figure 8. Extracted ion chronogram of bradykinin *m/z* 531 using a 30º tip on silane-modified surface.

Calibration curves were created by plotting the averaged ratio of extracted-ion-chronograms peak areas of the analyte to internal standard to their respective concentrations. The peak areas that were obtained after each spay event were integrated using Qual Browser software and the Genesis algorithm. The LOD and LOQ for the calibration curves were calculated by using 3 and 10 times the standard deviation of the blank, respectively, divided by the slope of the calibration curve, see equation 1 and 2 below.

$$LOD = \frac{3\ x\ Standard\ Deviation_{blank}}{Slope\ of\ Calibration\ Curve} \quad (1)$$

$$LOQ = \frac{10\ x\ Standard\ Deviation_{blank}}{Slope\ of\ Calibration\ Curve} \quad (2)$$

The standard deviation of the measurements at each concentration were calculated and used for the error bars in the calibration curves.

Comparing the two spectra for the unmodified copper and the silane-treated copper surface in Figure 9 and Figure 10, the absolute intensity of background for the silane-treated copper surface is lower compared to the background intensity for the unmodified surface by $5.4x10^6$ arbitrary units when looking at the spectral artifact at *m/z* 419. The analyte peaks for the triply charged bradykinin *m/z* 354 relative to the doubly charged base peak at *m/z* 531is also higher in relative intensity by 7.26 arbitrary units for the silane-modified surface than the unmodified surface using the same 25 μM concentration. This indicates that the ionization efficiency and sensitivity are greater for the silane-modified surface.

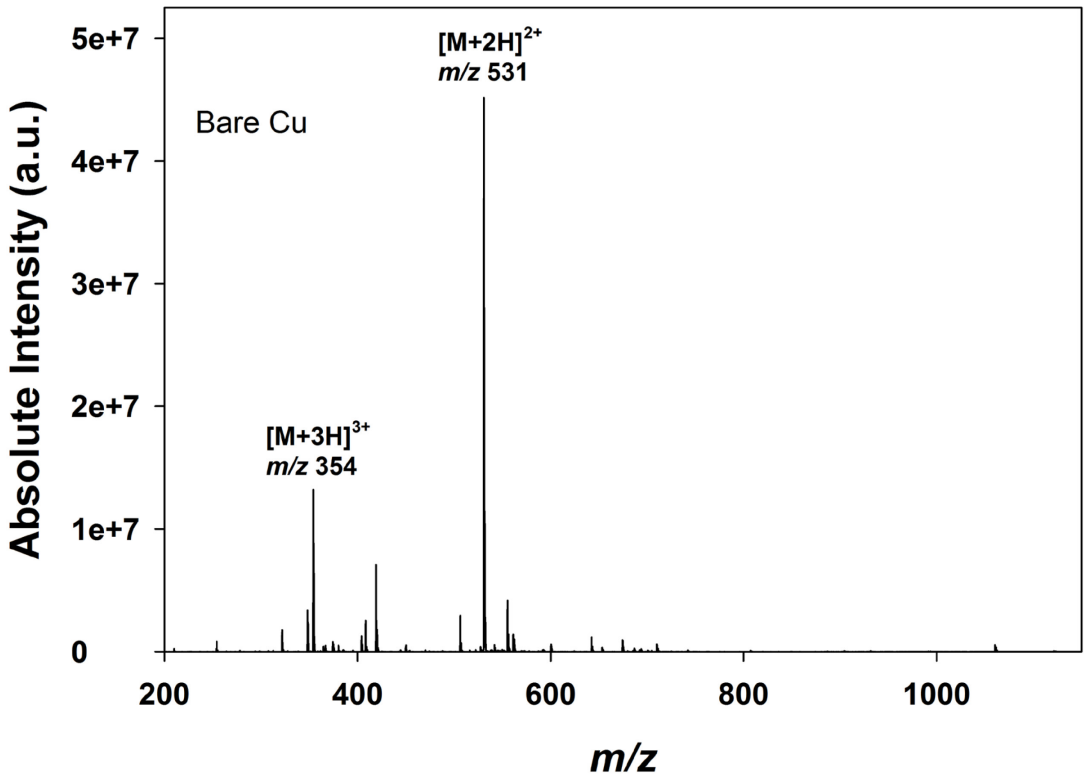

Figure 9. Background subtracted mass spectrum of 25 μM of bradykinin spiked with substance P as an IS using bare copper with a 90° tip.

These results were also consistent with a similar with paper spray experiment testing for a key biomarker indicative of liver injury in whole blood samples, where a hydrophobic filter paper was prepared.[69] We believe this is due to the preferential ejection of the peptide analyte due to the hydrophobic properties of silane. Because peptides are polar molecules interacting with the long silane groups, the peptides will not partition or adsorb to the surface very well. This was also noted in previous reports that used hydrophobic surfaces to preferentially extract analytes from a matrix.[81] In Figure 9, there is more partition between the analyte and the unmodified surface, therefore ejection of the analyte

over a given time is not as efficient because some of the analyte has adhered to the surface, resulting in a lower analyte peak intensity and higher background.

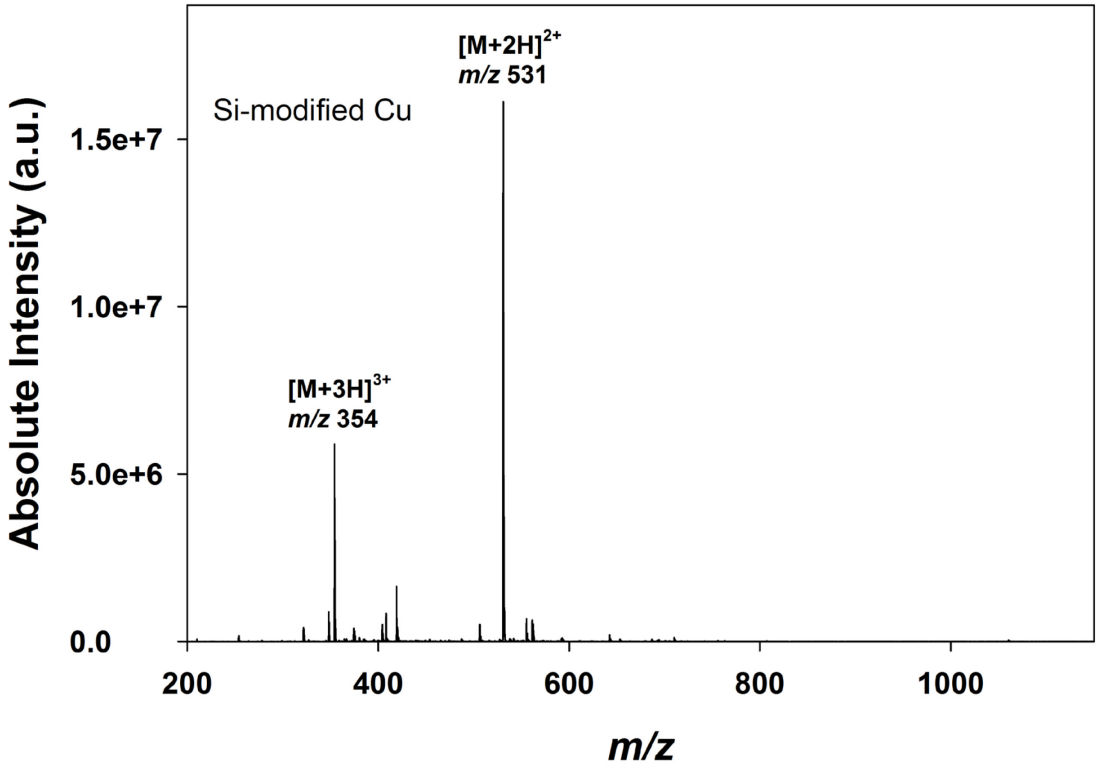

Figure 10. Background subtracted mass spectrum of 25 μM bradykinin spiked with substance P as an IS using Si-modified copper with 90° tip.

Here it is also worth mentioning that the substance P *m/z* is not easily observed, due to the background subtraction, which also contained the same concentration of substance P.

The calibration curve for bradykinin spiked with substance P with a 30º tip are shown below in Figure 11. These spray events were initiated with +4.3 kV for both surfaces and the LOD for the unmodified surface was 87.0 ng/mL and LOQ 209 ng/mL. The LOD and LOQ for the silane-treated copper surface were 10.4

ng/mL and 34.8 ng/mL. The slopes for each surface, shows that the sensitivity has gone up by almost a third for the silane-treated surface, as was expected. Both calibration curves in Figure 11 are very linear ($R^2 > 0.98$), and the small error bars indicate that there was not a lot of fluctuations in signal intensity from *n* = 3 number of measurements.

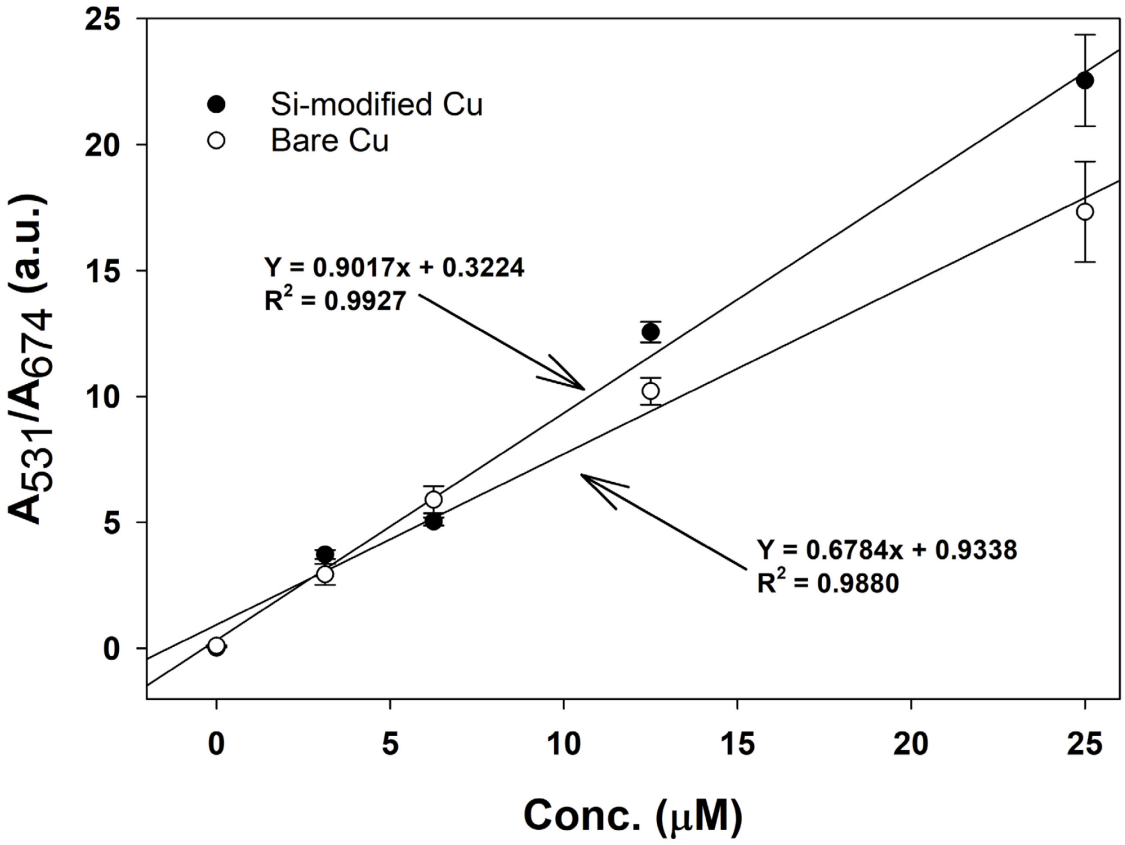

Figure 11. Calibration curves for bradykinin using Si-modified and bare copper surfaces with a 30º tip.

The ratio of the XIC peak are ratios for bradykinin spiked with substance p with the 60 º tip shown below in Figure 12 using the unmodified copper surface

gave an LOD of 35.9 ng/mL and LOQ of 119 ng/mL. The calibration curve for the silane-treated surfaces gave an LOD of 6.37 ng/mL and an LOQ 21.2 ng/mL.

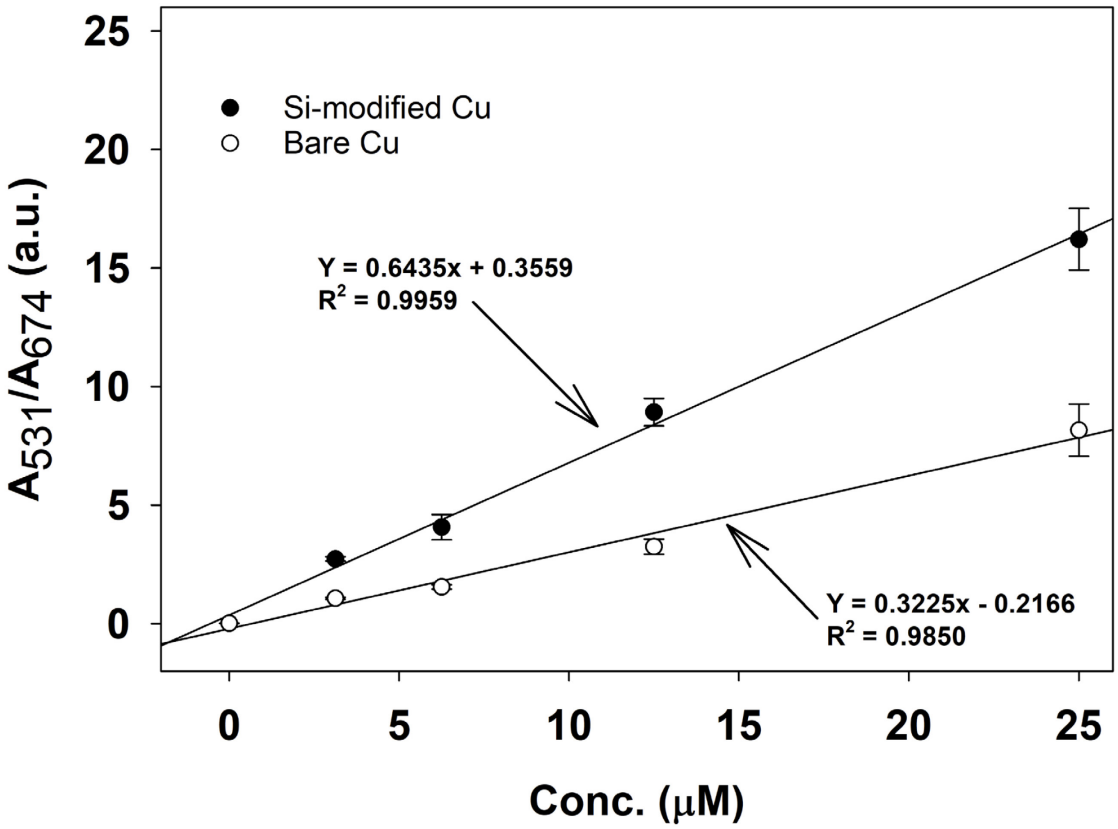

Figure 12. Calibration curves of bradykinin using Si-modified and bare copper surfaces with a 60° tip.

Interesting to note here, is that at 60° the silane-treated copper surface had the lowest limits of detection than any other calibration curve using bradykinin, but has the lowest sensitivity compared to 30° and 90° tips.

In Figure 13 below, the LOD and LOQ for the unmodified copper surface were 75.6 ng/mL and 252 ng/mL, respectively. The LOD and LOQ for the silane-treated copper surface were 55.9 ng/mL and 186 ng/mL, respectively. Looking at

the slopes of the calibration curves Figure 13, it is seen that the sensitivity (i.e. the slope) for the silane modified surface is nearly double that of the unmodified copper surface.

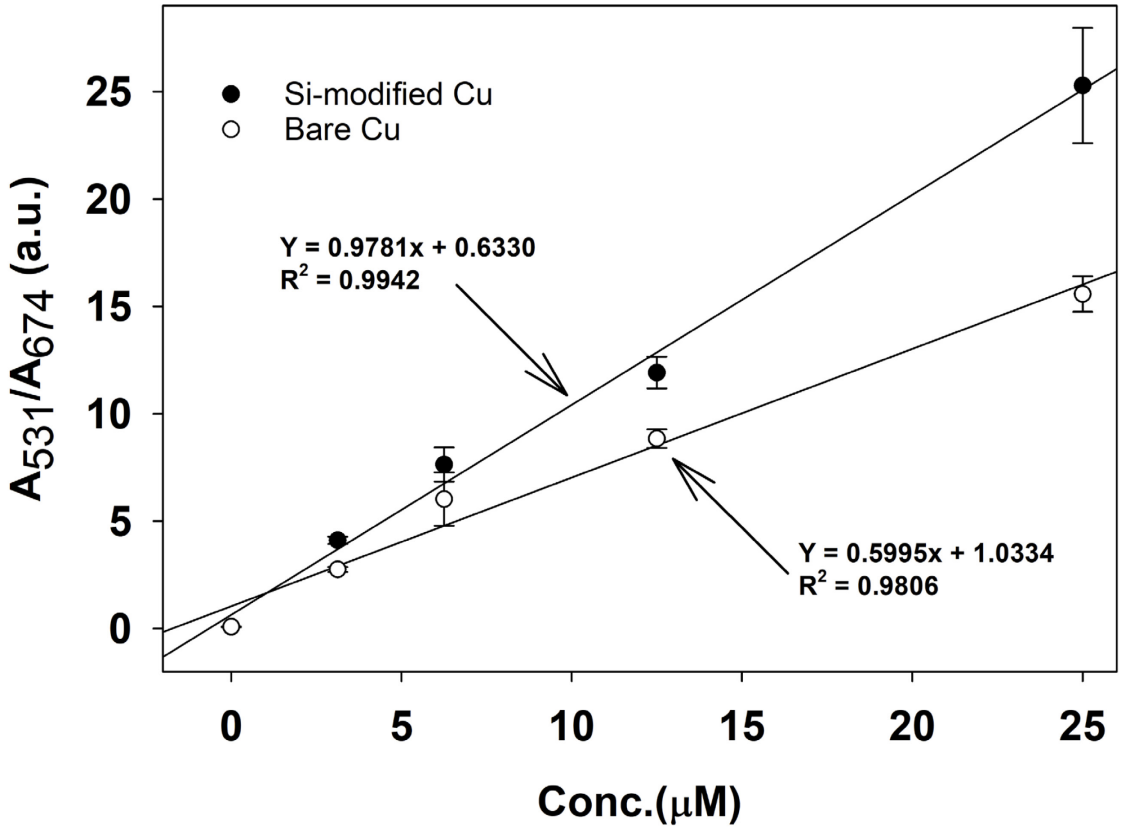

Figure 13. Calibration curves of bradykinin using Si-modified and bare copper surfaces with a 90° tip using (1μL).

As far as the analysis of singly charged peptides, such as leucine-enkephalin, you can see in Figure 14 below, that by comparing the slopes of the two surfaces, the silane-modified surface has almost 3x greater sensitivity than the untreated surface using a 30º tip.

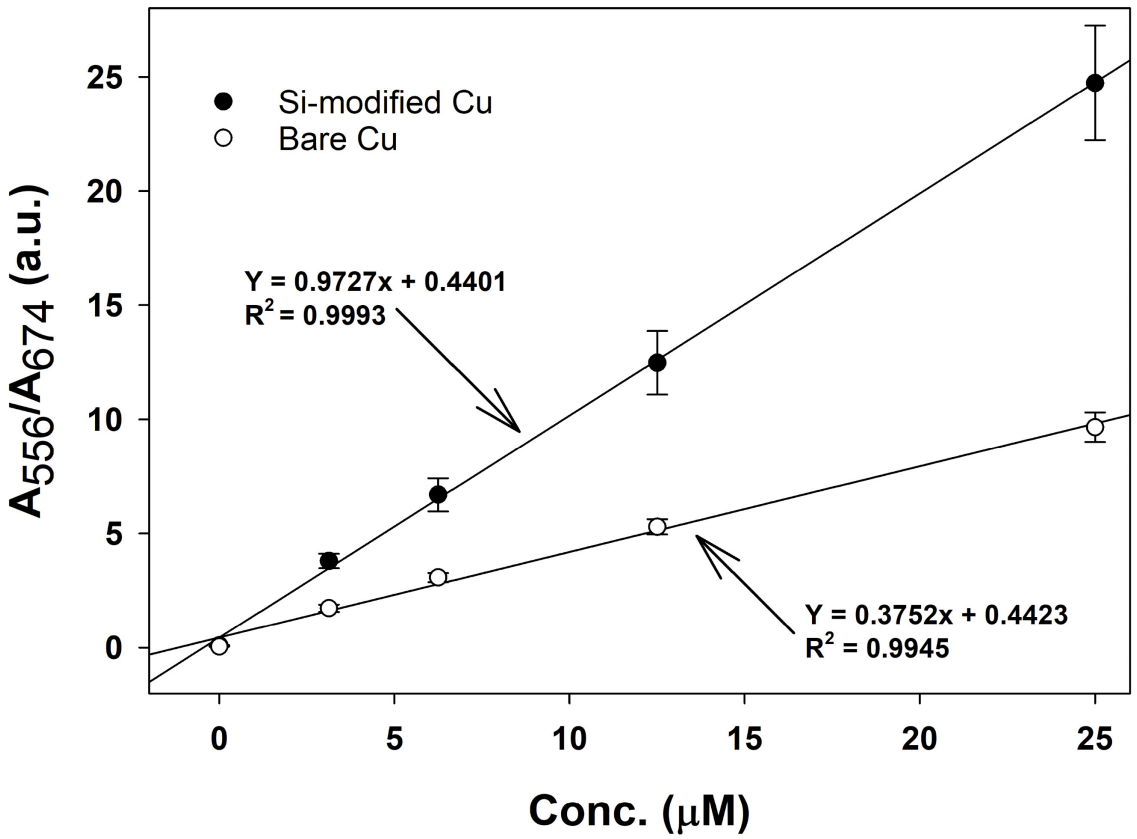

Figure 14. Calibration curves for YGGFL using Si-modified and bare copper surfaces with 30° tip.

The unmodified copper surface had a LOD 21.2 ng/mL and LOQ 67.2 ng/mL. The silane-modified surface had a LOD 18.2 ng/mL and LOQ 60.7 ng/mL. Note, that the LOD and LOQ for both surfaces are very similar, but the sensitivity between the two surfaces are vastly different. The base peak measured for leucine-enkephalin was singly charged, whereas the previous experiments with bradykinin were measuring a doubly charged analyte as the base peak. This is likely due to the differences in the isoelectric points between leucine enkephalin (5.9) and bradykinin (12.1). Under the present experimental conditions, the pH of the solution is ~2.7 which is far below the isoelectric point for bradykinin. It is

interesting to note that bradykinin had lower sensitivity and lower limits of detection and quantitation than YGGFL on a 30º silane-modified surface, (see Table 1 at the end of this section).

Comparing the sensitivity of the two calibration curves in Figure 15 below using a 60° tip, the silane-treated surface has almost twice the sensitivity as the unmodified copper surface.

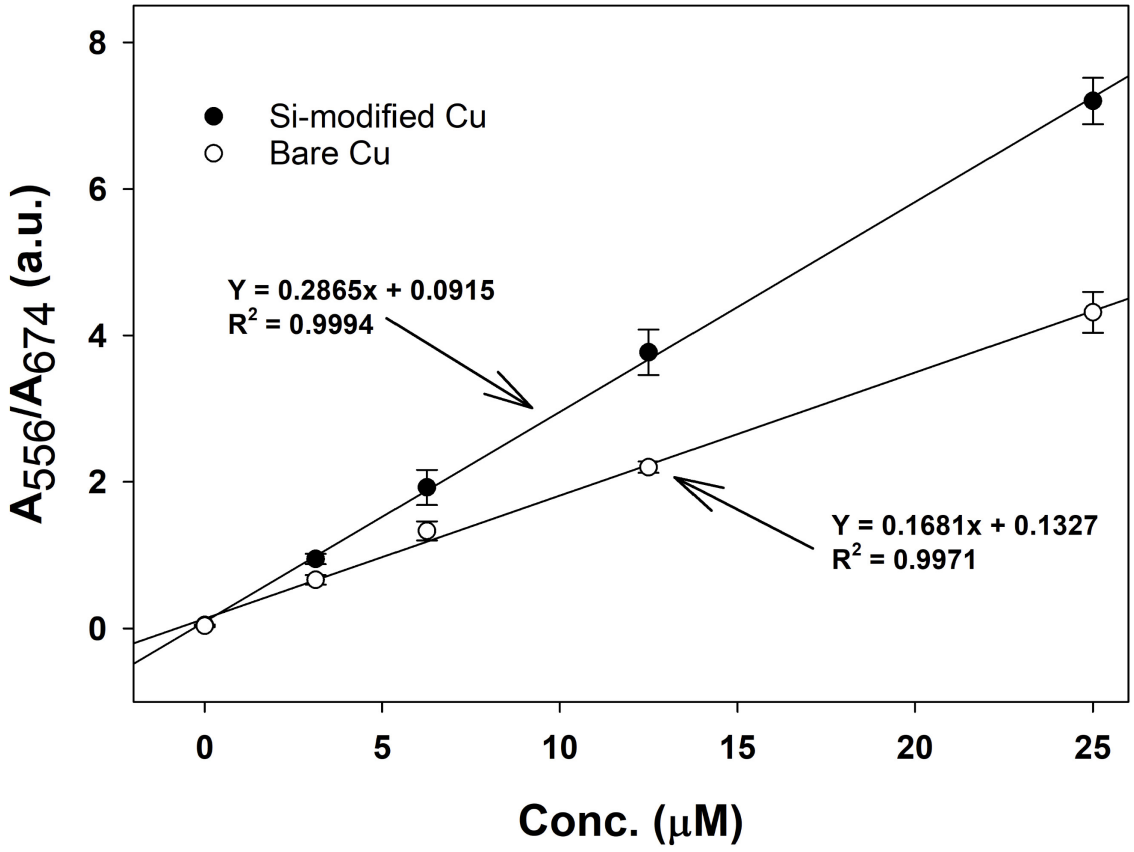

Figure 15. Calibration curves for YGGFL using Si-modified and bare copper surfaces with a 60°.

The unmodified surface in Figure 16, has a LOD of 158 ng/mL and LOQ of 527 ng/mL. The silane-modified surface has a LOD of 54.9 ng/mL and a LOQ of 183 ng/mL. Both spray events were initiated with a positively biased 4.3 kV.

Comparing the two calibration curves with a 90° tip in Figure 16 below, shows there is no significant difference in sensitivity between and unmodified and silane-modified surface.

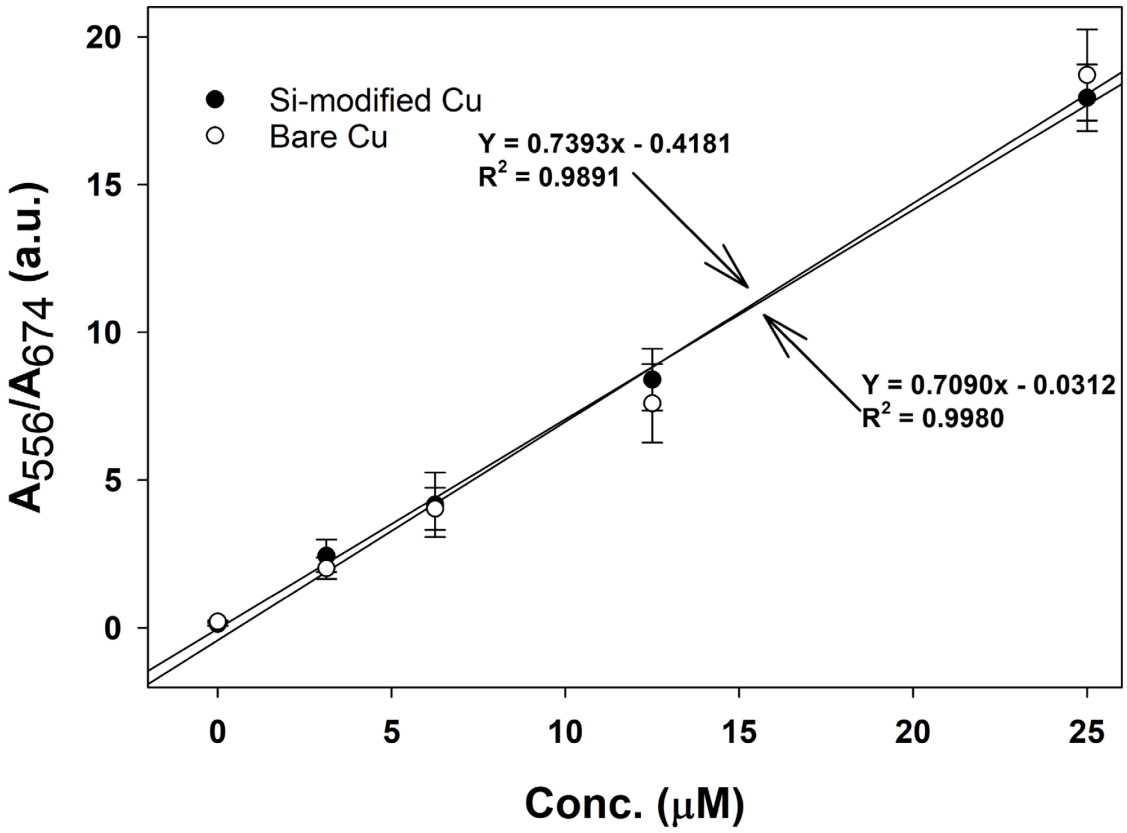

Figure 16. Calibration curves for YGGFL using Si-modified and bare copper surfaces with a 90° tip.

Comparing both slopes, this is the only case in all of these experiments where the sensitivity of the bare copper surface is slightly higher than that of the

silane-modified surface. However, it is important that the experimental uncertainty leads to overlapping error bars. In this case, it is difficult to say YGGFL is being preferentially ejected from a particular surface. This leads to the conclusion that when using a 90° surface with YGGFL, the type of surface is irrelevant.

Table 1 below, shows that the doubly charged bradykinin analyte on the silane-modified surfaces displayed a higher sensitivity, lower LOD and LOQ compared to the unmodified surface.

Table 1. Summary of all LOD/LOQ and sensitivity data for all bare and Si-modified copper surfaces using, 30, 60, and 90° tips

Tip Angle		Bare Copper LOD / LOQ (ng/mL)	Bare Copper Sensitivity	Si Modified Copper LOD / LOQ (ng/mL)	Si-Modified Copper Sensitivity
30	Bradykinin	87.0 / 209	0.6784	10.4 / 34.8	0.9017
	YGGFL	21.2 / 67.2	0.3752	18.2 / 60.7	0.9727
60	Bradykinin	35.9 / 120	0.3225	6.37 / 21.2	0.6435
	YGGFL	158 / 527	0.1681	54.9 / 183	0.2865
90	Bradykinin	75.6 / 252	0.5995	55.94 / 186	0.9781
	YGGFL	94.8 / 316	0.7393	119 / 397	0.7090

The lowest LOD and LOQ for bradykinin were from the silane-modified surfaces between 30 and 60°. It is suspected that as the angle on the tip is decreases, higher sensitivity is expected in these calibration curves, due to the increasing electric field. As it has been observed in other experiments using an HESI probe, the singly charged bradykinin peak at *m/z* 1061 is not the most abundant peak in the spectrum. The doubly charged bradykinin peak at *m/z* 531

is the base peak in this experiment using metal spray ionization, which was also consistent with past HESI experiments. All silane-modified surfaces displayed higher sensitivity, lower LOD, and LOQ for this particular analyte.

It was initially expected that higher sensitivity would be accomplished by using the superhydrophobic surface with a multitude of analytes of different classes. However, this might not be the case with nonpolar analytes such as lipids on a superhydrophobic surface, because of the attractiveness the lipids might display for the hydrophobic fluorinated-branched alkyl groups. These intermolecular interactions may cause the nonpolar analyte to bind too strongly through Van der Waal's or dipole forces, preventing the ejection of the analyte from the surface, in which no spray event would be observed. Preliminary data not shown in this work, found that steady spray events and calibration curves could not be obtained for the lipids 1,2-Dioeoyl-sn-glycero-3-phosphocholine (DOPC), and 1-Palmitoyl-2-oleoyl-sn-glycero-3-phosphocholine (POPC) using a bare copper surface or a silane-modified surface. In order to combat this problem with nonpolar analytes, a covalently attached or coated hydrophilic surface might be employed.

Conclusion

Using a hydrophilic, superhydrophobic, omniphobic, and unmodified copper surface, would give a continuum for different ionization efficiencies for analytes of differing polarity. These differing surfaces would provide a spectrometrist with four ionization surfaces that could easily be changed out

without changing probes, as is the case when looking at polar vs nonpolar molecules with ESI and APCI probes.

Referring back to Table 1 above, the singly charged YGGFL analyte on the 30 and 60° tip showed higher sensitivity and lower LOD and LOQ from the silane-modified surfaces, compared to the bare copper surfaces. The only exception in all these experiments where a higher sensitivity was not observed with a modified surface using YGGFL, was with the 90° tip. The conclusion was that with a 90° tip, the surface did not play a major role in the ability to detect or quantitate peptides. As observed in Table 1, the LOD and LOQ for the silane-modified surface for YGGFL using the 30° tip was almost twice that of the 90° tip. Overall, the singly charged YGGFL displayed the highest sensitivity when using the 30° silane-modified tip. The doubly charged bradykinin displayed the highest sensitivity between 30 and 60° silane-modified tip.

4. METAL SPRAY IONIZATION USING AN OMNIPHOBIC SURFACE

Omniphobic surfaces are ones that display a static contact angle greater than 150° and low hysteresis with low surface tension liquids.[82] Since their introduction into material science, omniphobic surfaces have been studied extensively for their highly commercializeable properties that mainly exist within high repellency to liquids, including low surface tension oils.[83] Some interesting facets that omniphobic surfaces have been used for include, but not limited to, self-cleaning[84], self-healing[85–88], anti-corrosion resistant materials[89–92], stain-free frabrics[83], anti-icing, water and oil separation[93], solar panels, windshields, and touch screens due to their transparency.[83,94–99]

By using an omniphobic surface as a spray initiator, these experiments aim to achieve ESI-like sensitivity, LOD/LOQ to a broad variety of analytes, where HESI sensitivity may suffer. The justification that an omniphobic surface might offer these advantages lies in the fact that omniphobic materials have been shown to have high liquid repellency to liquids with low surface tension, such as alcohols.[100] Typical solvents for direct infusion for APCI and ESI are equal volume mixtures of water and methanol. In these experiments, initial optimization was performed at quantitating the lipids, DOPC and POPC, and it was found that the 9:1 (V:V) methanol:water, provided the best results, which was used in this study.

In previous studies, metal spray ionization from a superhydrophobic surface, resulted in higher sensitivity to leucine-enkephalin when compared to electrospray ionization. In the case of doubly charged bradykinin, ESI had

greater sensitivity compared to metal spray. These studies also failed to generate reliable calibration curves for non-polar class of analytes, such as lipids. The conclusion from these experiments, was that the surface properties of the superhydrophobic to polar analytes achieved higher sensitivity, compared to HESI. This is likely due to the mismatch in polarity between the analyte and the surface. With non-polar analytes, reliable calibration curves could not be obtained using the superhydrophobic surface. This is likely because of the analytes affinity to adsorb onto the non-polar superhydrophobic surface.

Amongst these problems, the superhydrophobic surface mentioned in the previous chapter appeared to be oxidizing the copper underneath the coating. This could be due to the exposure to the ambient atmosphere or the application of a high voltage (+4.3 kV) necessary to induce a spray event. It is suspected that, over time, that the superhydrophobic surface would not have the same repellency to polar analytes. Rather than using a copper surface and covalently attaching a surface modifier, a copper surface was gold-plated and gold-thiol chemistry was used to attach 2-mercapto ethanol to the surface, which has an incredibly strong bond requiring an activation energy between 40-50 kcal/mol to desorb the thiol from gold.[101,102] Using the terminal hydroxy groups on the 2-mercapto ethanol, an omniphobic/superhydrophobic/hydrophilic can be covalently bonded to the surface as needed, depending on the polarity of analyte under study.

There are several advantages to using a gold-plated copper surface, instead of another conductive material. First, gold is more conductive than

copper, and in order to initiate a spray event the material needs to be capable of carrying a positive or negative voltage.[103] Given that gold is more conductive than copper, the argument could be made to use an entirely gold surface, however the cost of a gold surface precluded the use of a solid gold surface in this work.[104] Gold has a very high oxidation potential, does not oxidize below its melting point, and does not react with atmospheric O_2. Thus, oxidation, via exposure to air or application of a high voltage will not affect the underlying substrate.[101,102,105] Because gold has a high oxidation potential, the surface can be cleaned with a strong acid to remove any organic residue.[101,105] This also allows the analyst to change the surface coating, by using 3:1 pirana etch solution to rid the surface of the existing covalent bonds.[102] This provides a chemist with a reusable surface, where other coatings can be covalently bonded to change the surface properties.

Herein, these experiments report the use of a copper surface electroplated with gold. The gold surface was then submerged in an ethanolic solution of 2-mercapto ethanol to create a gold-thiol bond. Using the terminal alcohols in the thiol, an omniphobic surface can then be covalently attached that was prepared according to a paper by Wang et.al. to be used as a spray initiator, similar to PS experiments.[73]

Materials

1,2-Dioleoyl-sn-glycero-3-phosphocholine (DOPC), ≥99.0% 2-oleoyl-1-palmitoyl-sn-glycero-3-phosphocholine (POPC), ≥98% bradykinin acetate, ≥ 95% substance P, ≥ 90% (R)-(+)-pulegone were all purchased from Sigma and used

without any further purification. [Leu5]-enkephalin (YGGFL) was purchased from AnaSpec Inc. Aspartame ≥ 98%, propyl 4-hydroxybenzoate (paraben) ≥ 99%, and ≥98% dimethoxydimethylsilane were purchased from Tokyo Chemical Industry. 2-mercapto ethanol 99% was purchased from Aldrich. Analytical standards of Δ^9-tetrahydrocannibinol (THC) and cannabinol (CBN) were purchased from Cerilliant. HPLC LC-MS grade methanol, water, concentrated hydrochloric, and high purity formic acid were purchased form VWR. A 1' x 1' x 1 mm thick copper shim was purchased from McMaster Carr. X, y, z adjustable stage components were purchased from ThorLabs. Thermo-Scientific Velos Pro mass spectrometer equipped with a dual pressure linear ion trap with a high-pressure ion trap that allows for greater fragmentation efficiency, coupled to low-pressure ion trap for high resolution. Thermo Qual browser software and Genesis algorithm was used for data analysis.

Methods

Omniphobic surfaces were made by first cutting the desired dimensions of the copper (23 mm x 10 mm with a 30° tip) and then sonicating for 10 minutes in an acetone/methanol/isopropyl mixture and then triple rinsed with deionized water. The surface was placed into a 2.0M HCL solution for 10 minutes to remove any residual copper oxide. Surface was then rinsed three times with deionized water and dried with nitrogen. The surface is placed in a 0.25 troy once/1 quart solution of gold solution purchased from Technic Inc for 10 minutes supported via an electrode clip powered by a bipotentiostat model AFCBP1 purchased from Pine Instrument company. The instrument was set to galvanic

mode and a negative bias of 10 mA was used at 100 mV, which gave a -2.18 potential sweep. After the gold was successfully electroplated on the copper surface, the surface was rinsed with deionized water and placed in a solution of 3:1 sulfuric acid: hydrogen peroxide, pirana etch for 10 minutes to rid the surface of any hydrocarbons. The surface was triple rinsed with deionized water and submerged in a 10 mM solution of 2-mercapto ethanol in 100% ethanol with a stir bar for 24 hrs. This creates the strong gold-thiol bond and the procedure was adapted form Love et al. 2005[101], where the bond is typically formed in less than 10 minutes. Due to the minor surface deformities that are inherent from the manufacturing process, the surface was allowed to incubate overnight in order to form a closer packed monolayer. The omniphobic surface coating was formed by taking the 2-mercapto ethanol functionalized surface and placing it in a solution of 10% (wt) dimethoxydimethylsilane, 1% (wt) sulfuric acid in isopropyl alcohol. The original procedure for the instant omniphobic surface by Wang and McCarthy 2016 describes the coating being formed in minutes[106], whereas these surfaces were left in solution overnight, see Figure 17 below.

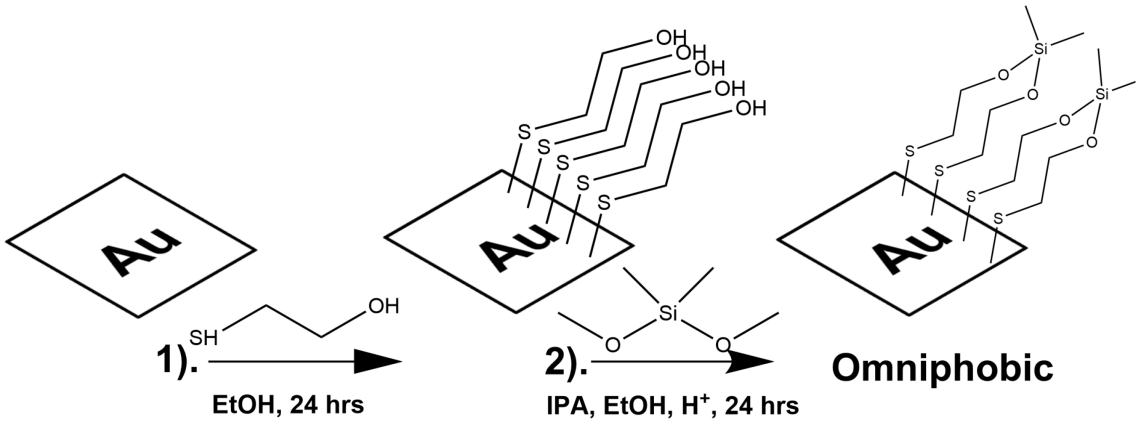

Figure 17. 1) Synthesis of the 2-mercapto ethanol-thiol coating, and 2) Formation of the omniphobic surface.

The crosslinking of the dimethoxydimethylsilane with the terminal hydroxy groups on 2-mercapto ethanol is initiated upon drying, so the surface was slowly removed from the solution over the course of 10 minutes. After removal, the surface was then rinsed with 98% ethanol and dried with nitrogen.

The power supply that was delivered to the surface was created using a copper insulated cable and soldered to an alligator clip. The copper cable was directly plugged into the voltage output of the MS on ionization probe housing. The optimal distance of the tip was oriented 3.17 mm away from the inlet of the mass spectrometer for optimal signal intensity.

Initial experiments used MS/MS via collision induced dissociation with a normalized collision energy of 35%. Using CID the transition of the protonated molecule to the most abundant fragment ion was monitored. Using these parameters, later experiments were conducted via selected reaction monitoring (SRM) where the mass spectrometer was only scanning the *m/z* window containing the most abundant product ion.

Calibration curves were created using the ratio of the most abundant product ion peak area collected with SRM, to the internal standard, if there was one. If there was no internal standard, then direct quantitation was performed using SRM for the peak area of the most abundant product ion. The peak areas were obtained using Qual Browser software and fitted using the Genesis algorithm. An n = 3 was performed with each concentration of analyte and the peak areas were averaged for each concentration and the standard deviations were also calculated for each of the averaged concentrations. The data was

normalized because the two calibration curves generated using metal spray and HESI were not scaled appropriately in relation to each other, making it hard to evaluate the error bars between the two methods. Normalizing the data for the ratios of analyte to internal standard was done by taking the ratio for each concentration and dividing that value by the maximum value (that usually corresponded to 25 μM solution) and multiplying that number by 100. The error bars were normalized by calculating the relative standard deviation, dividing by 100, and multiplying that value by the ratio of analyte to internal standard, divided by the maximum value, all multiplied by 100. All limits of detection and quantitation were calculated before the data was normalized.

Prior to each experiment the omniphobic surface was rinsed with methanol and dried with a cotton swab. Once the instrument was scanning, 0.5 μL of the analyte in 9:1 methanol:water (V:V) with 0.1% formic acid, is applied to the back channel as far away from the inlet of the and drug forward as the micro pipette is expelled. We understand that 9:1 (V:V) methanol:water with 0.1% formic acid is not a typical solvent system, and to prove that there was no noticeable difference we appended calibration curves of 50:50 (V:V) methanol:water with 0.1% formic acid. Solutions were run in order of 0, 1.5625, 3.125, 6.25, 12.5 and 25 μM, and all solutions were made with by serial dilutions.

Results and Discussion

Contact angle measurements were performed on a gold electroplated, 2-mercaptoethanol, and omniphobic surface during each stage of the synthesis process to confirm the desired chemistry was performed. Measurements were

taken using 18 µL of 1:1 (V:V) MeOH:H_2O solution. These measurements were taken with an n=11. Prior to each measurement, the surface was cleaned with a cotton swab to remove any residue. Figure 18 shows the resulting contact angles and the error bars represent the 95% confidence interval.

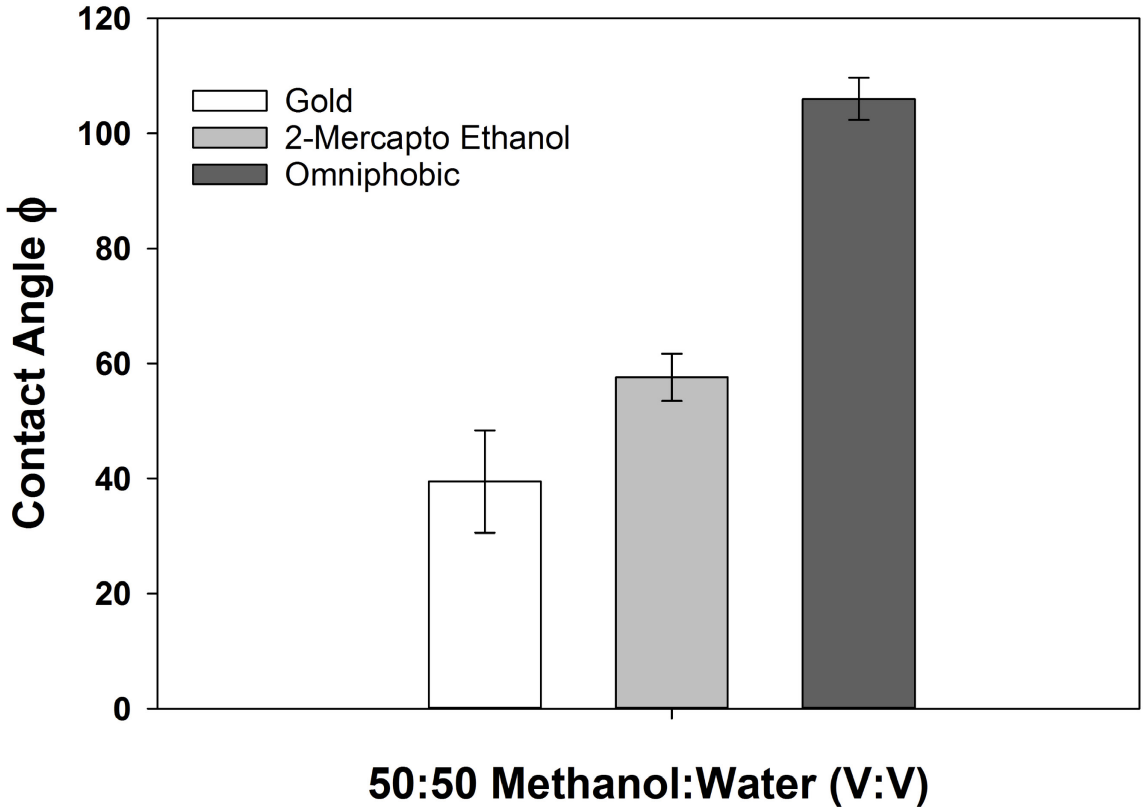

Figure 18. Contact angle measurements were performed on a copper-gold plated surface, 2-mercapto ethanol-gold surface, and the omniphobic surface with an n=11 and their respective 95% confidence intervals using 18 µL of 50:50 methanol:water (V:V).

As can be seen from Figure 18, each stage of the surface preparation results in an increase in the contact angle ensuring that the surface is becoming more repellant to aqueous solutions.

In order to validate the results in Figure 18, the same measurements were performed on the same surfaces using mineral oil as shown below in Figure 19.

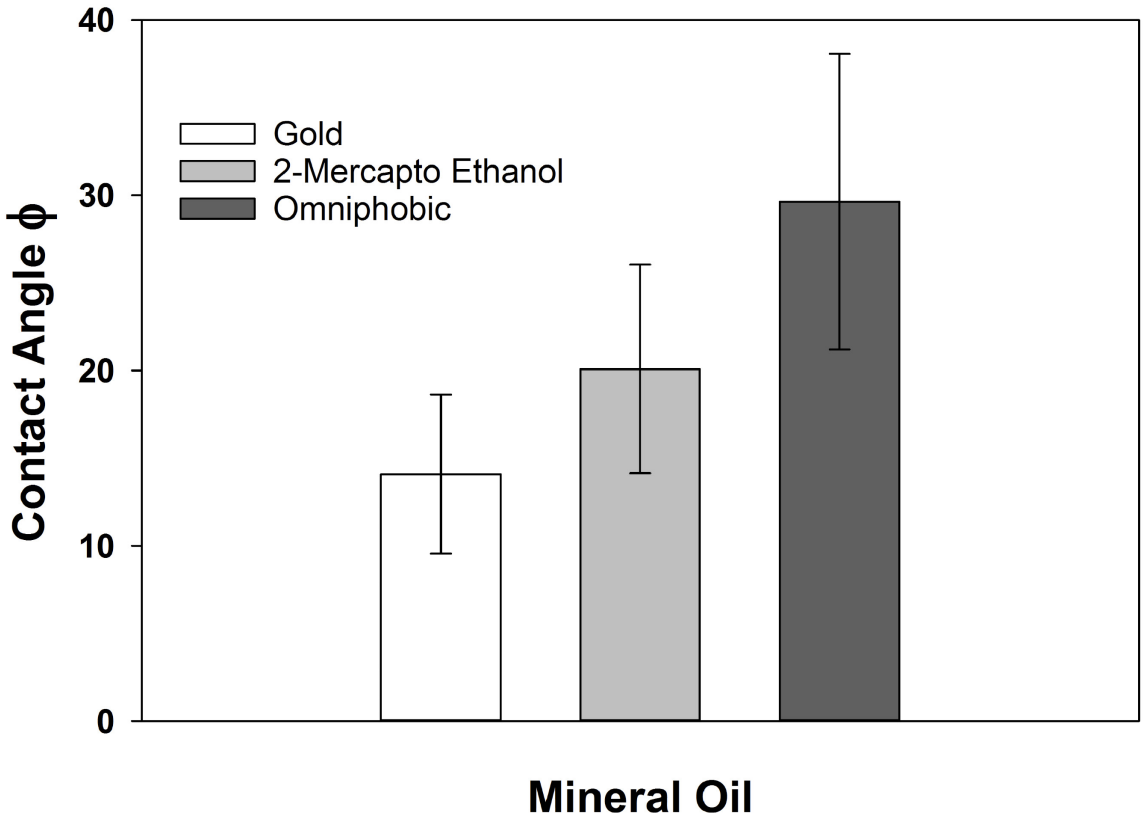

Figure 19. Contact angle measurements were performed on a copper-gold plated surface, 2-mecapto ethanol surface, and the omniphobic surface with an n=11 and their respective 95% confidence intervals using 18 μL of mineral oil.

As observed from Figure 19, the increased contact angles for each surface throughout the synthesis, shows greater repellency to non-polar solutions. The contact angles were much lower when mineral oil was applied to the surface rather than 1:1 (V:V) MeOH:H_2O. This is due to the high viscosity of mineral oil and its wetting ability on surfaces, because it has lower surface tension than water and lacks the intermolecular forces to hydrogen bond.[107]

The sensitivity, LOD and LOQ of a commercial HESI probe using flow injection analysis (FIA) were compared to omniphobic surfaces using metal spray, to compare the performance of the two methods.

In Figure 20 below, selective reaction monitoring was used to monitor serial dilutions of the doubly protonated peptide Bradykinin $[M+2H]^{2+}$ = *m/z* 531, spiked with the peptide substance P as an internal standard. In this SRM experiment the transition of *m/z* 531 to *m/z* 522.75 and the doubly protonated substance P $[M+2H]^{2+}$ = *m/z* 674 to 665 were monitored.

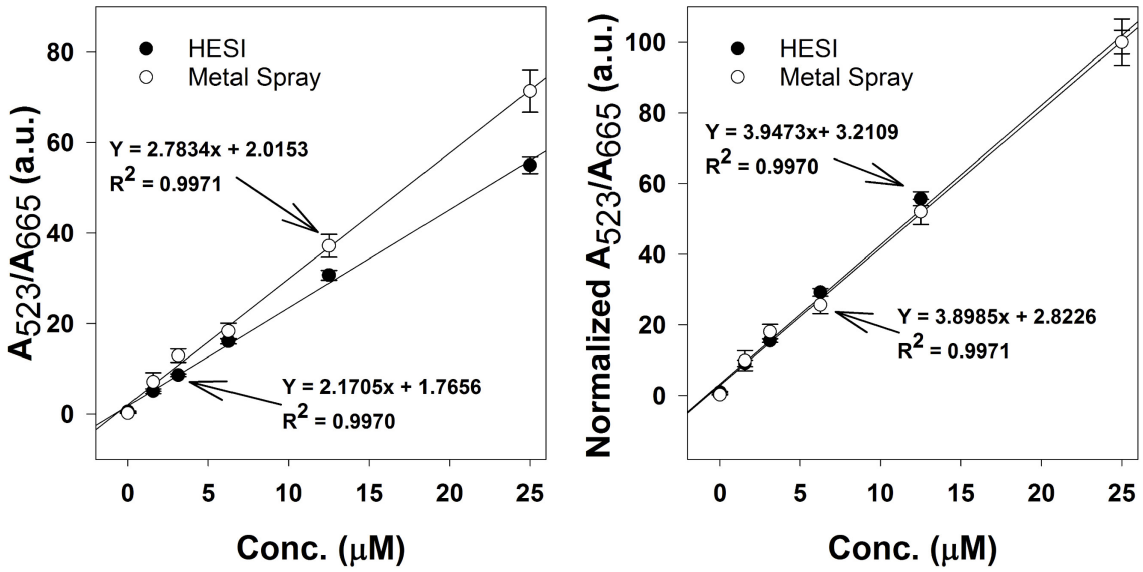

Figure 20. Raw data (left) and normalized data (right) using SRM of Bradykinin with substance P as an IS using HESI and metal spray.

The limits of detection and quantitation were 22.4 ng/mL and 74.5 ng/mL respectively, using metal spray. In Figure 20, the SRM instrumental method was applied to bradykinin and substance P using a constant flow from the HPLC pump with a 9:1 methanol:water mixture with 0.1% formic acid using a HESI

probe. The LOD and LOQ for the HESI experiment were 166 ng/mL and 554 ng/mL respectively. Comparing the slopes of the two calibration curves on the left in Figure 20, metal spray is 1.28 times more sensitive to doubly charged peptides and offers lower LOD and LOQ when compared to HESI analysis. This was the first-time using metal spay ionization that lower LOD/LOQ and higher sensitivity was observed using the doubly charged bradykinin, compared to HESI. This experiment also showed that metal spray can be used quantify doubly charged peptides in a LOD that would be comparable to concentrations found in blood plasma, urine, saliva, or sweat.[62]

In Figure 21 below, a similar experiment was performed on Leucine-enkephalin (YGGFL) with the difference being that the most abundant peak seen with YGGFL is the singly charged peptide $[M+H]^+$ *m/z* = 556.

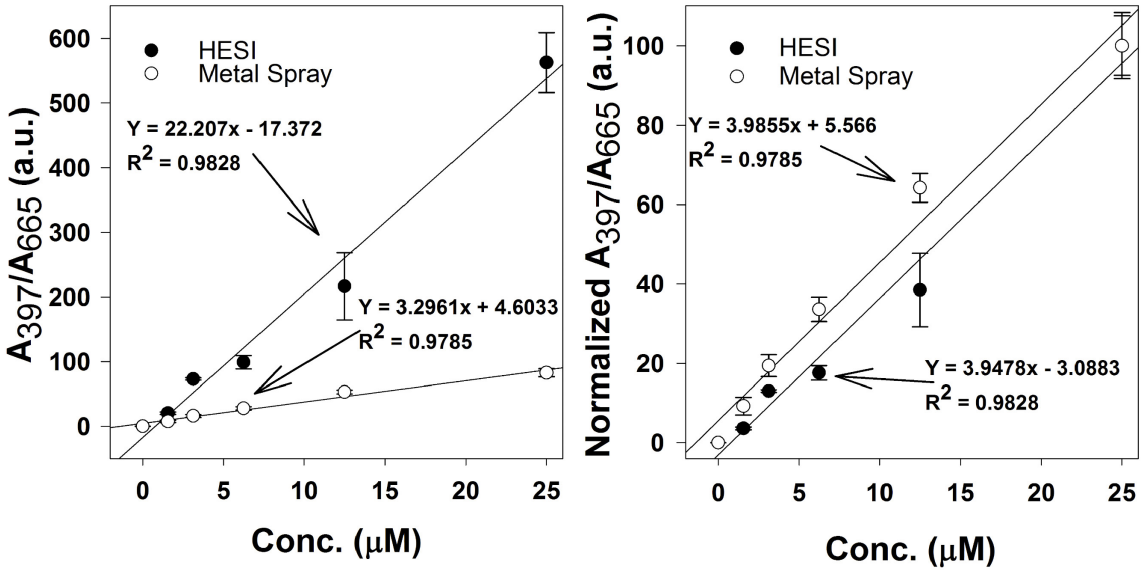

Figure 21. Raw data (left) and normalized data (right) using SRM of YGGFL with substance P as an IS using HESI and metal spray.

Figure 21 shows the calibration curve of YGGFL with substance P as I.S. The LOD and LOQ for Figure 21 using metal spray is 1.82 ng/mL and 6.06 ng/mL and 0.26 ng/mL and 0.87 ng/mL using HESI, respectively. As you can see in Figure 21, the slope of the raw data (left) calibration curve using metal spray with YGGFL displays a higher sensitivity compared to the raw data calibration curve using Bradykinin in Figure 20. However, we cannot conclusively say at this time if it is because metal spray is more sensitive to singly charged species.

After it was determined that peptides could be successfully detected and quantified from an omniphobic surface, the focus then turned to lipids.

In past experiments using superhydrophobic surfaces, reliable calibration curves for the lipids DOPC or POCP could not be obtained. This might be due to how the data was collected using direct quantitation of the analytes in full scan mode instead of using SRM. Here in Figure 22 below, the transition of *m/z* 786 to 496 for DOPC was monitored, while using POPC as I.S.

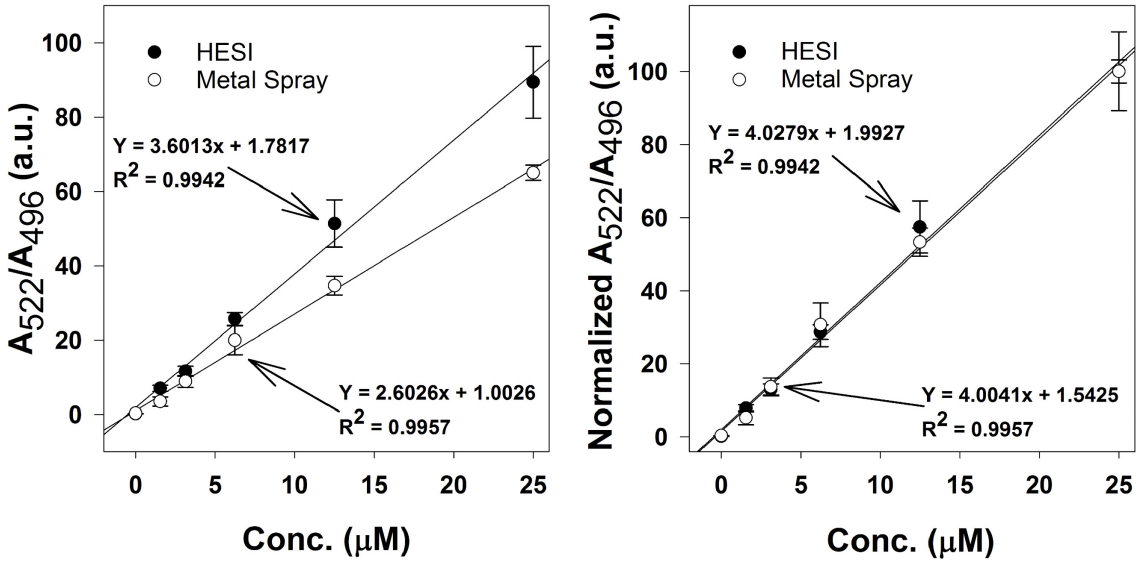

Figure 22. Raw data (left) and normalized data (right) using SRM of DOPC with POPC as an IS using HESI and metal spray.

As seen in Figure 22, metal spray resulted in LOD/LOQ of 2.41/8.04 ng/mL respectively, while HESI resulted in a LOD/LOQ of 5.05/16.9 ng/mL respectively. Looking at the slopes of the two curves using the raw data (left) in Figure 22, HESI was 1.38 times more sensitive to the nonpolar analytes, although the LOD/LOQ for metal spray was lower.

Calibration curves were constructed for the small polar molecule caffeine in Figure 23 below, which monitored the transition from *m/z* 195 to 138, corresponding to the loss of C_2H_3NO via homolytic cleavage.

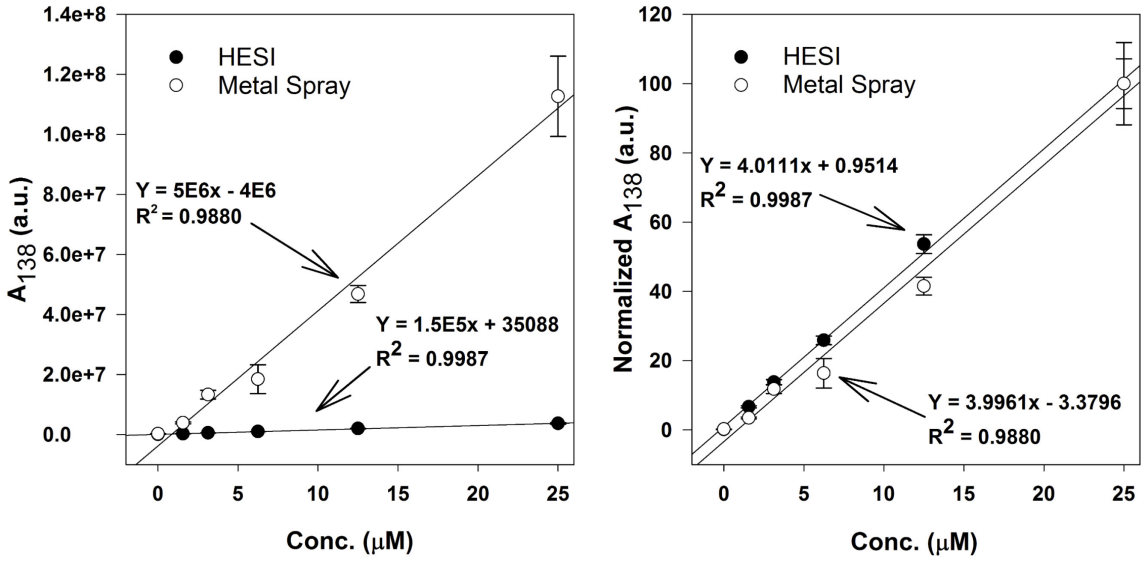

Figure 23. Raw data (left) and normalized data (right) using SRM of caffeine and with no IS using HESI and metal spray.

The calibration curves produced in Figure 23 with metal spray gives a LOD/LOQ 4.26/14.2 ng/mL. The calibration curves in Figure 23 produced with HESI gives a LOD/LOQ of 2.25/7.49 ng/mL respectively. Before normalizing the data, the slope of the metal spray calibration curve in Figure 23 was 33 times greater than that of HESI, (see Table 2 at the end of this section).

To further investigate the practicality of using metal spray over HESI, it would be interesting to look at drugs in concentrations that could be found in blood plasma or urine. Here we investigate the cannabinoids produced in *cannabis* and Δ^9-tetrahydrocannabinol (THC) and cannabinol (CBN).[108] It was also coincidence that THC and CBN are also small nonpolar molecules, whereas the majority of analytes investigated in these experiments are polar in nature.

SRM was used to observe the transition from *m/z* 315 to 193 for THC and *m/z* 311 to 241 for CBN, see Figure 24 below. The LOD/LOQ for THC obtained

using metal spray was 30.5/102 ng/mL respectively and the LOD/LOQ calculated using HESI was 4.29/14.3 ng/mL respectively.

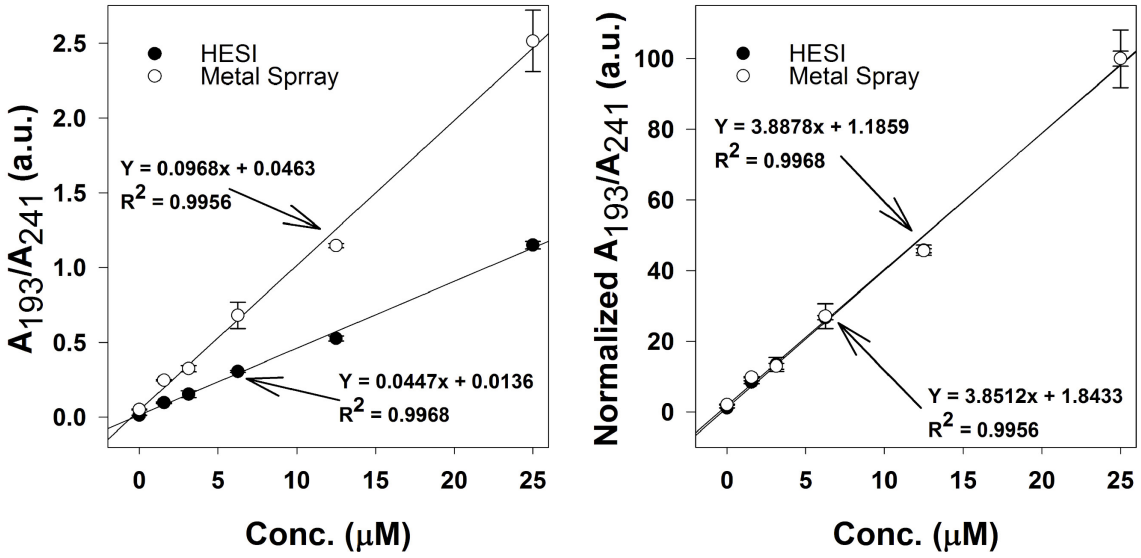

Figure 24. Raw data (left) and normalized data (right) using SRM of THC with CBN as an IS using HESI and metal spray.

The advised cut off detection limit for monitoring the presence of cannabinoids recommended by the Substance Abuse and Mental Health Services Administration (SAMHA) was found to be 50 ng/mL for habitual users, and sometimes can be detected up to 3 months after use.[109,110] Referring to the raw data on the left in Figure 24, it is interesting to note that metal spray had approximately twice the sensitivity compared to HESI, before normalizing the data. Both metal spray and HESI have detection limits well below the SAMHA recommendation, making metal spray an adoptable technique for quantifying drugs and their metabolites.

Aspartame is an artificial sweetener that is 180-200 times sweeter than sucrose, and often used as a sugar substitute in soft drinks.[111] The amount of aspartame in soft drinks is typically around two hundred milligrams[112], this lends metal spray as an alternative tool for fast quality control in soft drink formulation. Calibration curves were created with these two ionization sources, to see if their limits of detection/quantitation were comparable, data shown below in Figure 25.

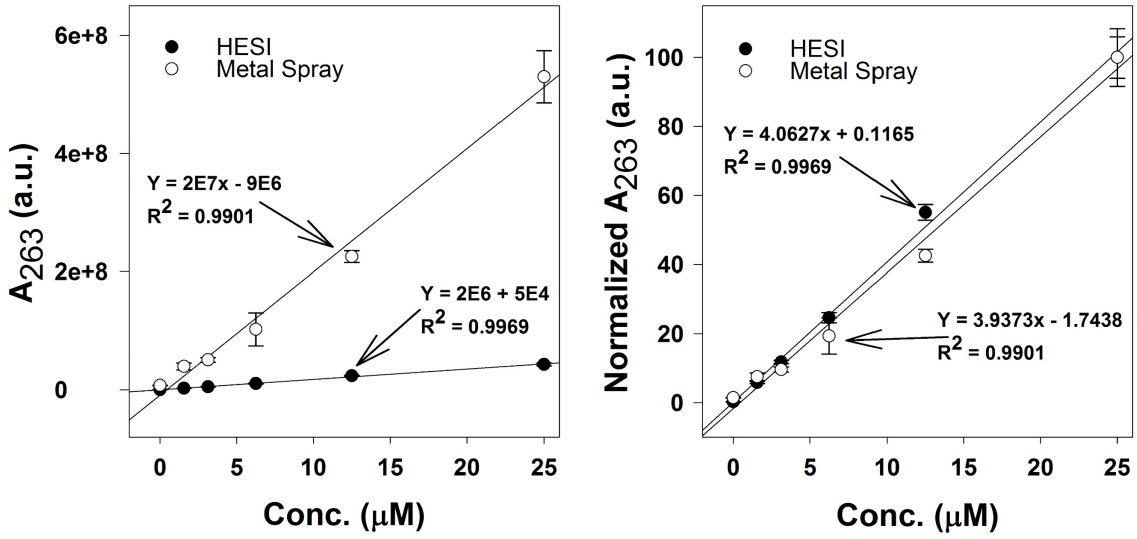

Figure 25. Raw data (left) and normalized data (right) using SRM of aspartame with no IS using HESI and metal spray.

In Figure 25 above, the R^2 values for both calibration curves were > 0.99, which was exemplary. The LOD/LOQ for metal spray was 14.8/49.3 ng/mL respectively, and the LOD/LOQ obtained using HESI was 3.57/11.9 ng/mL. These LOD/LOQ found with metal spray are well below what would be found being used as a food or soft drink additive, thus illustrating the utility of metal spray ionization. The sensitivity as indicated using the raw data (left) in Figure

25, shows metal spray was an order of magnitude greater than HESI. While HESI displayed lower LOD and LOQ compared to metal spray, sampling with metal spray might be easier, depending on the nature of the experiment.

4-Hydroxy-propylbenzoate also known as (paraben) is a preservative used in in cosmetics and food products, that prevents the growth of microorganisms.[113,114] Typically used at low concentrations in these products, it would be interesting to see what LOD/LOQ could be obtained using metal spray, and see if these values would mimic the concentrations found in these products, Figure 26 below.

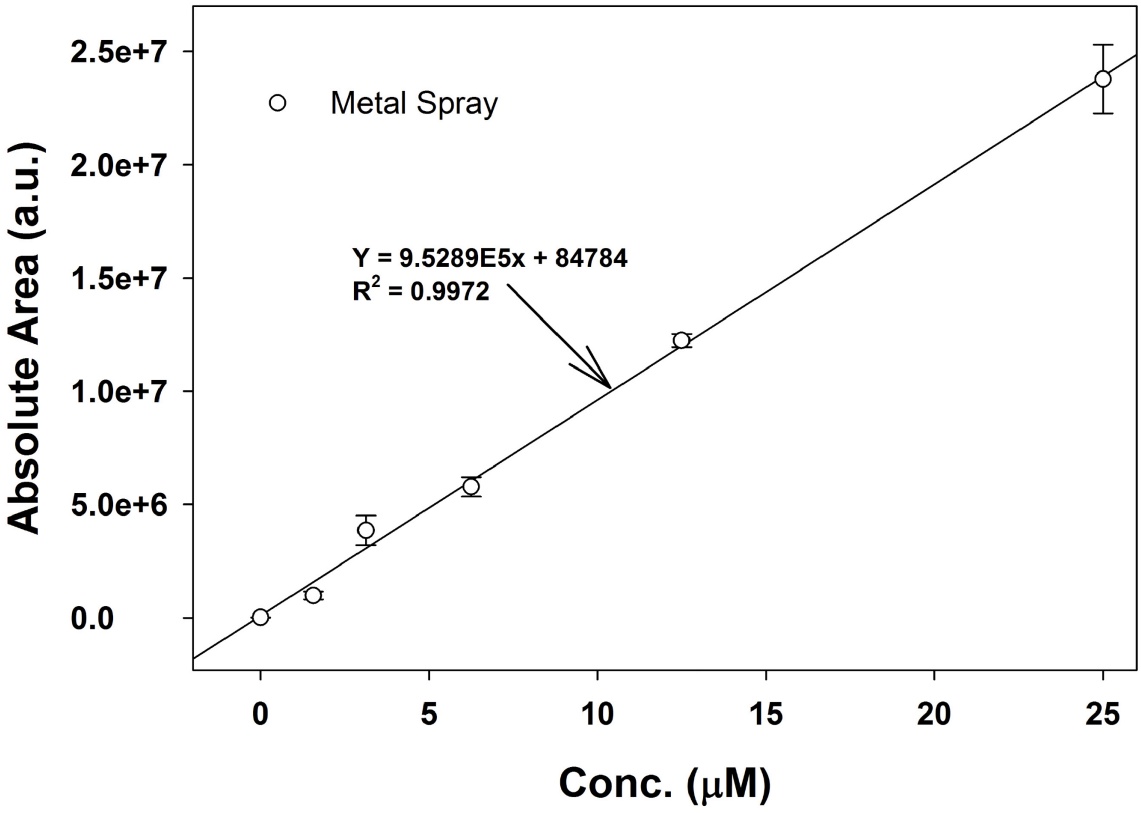

Figure 26. Paraben *m/z* 181 using SRM with no IS.

Figure 26 above, produced some the best limits of detection and quantitation that have been seen so far using metal spray (0.79/2.33 ng/mL respectively), suggesting that propyl 4-hydroxy benzoate ionizes very efficiently with metal spray. This is probably due to the proximal distance from the tip of the omniphobic surface to the inlet of the MS, as it is closer than a corona discharge needle, thus creating a stronger electric field. It is interesting to note, that there is no calibration curve for paraben with HESI. Several attempts were made, to produce a reliable calibration curve with HESI, but for whatever reason, this data could not be obtained. There was no attempt to analyze the sample in negative ion mode, so we cannot say for certain at this time, if it is due to poor ionization efficiency, or if the ions in metal spray are a quasi-combination of ESI/APCI in how the ions are produced.

To further demonstrate the utility of metal spray, a homeopathic pesticide was investigated. The ketone monoterpene pulegone, which is a naturally occurring pesticide from the mint family, is often used for hobby-gardening.[115] If metal spray ionization offers low LOD and LOQ comparable to HESI, then metal spray would lend itself to testing homegrown plants post pesticide application, to see if the concentrations were deemed suitable for human consumption, see Figure 27 below.

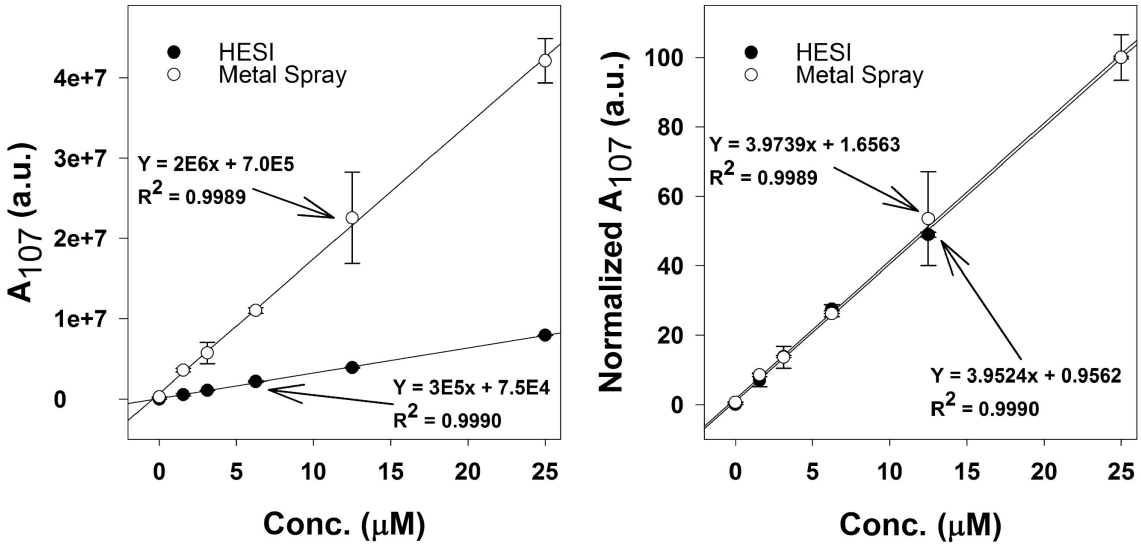

Figure 27. Raw data (left) and normalized data (right) using SRM of Pulegone with no IS using HESI and metal spray.

This data in Figure 27 above had to be normalized because the raw sensitivity data for metal spray (left) was 6.7 times higher than HESI. However, HESI gives lower LOD/LOQ, which was expected, as there is less sampling variability between each measurement using the LC autosampler. In retrospect, manual FIA should have been used, so that human induced error was similar. The LOD/LOQ using metal spray was 5.79/19.3 ng/mL respectively, while the LOD/LOQ calculated with HESI was 1.26/4.20 ng/mL in that respective order. In one *in vivo* study on humans where one individual was fatally poisoned, 18 ng/mL of pulegone was found in blood serum analyzed 26 hours post-mortem.[116,117] The values calculated for metal spray and HESI were well below the concentrations detected in the poisoned individual, therefore metal spray would be a suitable alternative for post-harvest pesticide quantitation. These LOD/LOQ found with metal spray ionization would be representative of the

natural concentrations found in post application of this pesticide in hobby gardens. The sampling for such applications might be as easy as swiping the metal surface across the leaf or stem of a plant, or vice versa.

Table 2. Summary of LOD/LOQ, and raw sensitivity data for metal spray and HESI.

Analyte	Metal Spray LOD/LOQ (ng/mL)	Metal Spray Sensitivity	HESI LOD/LOQ (ng/mL)	HESI Sensitivity
Bradykinin*	22.3 / 74.5	2.78	116 / 554	2.17
YGGFL*	1.82 / 6.06	3.29	0.26 / 0.87	22.2
Lipids*	2.41 / 8.04	2.60	5.50 / 16.9	3.60
Caffeine	4.26 / 14.2	$5x10^6$	2.25 / 7.49	$1x10^5$
THC*	30.5 / 102	0.097	4.29 / 14.3	0.045
Aspartame	14.8 / 49.3	$2x10^7$	3.57 / 11.9	$2x10^6$
Paraben	0.79 / 2.33	$1x10^6$	NA	NA
Pulegone	5.79 / 19.3	$2x10^6$	1.26/4.20	$3x10^5$

*Indicates an internal standard was used

Conclusion

Overall, metal spray proved to be an exemplary tool for quantitation as far as ambient ionization techniques. Quantitation can be performed in seconds, with high sampling throughput, and is very easy to use. In some cases, metal spray offered lower LOD/LOQ compared to HESI, (see Table 2 above). Surfaces are reusable, do not require wicking, have a fixed geometry, and can be functionalized and tuned to increase sensitivity for a broad range of analytes. For these reasons, metal spray ionization has many advantages over paper spray.

Future directions for this project would include quantification of analytes in complex matrices such as hair, urine, sweat, blood and soil without any pre-dilution, and compared the sensitivity, LOD/LOQ to that of ESI or GC-MS.

5. ATMOSPHERIC SOLIDS ANALYSIS PROBE FOR DIFFERENTIATION OF ISOMASS DRUG MIXTURES USING ONLINE DERIVATIZATION

Differentiation of Δ^9-tetrahydrocannabinol from cannabidiol presents a significant challenge in the forensic community because these molecules are constitutional isomers. The net result is that, high mass accuracy, high resolving power instruments cannot contribute to the separation of these two molecules. Though GC-MS and LC-MS are the gold standard for accomplishing this differentiation, both techniques suffer from a temporal bottleneck. Typical analysis time for GC and LC is about 20 minutes, depending on the nature of the analyte under investigation. Because of the temporal restriction imposed by chromatographic separation, ambient ionization techniques have been under investigation. Rather than using these classical chromatographic techniques, we are utilizing an online, rapid derivatization technique capable of differentiating molecules with different numbers of exchangeable protons. The full scan mass spectra of CBD were distinct to that of THC so that this may provide a valuable route for differentiation.

Rather than using these classical chromatographic techniques, these experiments utilize an online, rapid derivatization technique capable of differentiating molecules with different number of exchangeable protons. To facilitate this, an atmospheric solids analysis probe (ASAP) is positioned between the ESI source and the APCI corona discharge needle. Solids or liquids of CBD and THC are placed on a closed capillary without any dilution or pretreatment, by placing the capillary into the solid sample or liquid solution. A stream of nitrogen

gas flows from the outlet of the ESI probe, which the sample is thermally desorbed from the surface using high temperatures, where the analytes subsequently become ionized before entering the inlet of the mass spectrometer. A derivatizing agent, *N,O*-Bis(trimethylsilyl)trifluoroacetamide (BSTFA) is diffused from the syringe through the ESI source as an aerosol along with the high temperature nitrogen gas, to allow the reaction between the derivatizing agent and the analytes, see Figure 28 below.

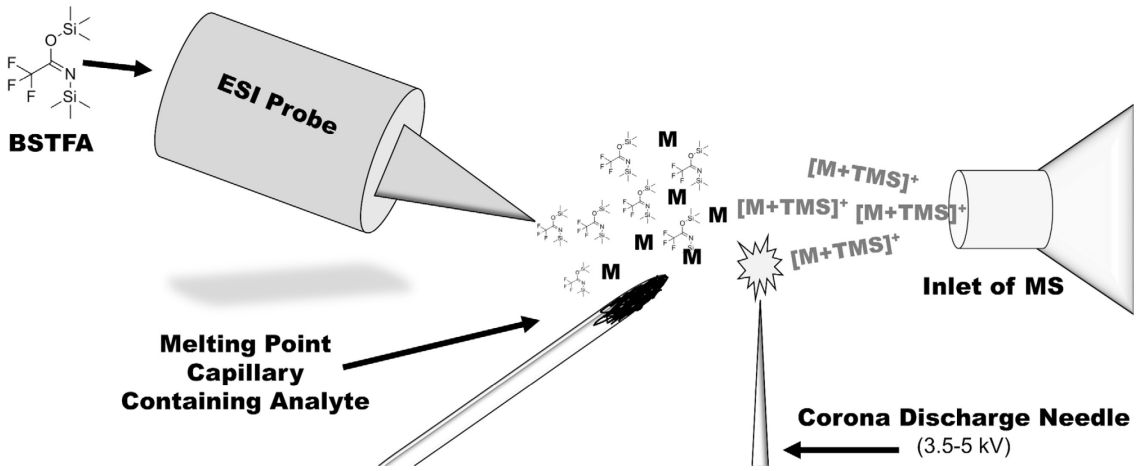

Figure 28. ASAP schematic using direct infusion of BSTFA for online derivatization.

These reactions are carried out under ambient conditions which are well suited to high throughput analyses and allow identification of target molecules in complex matrices on the order of seconds rather than several minutes needed for conventional chromatographic techniques. Additionally, ASAP provides soft ionization conditions which results in little to no fragmentation. This sampling

technique is also a way to bypass traditional chromatographic separation, as quantitation has been achieved with a variety of analytes, including: leanness-enhancing drugs found in the tissues of sheep[118],ergosterol inhibitors in fungal cells[119], flavonoid patterns from pollen[120], and saturated fractions of crude oil just to name a few.[121]

The nature of the differing structures of the molecules, cannabidiol (CBD) has two hydroxyl groups whereas THC has only one, shown in Figure 29 below.

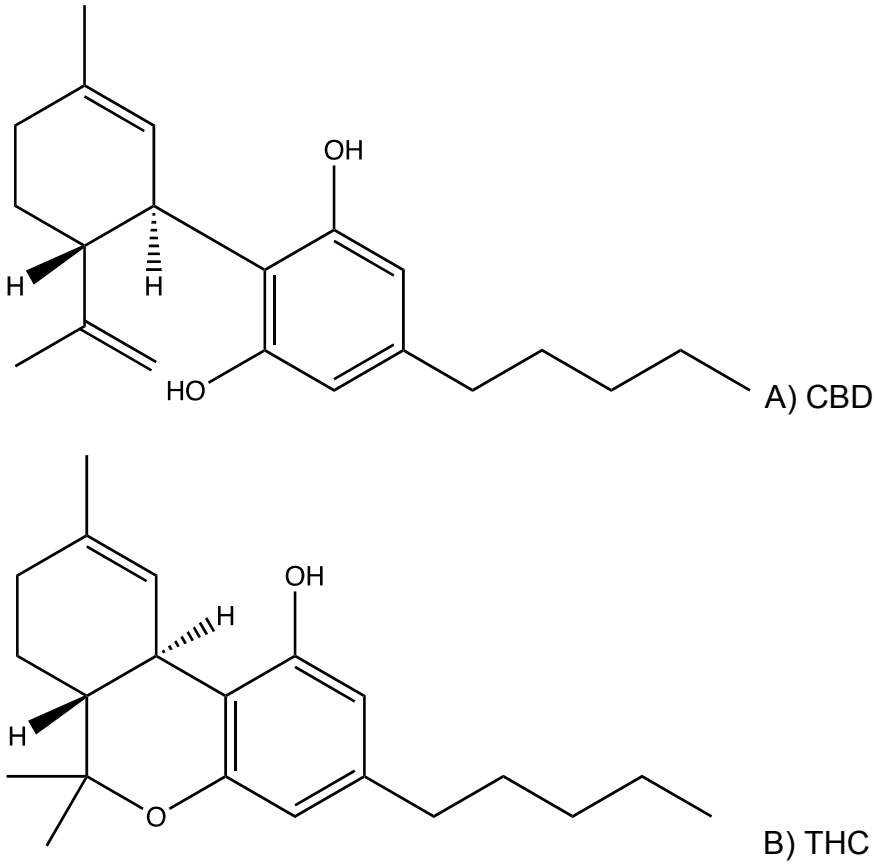

Figure 29. A) Molecular structure of CBD with two exchangeable hydroxy protons; B) Molecular structure of THC with one exchangeable hydroxyl proton.

In principle, this means that there are two potential exchangeable sites on CBD, compared to only one for THC. This will greatly simplify spectral interpretation because the presence of the CBD peak corresponding to $[M-H+2D]^+$, where D is the derivatization reagent chosen for the experiment.

To date others have investigated D_2O, BSTFA, and MSTFA. While all three reagents yield similar results in the ability to distinguish the constitutional isomers, BSTFA provides the greatest potential for differentiation because the reaction rate for derivatization is the highest, which was also reported by Leghissa in 2016 on multiple cannabinoids using GC-MS.[122]

Recent archeological studies on fossil pollen suggest that cannabis may have originated from the Tibetan plateau nearly 28 million years ago. Archeological studies examining the contents of a Caucasoid shaman in China and clay fragments/baskets in eastern Gravettian settlements, hypothesize humans have long used cannabis for centuries, between 27,000-29,000 years ago.[123,124] Humans have used specifically *cannabis sativa*, *cannabis indica*, *cannabis sativa L.*, and *cannabis ruderalis* for their robust properties in textiles, and their abundance of unique chemicals called cannabinoids.[125] These cannabinoids have been noted for a plethora of medicinal properties dating back nearly 5,000 years, some of which include antitumor potential, and has also been used for divination purposes.[126–128] Two of the major cannabinoids of marijuana are the main psychoactive component Δ^9-tetrahydrocannabinol (THC) and a non-psychoactive component, cannabidiol (CBD).

With recent legalization for medicinal and recreational use of cannabis in thirty-three states and the District of Columbia in the US, severe attention needs to be drawn to the area of quality control in order to protect the consumer.[129] This is particularly difficult, because there are no laws currently in place that unify the overall testing standards and quality parameters and requirements of cannabis from state to state.[130–135] With the recent introduction of the 2018 farm bill, which allows any state in the US to cultivate hemp for industrial purposes, quality of the cannabis and percent composition of THC and CBD is particularly important, especially in states that do not permit the use, be it medicinal or recreational.[136,137] The caveat being, that every state has a unique set of guidelines as far as what is being tested for, but the federal threshold percentage of THC (typically < 0.3%) content at which the level is too high, and deemed illegal. The reason for placing restrictions on the percentage of THC in hemp, is because many legislators fear that hemp cultivation will be garnered towards producing higher percentages of THC in order to skirt the laws in state states that do not permit the use of *cannabis sativa*, but allow the use of hemp.

The two compounds CBD and THC are structurally similar and share the same molecular mass. Despite their identical chemical formula ($C_{21}H_{30}O_2$) and similar structure, the GC retention times and electron ionization mass spectra of the two compounds are very distinct, so CBD and THC are easily differentiated using GC-MS. However, one downside to GC-MS is the relatively long analysis times of 20-30 minutes,[122,138] which can restrict the analysis throughput in crime labs.[139] Another flaw with using GC-MS is because the instrument uses high

temperatures to vaporize the analyte into the gas phase, carboxylated forms of THC and CBD are often not observed, so quantitation of total cannabinoid content is often inaccurate.[4–6] Liquid chromatography mass spectrometry (LC/MS) has classically been used to distinguish between the two compounds and their metabolites as well but suffers the same temporal drawback in terms of sample preparation and analysis time.

Ambient ionization techniques, which oftentimes bypass chromatographic separations, are therefore seen as an attractive alternative for fast drug identifications. Over the last several years, a number of ambient ionization and sampling techniques have emerged to facilitate rapid analyses with minimal or no sample preparation. In negative ion mode, the deprotonated forms of CBD and THC have distinct CID fragmentation patterns and can therefore by readily distinguished.[140–142] In positive mode, however, tandem mass spectra of the protonated forms of CBD and THC are indistinguishable.[143] Therefore these studies explore the possibility to quickly and easily differentiate CID of the two cannabinoids in positive ion mode.

Although the structures are very similar, the full and tandem mass spectra of CBD and THC are virtually indistinguishable in the protonated form, thus negating the ability to use standard tandem mass spectrometry to distinguish the two.[143,144] One potential route for rapid differentiation lies in derivatizing the molecules so that they can be distinguished. Cannabidiol has more exchangeable hydrogen atoms than tetrahydrocannabinol and using hydrogen/deuterium exchange (HDX), one can shift the isotope envelope of CBD

more so than THC. The difference in isotopic distributions for cannabidiol and tetrahydrocannabinol prepared with D_2O suggests that the known interconversion of cannabidiol and tetrahydrocannabinol is slow relative to the hydrogen/deuterium exchange process and therefore permits the use of HDX. Provided that the reaction kinetics hold for the interconversion process, it is also reasonable to assume the use of alternative derivatization agents in order to more fully distinguish between the two constitutional isomers, such as methylation, esterification or silylation agents.[133]

The use of derivatization methods for cannabinoids has been widely reported and is typically used to make metabolites of the drugs more volatile and therefore amenable to analysis by GC/MS, and consequently increase peak shape as well.[133]

Materials and Methods

Standards of THC and CBD were obtained from Cerilliant Corporation (Round Rock, TX) at 1 mg/mL in methanol. LC-MS grade methanol and water were obtained from VWR (Radnor, PA). BSTFA was obtained from Sigma Aldrich (St. Louis, MO) and used without further purification. The structures of CBD, THC, and their silylated analogs can be found in Figure 30 below.

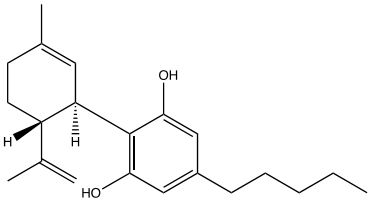

CBD – *m/z* 315

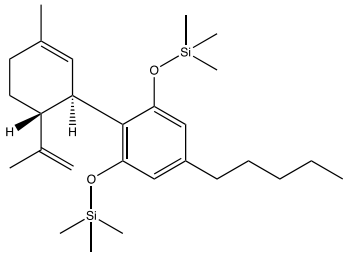

Doubly Silylated CBD - *m/z* 459

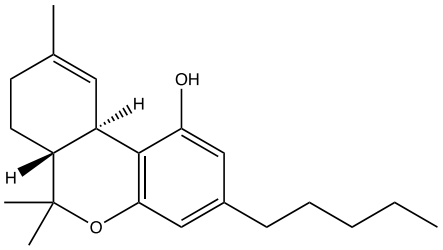

THC – *m/z* 315

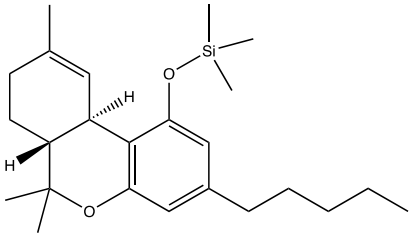

Singly Silylated THC – *m/z* 387

Figure 30. Structures and molecular weights of CBD (top) and THC (bottom) in their native states before and after silylation.

In Figure 30, by derivatizing with trimethylsilane, it is now apparent that the protonated molecule of CBD $[M+H]^+$ = *m/z* 315 has now shifted in mass by 114 mass units by exchanging the two phenolic hydrogens with two trimethylsilyl (TMS) groups, resulting in a peak $[M-H+2TMS]^+$ = *m/z* 459 for the doubly silylated CBD. After derivatizing THC we have now shifted the pronated mass [M-H+TMS] = *m/z* 387. Both structures of CBD and THC share the same chemical formula and $[M+H]^+$ = *m/z* 315. After derivatizing CBD and THC the *m/z* masses can now be differentiated by 72 mass units from the addition of an extra TMS group to CBD. It is important to mention however, that if only one TMS group is adducted onto the CBD molecule, then the two *m/z* cannot be differentiated.

GC-MS

A solution containing 25 μM each CBD and THC was prepared in MeOH. This solution was then analyzed using an Agilent 6890 GC coupled to a 5970 Mass Selective Detector (MSD). An HP-1 column was used with helium as the carrier gas at 1.0 mL/min. Vacuum compensation was used in constant flow mode. The GC/MS temperature program parameters are outlined in Table 3.

Table 3. Temperature program details used for GC-MS separation of CBD and THC.

Parameter	Value
Injector Mode	Split – 20:1 split ratio
Initial Temperature	50 °C – hold for 2 min
Ramp	20 °C/min
Final Temp	300 °C – hold for 5 min

Direct Infusion ESI

ESI studies were carried out on a Thermo LTQ Velos Pro (Thermo-Fisher Scientific, Waltham, MA) linear ion trap mass spectrometer with a heated ESI source. Solutions were made by diluting the standard solutions to 60 μM in 1:1 (V:V) H_2O:MeOH and acidified to 0.1% (V) with formic acid (Acros Organics, New Jersey). Samples were directly infused through the ESI source at 5μL/min with 4.5 kV spray voltage. MS/MS experiments were carried out with a normalized collision energy of 35%.

LC-MS

An Agilent 1100 Quaternary LC system was coupled to the aforementioned Thermo LTQ Velos Pro Mass spectrometer. Separation of the cannabinoid species was carried out in reverse phase using a C18 column. The mobile phase was ACN/H_2O with 0.1% (V) formic acid. The initial mobile phase composition was 80:20 H_2O:ACN and was ramped to 10:90 H_2O:ACN over 14 minutes with the mass spectrometer operating in full scan mode.

ASAP

A Thermo heated electrospray ionization probe (HESI) was used with a standard corona discharge needle, and the configuration used is described by McEwen in 2005 with its advent.[48] In this study, samples were analyzed directly from the closed end of a melting point capillary. Analytical standards of THC and CBD were sampled directly out of their vials at concentrations of 1 mg/mL in methanol, without any further pretreatment. After the melting point capillaries were dipped into their respective solutions, they were dried in atmospheric conditions for approximately 15 minutes prior to analysis.

Online Derivatization

Following analysis using standard ASAP, experiments were carried out using BSTFA as an online derivatization agent. This was accomplished by directly infusing BSTFA though the HESI probe at a rate of 5 µL/min. The remaining parameters, shown below in Table 4, were similar to those used for standard ASAP.

Table 4. Temperature program details used for ASAP separation of CBD and THC.

Parameter	Value
Vaporizer Temperature	250°C
Capillary Temperature	250 °C
Sheath Gas	15
Auxiliary Gas	5
Spray Voltage	3.8 kV
Syringe Flow Rate	5 µL/min.

Results and Discussion

Standard routes to differentiation between CBD and THC include GC-MS and LC-MS. GC-MS and LC-MS data can be seen in Figure 31 and Figure 32, respectively.

In the case of GC-MS, we can see that there is approximately 0.5 minutes separating the peak maxima for CBD from that of THC. In addition, the electron ionization mass spectra of CBD is distinct from that of THC. As seen in Figure 31, CBD gave rise to a single fragment ion at *m/z* 231 with limited intensity from the molecular ion. In contrast, the mass spectrum of THC had a significant intensity of the molecular ion along with several fragment ions that are unique for when compared to the CBD mass spectrum.

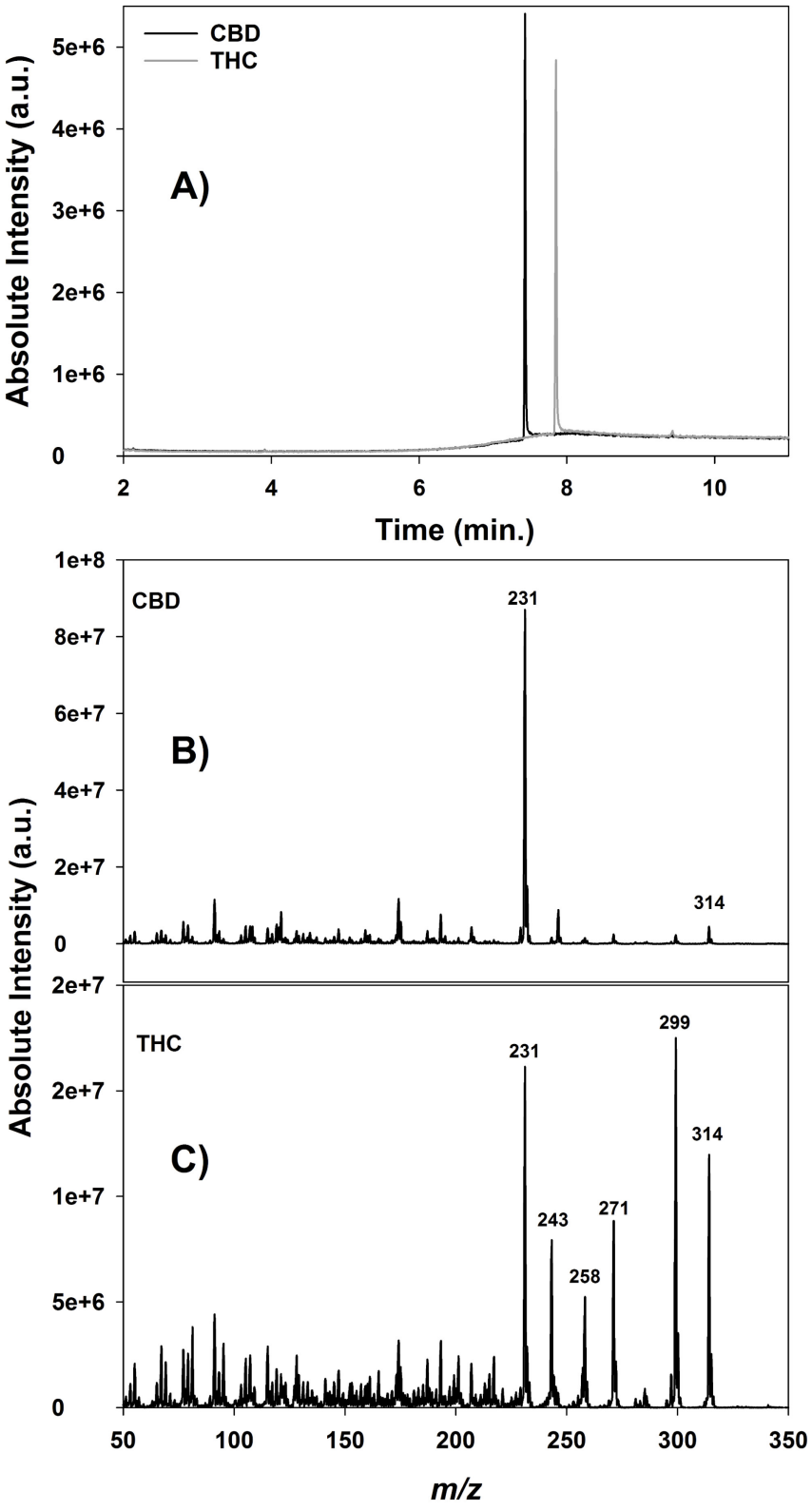

Figure 31. A) Gas chromatogram of CBD (black) vs THC (gray), the retention times are separated by approximately 0.5 minutes; B) Electron ionization mass spectra of CBD (top) vs THC (bottom) showing the fragment ions distinct to THC.

LC-MS separation of the constitutional isomers provided similar retention times to GC-MS, Figure 32 below.

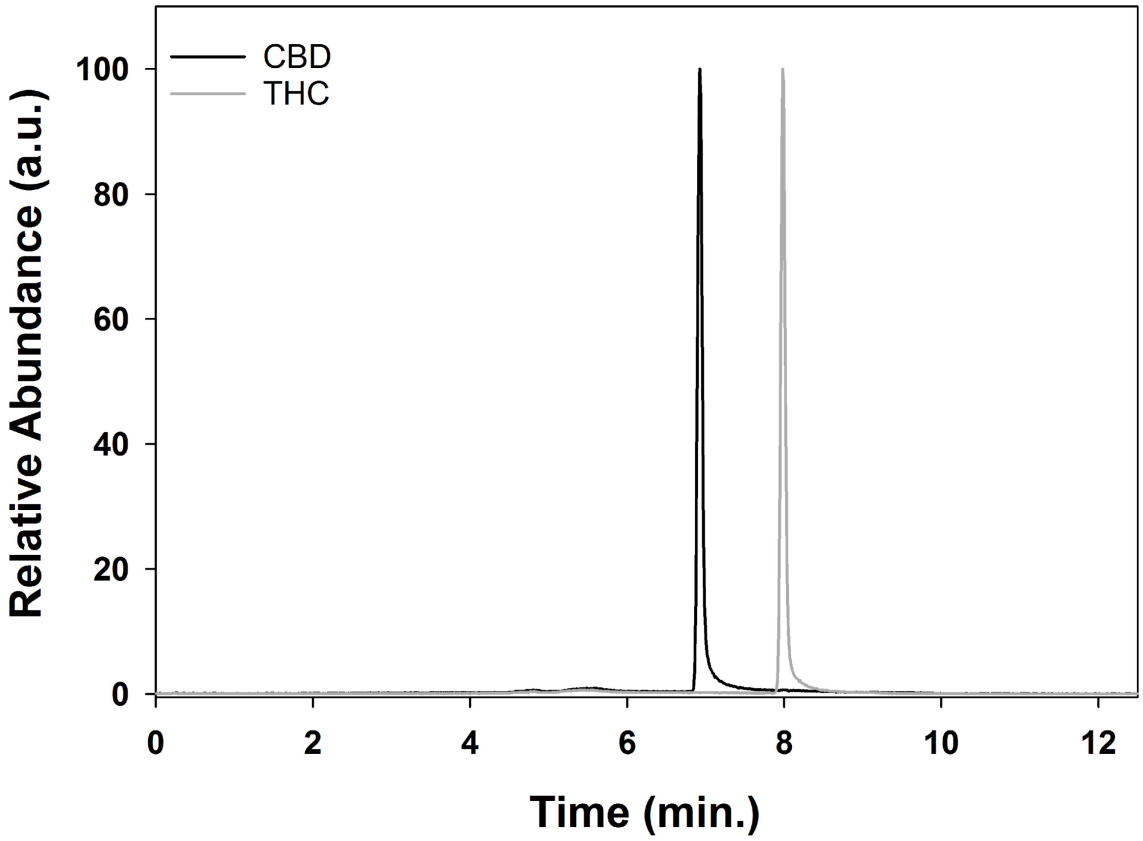

Figure 32. Reverse phase LC chromatographic separation of CBD (black) and THC (gray) in a 12.5-minute run.

Figure 32 shows reverse-phase liquid chromatography using gradient elution with water: acetonitrile + 0.1% formic acid as the mobile phase. By injecting a 5 µL sample of pure CBD, the analyte eluted off the column at 6.9 minutes while THC eluted at 8.1 minutes. Although this separation could be feasible in under 10 minutes, one must take into account that the

chromatography represented here is not indicative of a natural cannabis sample that would contain a plethora of other cannabinoids.

The major downside to these methodologies is that sample throughput is limited. Using LC or GC techniques CBD and THC can be separated, but these processes are time consuming, taking between 15-20 minutes for each sample. The increased caseload and decreased workforce experienced by forensic labs across the country have prompted the research into alternative tools that allow higher-throughput analyses.

Initial experiments focused on the ability to differentiate CBD from THC using tandem mass spectrometry. 25 μM solutions containing CBD and THC were prepared in 1:1 (V:V) MeOH:H_2O and acidified to 0.1% (V) with formic acid. These solutions were infused through a standard HESI probe at 5 μL/min. These solutions were infused through a standard HESI probe at 5 μL/min. The protonated molecule, *m/z* 315, was isolated with a 1.0 *m/z* window and fragmented with 30% normalized collision energy under conventional CID conditions.

When fragmented using standard, low-energy CID, the tandem mass spectra of CBD and THC, shown below in Figure 33, are visually indistinguishable. Due to the lack of unique transitions, the tandem mass spectrometry approach to differentiation was ineffective

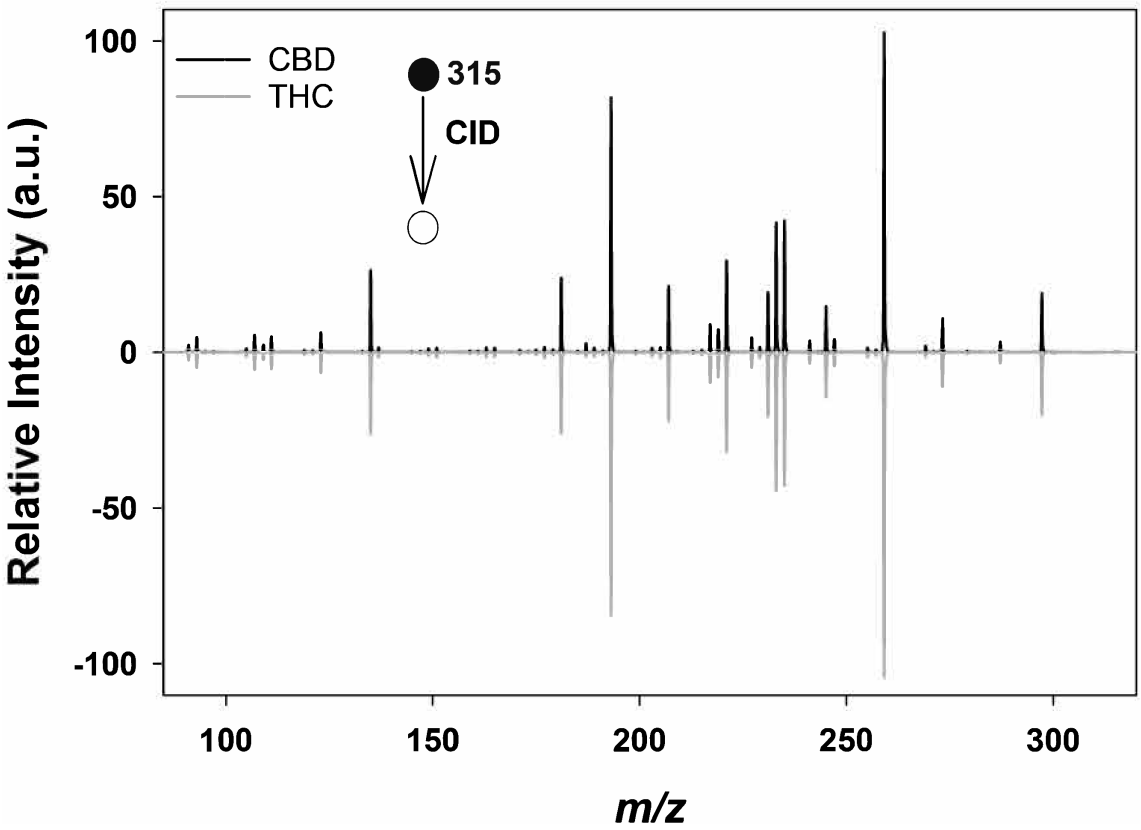

Figure 33. CID of CBD (black) and THC (gray) *m/z* 315 in positive ion mode.

An interesting observation was noted in the full scan mass spectra of CBD and THC. There appeared to be a discernable difference in the relative affinity for sodium adduction (data not shown, as evidenced by the ratio of *m/z* 337/315), but due to the variability of this ratio, this was not explored further.

Looking at the head-to-tail mass spectrum of the underivatized CBD and THC in Figure 33, it is apparent that the CID in positive ion mode produces mass spectra that look exactly identical. This makes MS/MS impossible to differentiate the two species in positive ion mode.

Ambient ionization such as ASAP, DART, and DESI are enticing alternatives to LC and GC techniques, due to their ease of sampling, increased

throughput, and lack of sample pretreatment. Using ASAP, initial experiments had to determine whether the cannabinoids could be desorbed from the melting point capillary surface and ionized sufficiently to produce sufficient mass spectral signal.

Closed end melting point capillaries were dipped into 1 mg/mL solutions of THC and CBD in MeOH. The solvent was subsequently evaporated under ambient conditions for approximately 5 minutes prior to analysis. Positive mode ASAP mass spectra, shown in Figure 34, shows that both CBD (top) and THC (bottom) give rise to the protonated molecule, $[M+H]^+$, at *m/z* 315.

Looking at Figure 34, it is apparent that the base peak in each spectrum is *m/z* 315, corresponding to both CBD and THC, and on the basis of full scan mass spectra, that differentiating the two species is impossible without the use of a derivatizing agent

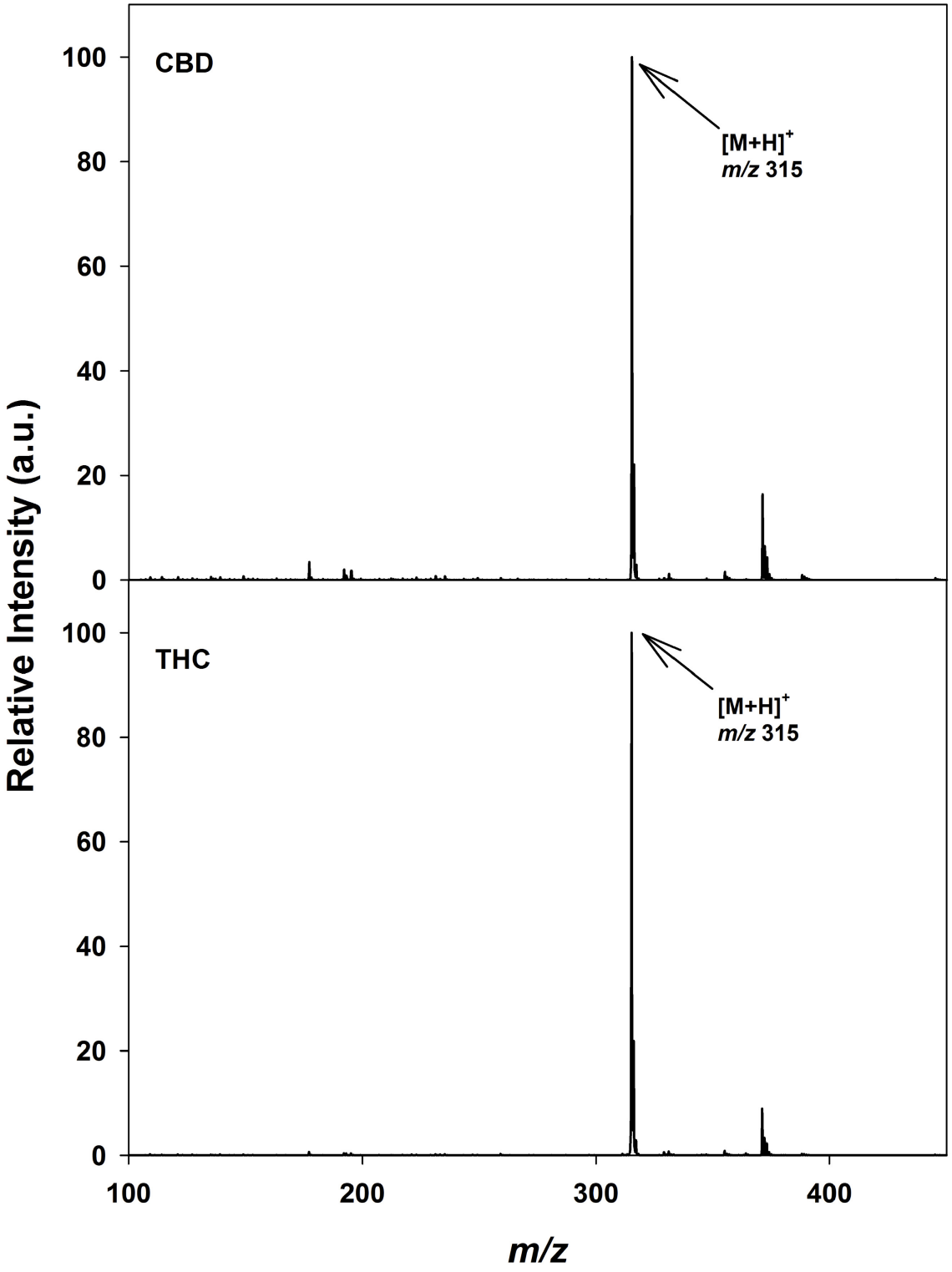

Figure 34. ASAP full scan mass spectra of CBD (top) and THC (bottom), both spectra show a dominant peak at *m/z* 315 from the protonated molecule.

After demonstrating sufficient desorption of THC and CBD to generate protonated molecules, online derivatization was carried out using BSTFA. This was accomplished by directly infusing a solution of BSTFA through the HESI source at 3 µL/min while sampling from the closed end of a melting point capillary as described earlier. By using the derivatizing agent, BSTFA, a portion of the exchangeable hydroxy protons will be displaced by the trimethylsilyl group, adding a 72-unit mass shift for every proton that is exchanged in the gas phase. The resulting spectra, shown below in Figure 35, demonstrate the silylated species of THC and CBD, respectively. Both analytes still showed peaks at *m/z* 315 resulting from the protonated molecule, suggesting that either the reaction is not 100% efficient, or there is not enough BSTFA present to fully react with the cannabinoid molecules present.

The base peak for both molecules occurred at *m/z* 387 from the addition of one TMS group replacing a hydroxyl hydrogen in both molecules, with as spectral artifact at *m/z* 371. Because THC contains only one exchangeable site, the reaction is limited to producing $[M+TMS]^+$. Interestingly, the base peak for CBD is also observed at *m/z* 387 with the exchange of a single hydroxyl group

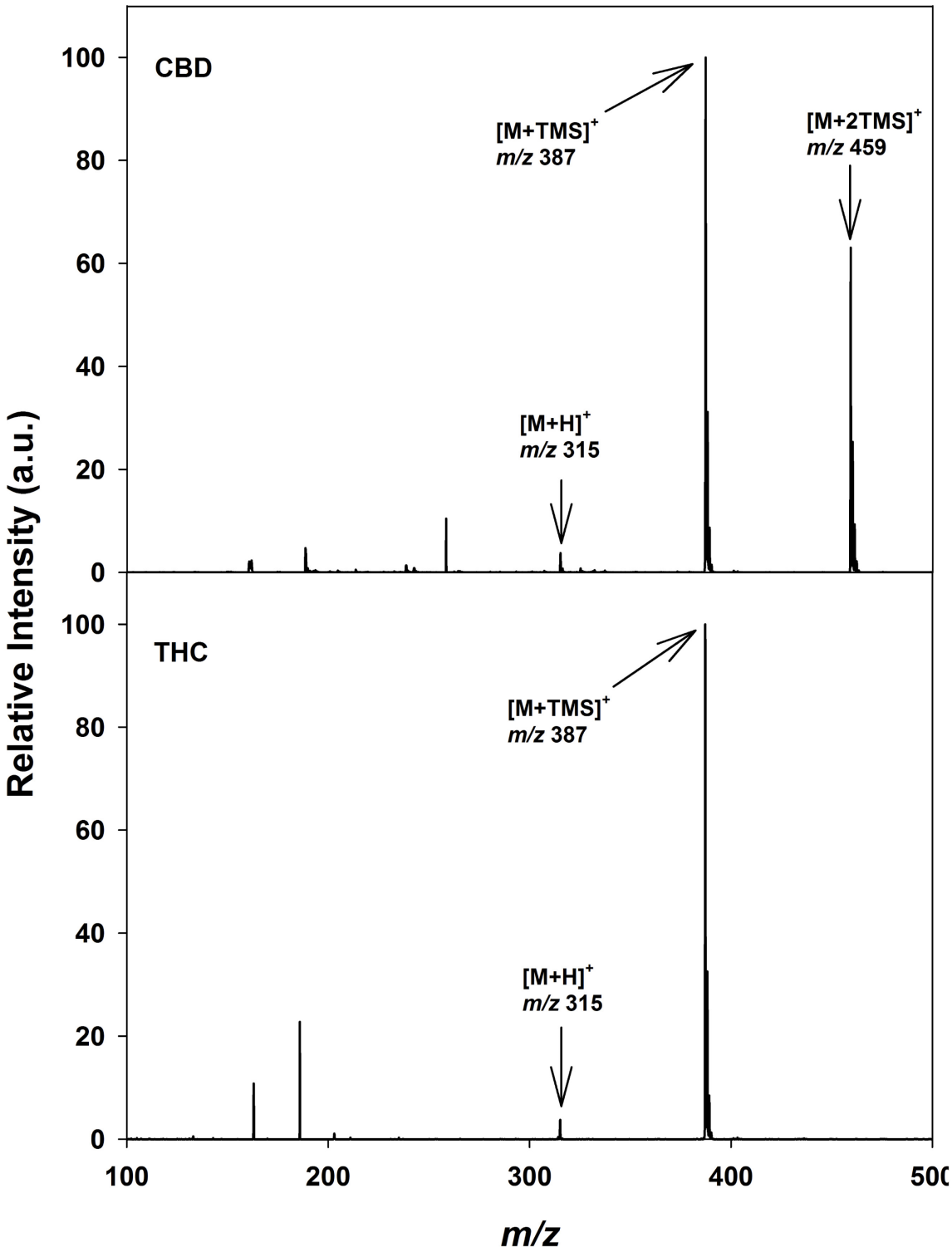

Figure 35. ASAP mass spectra collected while infusing BSTFA through the ionization source at 3 µL min^{-1}, CBD (top) and THC (bottom).

It is not known yet whether this was a result of a kinetic limitation, like the timescale from desorption of the analyte to initiate the reaction was longer than the transport time between the melting point capillary and the inlet of the of the mass spectrometer. Or if it was a result of a limiting reagent, i.e. the number of BSTFA molecules available to react was exceeded by the number of CBD molecules being desorbed and the number of water molecules present in the atmosphere. In both cases, the analyte molecules are desorbed off the surface and come in direct contact with the sheath gas that is carrying aerosolized BSTFA. As the aerosol BSTFA meets contact with the dried THC or CBD on the capillary tube, proton exchange occurs, and desorption is facilitated by the 250 °C vaporized stream of nitrogen sheath gas.

In addition, the CBD spectrum exhibited the presence of a significant peak at *m/z* 459 resulting from the addition of two TMS groups to the hydroxyl groups present on CBD giving rise to $[M\text{-}H+2TMS]^+$. This peak was lower in intensity than the singly silylated product, and this was expected because the likelihood of exchanging two TMS groups in the gas phase should be lower due to the number of collisions between the ESI probe and inlet of the mass spectrometer. It is interesting to note, that the *m/z* 315 peak for the protonated THC and CBD molecule had less than a 10% relative abundance, implying that most of the analyte molecules undergo at least one TMS exchange between protons.

It is apparent that by using just ASAP in the positive ion mode with full MS, that differentiating the two species is impossible. Whereas, in a typical direct

infusion experiment the CBD and THC molecules would be pre-silylated in solution, likely giving full conversion to the *m/z* 459 for CBD and *m/z* 387.

Using ambient ionization ASAP, this experiment was able to qualitatively shift the isotopic envelope of CBD and THC, which could prove as a means for instantaneous separation for the two isomers once a better method for quantitation can be established. Once a better method to quantitate cannabinoids is secured, direct analysis from leaf tissue, whole buds, or extracts could be preliminarily be performed, to see if further analysis using GC/LC-MS is needed. This methodology would greatly reduce analysis time in laboratories in states where the laws prohibit medical and recreational use of cannabis. The initial derivatization step could also be used as a preliminary protocol for forensic and crime lab testing for other classes of narcotics that share the same *m/z* value.

An ideal way to separate isobaric molecules using ASAP would be if one of the constitutional isomers did not have any labile protons that would undergo silylation. That way a deuterated standard could be used to properly mimic the silylation rate of any the isomers as a control. However, in real world applications this is often not the case.

In the case of separating CBD from THC using ASAP, many questions were raised as how to tackle this problem with quantitation. Is there something obscure about the nature of these two analytes that makes this task so cumbersome?

To test this hypothesis, the same online derivatization methodology was to a different class of drugs, to see if the nature of this chemistry was inherently

different. Hydromorphone and morphine was investigated, which both share the $[M+H]^+$ = *m/z* 286, and belong to the opioid class of narcotics. Morphine is a naturally occurring alkaloid, and the active ingredient derived from the opium poppy latex.[145] Morphine has a long history of use in humans as a pain reliever and once it was successfully isolated, it was noted to have greater analgesic potency compared to raw opium.[145,146] Hydromorphone is a synthetic morphine analogue that is more potent than morphine and is often used to treat chronic and acute pain.[136]

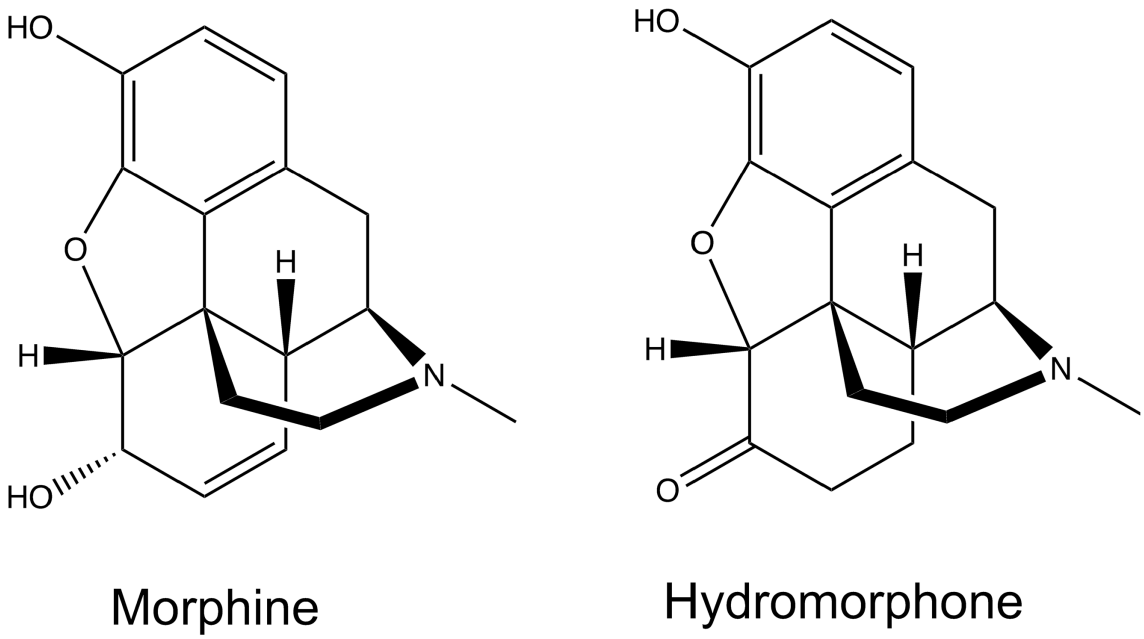

Figure 36. Molecular structure of morphine and hydromorphone.

Referring to Figure 36 above, morphine has two labile protons, being the phenolic hydrogen and they hydroxyl group, whereas hydromorphone only has the phenolic hydrogen.

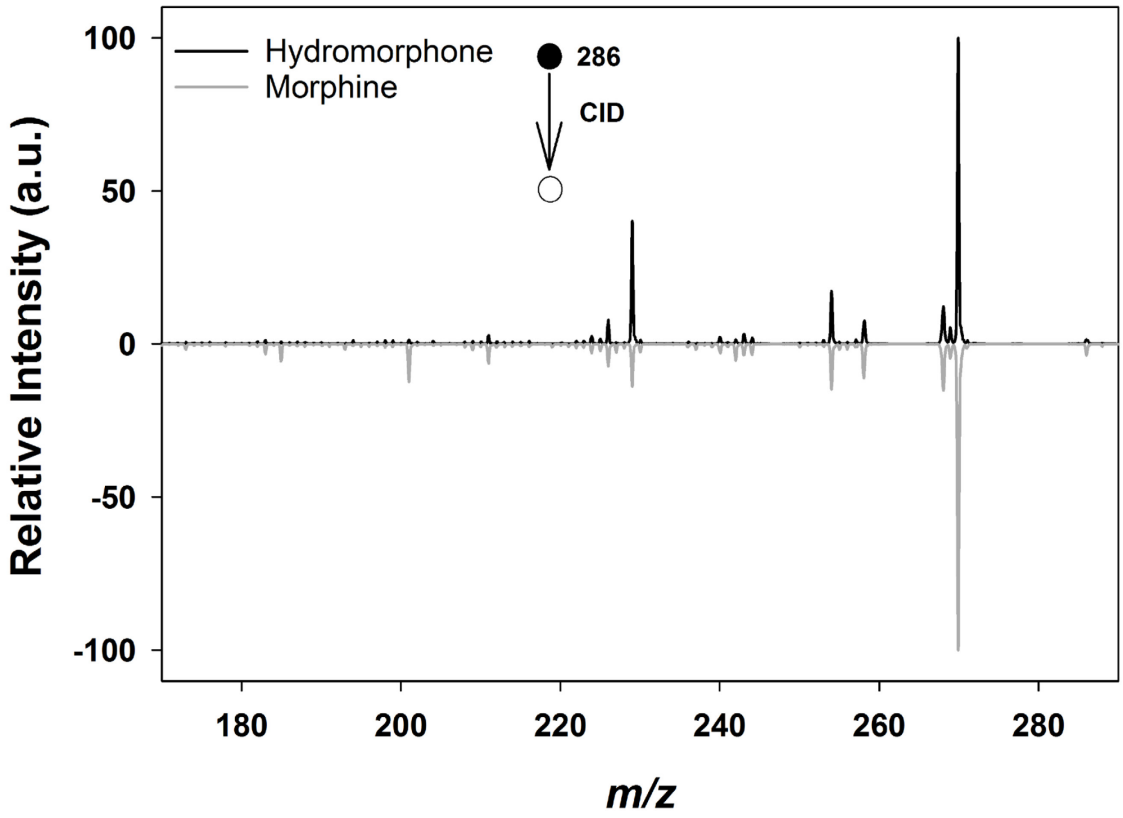

Figure 37. ASAP CID of hydromorphone (black) and morphine (gray) *m/z* 286 in positive ion mode.

Figure 37 above, shows the tandem MS of 10 µg/mL solutions of hydromorphone and morphine that were analyzed separately using ASAP. The protonated molecule, *m/z* 286, was isolated with a 1.0 *m/z* window and fragmented with 30% normalized collision energy under conventional CID conditions.

When fragmented using standard, low-energy CID, the tandem mass spectra of hydromorphone and morphine, shown in Figure 37, are visually indistinguishable. Due to the lack of unique transitions, the tandem mass spectrometry approach to differentiation was ineffective. The head-to-tail mass spectrum of the underivatized hydromorphone and morphine in Figure 37, shows

that CID in positive ion mode produces mass spectra that look exactly identical. This makes MS/MS impossible to differentiate the two species in positive ion mode.

With the recent opioid epidemic, new government regulations call for more strict guidelines with patients that have been suffering acute and chronic pain, so that they do not fall victim to the addictive properties of prescribed opioids.[148] Lax regulation and oversight, as well as the misrepresentation of addictive properties with oxycontin by Purdue pharmaceutical has led to many people suffering from chronic pain to seek relief elsewhere.[149] This “relief” is typically in the form of illicit street opiates such as heroin and fentanyl.[150] Pain management analysis could overlook the presence of isobaric opiates if adequate chromatography is not used.

So, the dilemma arises, what if prescribed morphine is being used in tandem with illicit hydromorphone or vice versa? Can ASAP be used to differentiate these molecules in the same way that was tried previously with THC and CBD? It is possible that the same methodology could apply to differentiate the two molecules, and perhaps the nature of opioids compared to cannabinoids are vastly different, making this analytical feat much easier than expected.

Initial experiments used single component solutions of either morphine or hydromorphone with a D3-deuterated morphine and D6-hydromorphone as an internal standard. Several experiments were performed to create a series of calibration curves using different ratios singly and doubly silylated peaks to the internal standards in order to see which internal standard gave the best

correlation coefficient with each single component solution. Solutions were typically 0, 25, 50, 75, and 100 µM with 75 µM internal standards of D3 or D6, using the same experimental conditions for each single component calibration curves. Overall, it appeared that using the deuterated D3-morphine gave the best linearity of the two, see Figure 38 below.

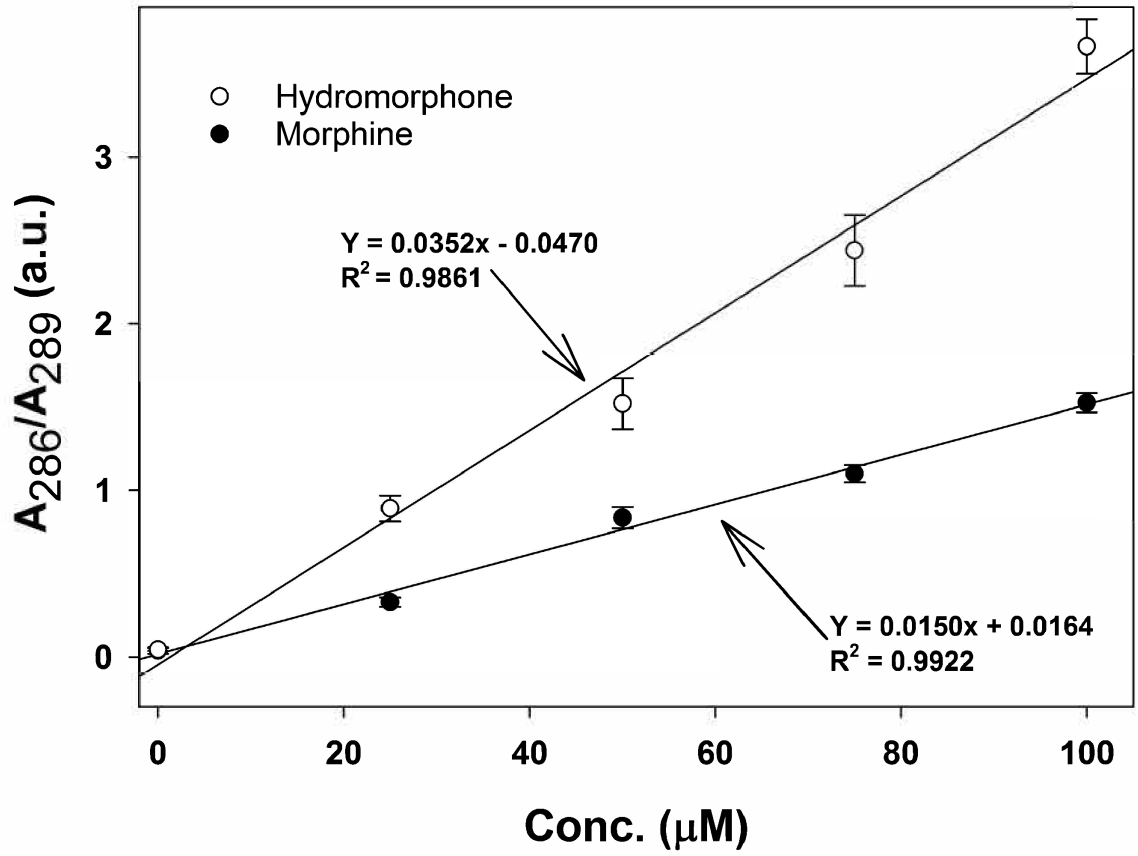

Figure 38. Calibration curve of single component solutions of hydromorphone and morphine using D_3-morphine as an IS.

After some deliberation, this made sense as morphine solutions would give the most variable change as far as silylating both labile protons, whereas D6-hydromorphone would only be representative of a system where only one site

was open to silylation. After creating calibration curves for the single component solutions, a series of binary component mixtures were made that contain 100 µM total of the two analytes, each spike with D3-morphine as an internal standard. For example, 100:0, 75:25, 50:50, 25:75, and 0:100 µM hydromorphone: morphine with 75 µM of D3-morphine in each sample. It worth mentioning, that the single component and multi-component solutions were run on different days, meaning that the humidity and temperature in the lab varied. This becomes important, because strong linearity was reported for the single component solution of hydromorphone, plotting the ratio of the doubly silylated hydromorphone to the doubly silylated D3- morphine. Hydromorphone only contains one labile proton, so the doubly silylated peak at $[M+2TMS]^+$ = *m/z* 430, should contribute very little to the overall peak contribution, so in theory this background contribution of *m/z* 430 to any of the internal standard peaks could be additive from the two single component solutions to add up to the multicomponent mixture, see Figure 39 below.

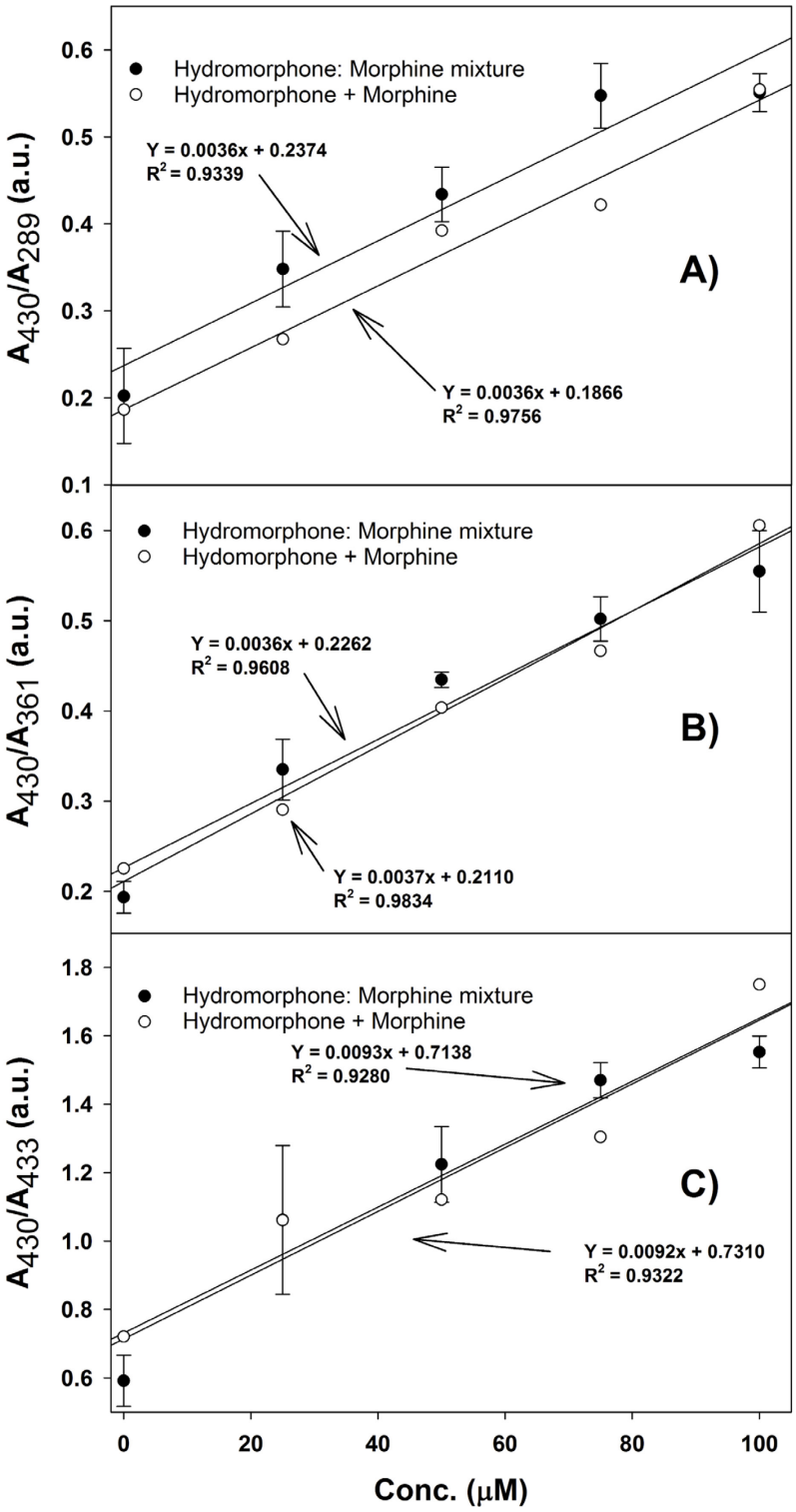

Figure 39. Linear combinations of peak area ratios for mixtures of hydromorphone: morphine, compared to single component solutions of each opioid; A) The doubly silylated analyte to the protonated internal standard; B) The doubly silylated to the singly silylated internal standard; C) The doubly silylated to the doubly silylated internal standard.

This experiment was performed to see if the calibration curves for the single component mixtures would be a linear combination between the two, resulting in the ratio of the calibration curves for the multi-component solutions. This data was collected on the same day in random block order, in hopes that the data for the single component solutions would be additive, resulting in the peak ratios for the binary component solutions. In Figure 39, the ratio of the doubly silylated analyte peaks to the protonated, singly, and doubly silylated internal standard peaks were chosen, because hydromorphone should not contain the doubly silylated peak at *m/z* 430, so the contribution of these peaks would be minimized as much as possible. This would indicate most of the contribution of these peaks in comparison to the binary component solutions, should arise from the morphine single component solutions. The data displayed in Figure 39 seems to be in agreement with this conclusion, as the slopes are very similar, and the 100 μM solutions share very similar peak ratios.

Conclusion

Using ambient ionization ASAP with the direct infusion of a derivatizing agent, this experiment was able to qualitatively shift the isotopic envelope of cannabinoids and opioids. This could prove as a means for instantaneous separation for the two isomers once a better method for quantitation can be established. Once a better method to quantitate isomass drug mixtures is secured, direct analysis from leaf tissue, whole buds, extracts, or raw pill tablets could be preliminarily performed to see if further analysis using GC/LC-MS is necessary. This methodology would greatly reduce analysis time in narcotic

testing laboratories, and the ease of sampling makes this methodology ideal for bypassing traditional chromatographic separation techniques. The initial derivatization step could also be used as a preliminary protocol for forensic and crime lab testing for other classes of narcotics that share the same *m/z* value.

6. CONCLUSION

Metal spray ionization using a bare copper surface produced reproducible spray events and enabled reusable surfaces. Ability to detect singly and doubly charged peptides was demonstrated. In addition to the ability to qualitatively observe the analytes, quantitation was carried out as well. Linear calibration curves ($R^2 > 0.99$) were produced for all analytes. Metal spray ionization may provide a viable alternative to other ambient ionization techniques.

Applying 4.3 kV to a copper the surface, a steady spray event was observed, such as seen with paper spray experiments, using as little as 0.5 µL of analyte applied. By covalently bonding trichloro(1H, 1H, 2H, 2H-perflourooctyl)-silane to copper (II) oxide to create a superhydrophobic surface, a higher degree of sensitivity and lower limits of detection and quantitation for the peptides bradykinin and leucine-enkephalin were calculated. There was only one instance in this paper where this was not observed using superhydrophobic surfaces compared to bare copper. Calibration curves for modified and unmodified surfaces were constructed using 30, 60, and 90° tips with 0, 3.125, 6.25, 12.5 and 25µM solutions of the peptides spiked with substance P as an internal standard. Overall, the highest degree of sensitivity and lowest limits of detection and quantitation, resulted from using the superhydrophobic surfaces with the tips between 30 and 60° for doubly charged bradykinin and a 30° tip for the singly charged YGGFL.

Overall, metal spray ionization proved to be an exemplary tool for quantitation as far as ambient ionization techniques. Quantitation can be

performed in seconds, with high sampling throughput, and is very easy to use. In some cases, metal spray offered lower LOD/LOQ compared to HESI, see Table 1 above. Surfaces are reusable, do not require wicking, have a fixed geometry, and can be functionalized and tuned to increase sensitivity for a broad range of analytes. For these reasons, we believe that metal spray has many advantages over paper spray. Future directions for this project would include quantification of analytes in complex matrices such as hair, urine, sweat, blood and soil without any pre-dilution, and compared the sensitivity, LOD/LOQ to that of ESI or GC-MS

Using ASAP coupled to online derivatization, we were able to qualitatively separate CBD from THC, which could prove to be a useful method to separate the two isomers based on ambient ionization methods. The presence of the *m/z* 459 peak is unique to CBD, thus the potential for separation. If this method proves to be quantitative, this may be a useful tool for forensic labs to help reduce backlogs.

7. FUTURE WORK

As far as improving on metal spray ionization and expanding its utility, I would like to use photolithography techniques used to develop film and circuit boards to acid etch the metal in order to accurately control dimensions of channel. The channel could extend in a linear fashion coated with a polar or non-polar surface to recreate normal or reverse-phase stationary phase you would find in GC and LC columns. If a linear channel is not sufficient to separate analytes from a mixture because of the short length, the possibility of snaking the channel might give the analytes of differing polarity long enough create chromatographic separation (hopefully on a faster time scale than GC and LC), provided the applied voltage is strong enough to elute the analytes off of the surface. I would also like to look at actual complex matrices (i.e. blood, urine, saliva), and the ability to quantitate from these matrices. In a paper by the Pawliszyn's group, they used a C-18 polyacrylonitrile coated blade spray as an extraction tool, where they were able to wash off the complex matrix and quantify the analytes with the coated blade as a spray initiator in order to bypass chromatographic separation. More work should be done in this realm in relation to metal spray ionization.

As far as using ASAP to quantitate isobaric drugs, once a better method to quantitate is established, looking at other isobaric drugs such as: scopolamine/cocaine, codeine/hydrocodone, lysergic acid diethylamide/lysergic acid N,N-methyl propylamide, bufotenine/5-Meo DMT/psilocin, ketamine HCl/5-Meo-diisopropyl tryptamine, would really solidify the adoption of ASAP for

preliminary psychoactive compound screening. This would also eliminate the need for a trained chemist to operate the instrumentation, as no sample preparation is needed, and sampling is easy to use.

REFERENCES

(1) Seger, C. Usage and Limitations of Liquid Chromatography-Tandem Mass Spectrometry (LC–MS/MS) in Clinical Routine Laboratories. *Wien. Med. Wochenschr.* **2012**, *162* (21), 499–504. https://doi.org/10.1007/s10354-012-0147-3.

(2) Pravallika, S. Gas Chromatography: A Mini Review. *Res. Rev. J. Pharm. Anal.* **2016**, *5* (2).

(3) Sidisky, L.; Baney, G.; Stenerson, K.; Desorcie, J. L. Carrier Gas Selection for Capillary Gas Chromatography. 27.

(4) Wang, M.; Wang, Y.-H.; Avula, B.; Radwan, M. M.; Wanas, A. S.; van Antwerp, J.; Parcher, J. F.; ElSohly, M. A.; Khan, I. A. Decarboxylation Study of Acidic Cannabinoids: A Novel Approach Using Ultra-High-Performance Supercritical Fluid Chromatography/Photodiode Array-Mass Spectrometry. *Cannabis Cannabinoid Res.* **2016**, *1* (1), 262–271. https://doi.org/10.1089/can.2016.0020.

(5) Dussy, F. E.; Hamberg, C.; Luginbühl, M.; Schwerzmann, T.; Briellmann, T. A. Isolation of Δ9-THCA-A from Hemp and Analytical Aspects Concerning the Determination of Δ9-THC in Cannabis Products. *Forensic Sci. Int.* **2005**, *149* (1), 3–10. https://doi.org/10.1016/j.forsciint.2004.05.015.

(6) Quantitative GC-MS Analysis of Δ9-Tetrahydrocannabinol in Fiber Hemp Varieties | Journal of Analytical Toxicology | Oxford Academic https://academic.oup.com/jat/article/29/4/258/730079 (accessed Mar 19, 2020).

(7) Konermann, L.; Ahadi, E.; Rodriguez, A. D.; Vahidi, S. Unraveling the Mechanism of Electrospray Ionization. *Anal. Chem.* **2013**, *85* (1), 2–9. https://doi.org/10.1021/ac302789c.

(8) Awad, H.; Khamis, M. M.; El-Aneed, A. Mass Spectrometry, Review of the Basics: Ionization. *Appl. Spectrosc. Rev.* **2015**, *50* (2), 158–175. https://doi.org/10.1080/05704928.2014.954046.

(9) Whitehouse, C. M.; Dreyer, R. N.; Yamashita, Masamichi.; Fenn, J. B. Electrospray Interface for Liquid Chromatographs and Mass Spectrometers. *Anal. Chem.* **1985**, *57* (3), 675–679. https://doi.org/10.1021/ac00280a023.

(10) Smith, R. D. Future Directions for Electrospray Ionization for Biological Analysis Using Mass Spectrometry. *BioTechniques* **2006**, *41* (2), 147–148. https://doi.org/10.2144/000112217.

(11) Correa, D. N.; Santos, J. M.; Eberlin, L. S.; Eberlin, M. N.; Teunissen, S. F. Forensic Chemistry and Ambient Mass Spectrometry: A Perfect Couple Destined for a Happy Marriage? *Anal. Chem.* **2016**, *88* (5), 2515–2526. https://doi.org/10.1021/acs.analchem.5b02397.

(12) Jagerdeo, E.; Wriston, A. Rapid Analysis of Forensic-Related Samples Using Two Ambient Ionization Techniques Coupled to High-Resolution Mass Spectrometers: Ambient Techniques Coupled to High-Resolution Mass Spectrometers. *Rapid Commun. Mass Spectrom.* **2017**, *31* (9), 782–790. https://doi.org/10.1002/rcm.7844.

(13) Graves, P. R.; Haystead, T. A. J. Molecular Biologist's Guide to Proteomics. *Microbiol. Mol. Biol. Rev.* **2002**, *66* (1), 39–63. https://doi.org/10.1128/MMBR.66.1.39-63.2002.

(14) Aebersold, R.; Mann, M. Mass Spectrometry-Based Proteomics. *Nature* **2003**, *422* (6928), 198–207. https://doi.org/10.1038/nature01511.

(15) Vidova, V.; Spacil, Z. A Review on Mass Spectrometry-Based Quantitative Proteomics: Targeted and Data Independent Acquisition. *Anal. Chim. Acta* **2017**, *964*, 7–23. https://doi.org/10.1016/j.aca.2017.01.059.

(16) Wenk, M. R. The Emerging Field of Lipidomics. *Nat. Rev. Drug Discov.* **2005**, *4* (7), 594–610. https://doi.org/10.1038/nrd1776.

(17) Harkewicz, R.; Dennis, E. A. Applications of Mass Spectrometry to Lipids and Membranes. *Annu. Rev. Biochem.* **2011**, *80* (1), 301–325. https://doi.org/10.1146/annurev-biochem-060409-092612.

(18) Yang, K.; Han, X. Lipidomics: Techniques, Applications, and Outcomes Related to Biomedical Sciences. *Trends Biochem. Sci.* **2016**, *41* (11), 954–969. https://doi.org/10.1016/j.tibs.2016.08.010.

(19) Ong, S.-E.; Pandey, A. Using Mass Spectrometry for Drug Discovery. *Trends Biotechnol.* **2002**, *20* (5), 227. https://doi.org/10.1016/S0167-7799(02)01956-X.

(20) Mei, H.; Hsieh, Y.; Nardo, C.; Xu, X.; Wang, S.; Ng, K.; Korfmacher, W. A. Investigation of Matrix Effects in Bioanalytical High-Performance Liquid Chromatography/Tandem Mass Spectrometric Assays: Application to Drug Discovery. *Rapid Commun. Mass Spectrom.* **2003**, *17* (1), 97–103. https://doi.org/10.1002/rcm.876.

(21) Rousu, T.; Herttuainen, J.; Tolonen, A. Comparison of Triple Quadrupole, Hybrid Linear Ion Trap Triple Quadrupole, Time-of-Flight and LTQ-Orbitrap Mass Spectrometers in Drug Discovery Phase Metabolite Screening and Identification in Vitro – Amitriptyline and Verapamil as Model Compounds. *Rapid Commun. Mass Spectrom.* **2010**, *24* (7), 939–957. https://doi.org/10.1002/rcm.4465.

(22) Pacholarz, K. J.; Garlish, R. A.; Taylor, R. J.; Barran, P. E. Mass Spectrometry Based Tools to Investigate Protein–Ligand Interactions for Drug Discovery. *Chem Soc Rev* **2012**, *41* (11), 4335–4355. https://doi.org/10.1039/C2CS35035A.

(23) Chen, H.; Gamez, G.; Zenobi, R. What Can We Learn from Ambient Ionization Techniques? *J. Am. Soc. Mass Spectrom.* **2009**, *20* (11), 1947–1963. https://doi.org/10.1016/j.jasms.2009.07.025.

(24) Liu, J.; Wang, H.; Manicke, N. E.; Lin, J.-M.; Cooks, R. G.; Ouyang, Z. Development, Characterization, and Application of Paper Spray Ionization. *Anal. Chem.* **2010**, *82* (6), 2463–2471. https://doi.org/10.1021/ac902854g.

(25) Jackson, S.; Swiner, D. J.; Capone, P. C.; Badu-Tawiah, A. K. Thread Spray Mass Spectrometry for Direct Analysis of Capsaicinoids in Pepper Products. *Anal. Chim. Acta* **2018**, *1023*, 81–88. https://doi.org/10.1016/j.aca.2018.04.008.

(26) Gómez-Ríos, G. A.; Pawliszyn, J. Development of Coated Blade Spray Ionization Mass Spectrometry for the Quantitation of Target Analytes Present in Complex Matrices. *Angew Chem* **2014**, 6.

(27) Gómez-Ríos, G. A.; Tascon, M.; Reyes-Garcés, N.; Boyacı, E.; Poole, J.; Pawliszyn, J. Quantitative Analysis of Biofluid Spots by Coated Blade Spray Mass Spectrometry, a New Approach to Rapid Screening. *Sci. Rep.* **2017**, *7* (1), 1–7. https://doi.org/10.1038/s41598-017-16494-z.

(28) Jiang, J.; Zhang, H.; Li, M.; Dulay, M. T.; Ingram, A. J.; Li, N.; You, H.; Zare, R. N. Droplet Spray Ionization from a Glass Microscope Slide: Real-Time Monitoring of Ethylene Polymerization. *Anal. Chem.* **2015**, *87* (16), 8057–8062. https://doi.org/10.1021/acs.analchem.5b02390.

(29) Dulay, M. T.; Zare, R. N. Polymer-Spray Mass Spectrometric Detection and Quantitation of Hydrophilic Compounds and Some Narcotics. *Rapid Commun. Mass Spectrom.* **2017**, *31* (19), 1651–1658. https://doi.org/10.1002/rcm.7952.

(30) Frey, B. S.; Damon, D. E.; Badu-Tawiah, A. K. Emerging Trends in Paper Spray Mass Spectrometry: Microsampling, Storage, Direct Analysis, and Applications. *Mass Spectrom. Rev. n/a* (n/a). https://doi.org/10.1002/mas.21601.

(31) Li, A.; Wang, H.; Ouyang, Z.; Cooks, R. G. Paper Spray Ionization of Polar Analytes Using Non-Polar Solvents. *Chem. Commun.* **2011**, *47* (10), 2811–2813. https://doi.org/10.1039/C0CC05513A.

(32) Yang, Q.; Wang, H.; Maas, J. D.; Chappell, W. J.; Manicke, N. E.; Cooks, R. G.; Ouyang, Z. Paper Spray Ionization Devices for Direct, Biomedical Analysis Using Mass Spectrometry. *Int. J. Mass Spectrom.* **2012**, *312*, 201–207. https://doi.org/10.1016/j.ijms.2011.05.013.

(33) Zhang, Y.; Ju, Y.; Huang, C.; Wysocki, V. H. Paper Spray Ionization of Noncovalent Protein Complexes. *Anal. Chem.* **2014**, *86* (3), 1342–1346. https://doi.org/10.1021/ac403383d.

(34) Wang, H.; Liu, J.; Cooks, R. G.; Ouyang, Z. Paper Spray for Direct Analysis of Complex Mixtures Using Mass Spectrometry. *Angew. Chem. Int. Ed.* **2010**, *49* (5), 877–880. https://doi.org/10.1002/anie.200906314.

(35) Manicke, N. E.; Yang, Q.; Wang, H.; Oradu, S.; Ouyang, Z.; Cooks, R. G. Assessment of Paper Spray Ionization for Quantitation of Pharmaceuticals in Blood Spots. *Int. J. Mass Spectrom.* **2011**, *300* (2), 123–129. https://doi.org/10.1016/j.ijms.2010.06.037.

(36) Manicke, N. E.; Abu-Rabie, P.; Spooner, N.; Ouyang, Z.; Cooks, R. G. Quantitative Analysis of Therapeutic Drugs in Dried Blood Spot Samples by Paper Spray Mass Spectrometry: An Avenue to Therapeutic Drug Monitoring. *J. Am. Soc. Mass Spectrom.* **2011**, *22* (9), 1501–1507. https://doi.org/10.1007/s13361-011-0177-x.

(37) Espy, R. D.; Manicke, N. E.; Ouyang, Z.; Cooks, R. G. Rapid Analysis of Whole Blood by Paper Spray Mass Spectrometry for Point-of-Care Therapeutic Drug Monitoring. *Analyst* **2012**, *137* (10), 2344–2349. https://doi.org/10.1039/C2AN35082C.

(38) Ren, Y.; Wang, H.; Liu, J.; Zhang, Z.; McLuckey, M. N.; Ouyang, Z. Analysis of Biological Samples Using Paper Spray Mass Spectrometry: An Investigation of Impacts by the Substrates, Solvents and Elution Methods. *Chromatographia* **2013**, *76* (19–20), 1339–1346. https://doi.org/10.1007/s10337-013-2458-y.

(39) Park, H. M.; Kim, H. J.; Jang, Y. P.; Kim, S. Y. Direct Analysis in Real Time Mass Spectrometry (DART-MS) Analysis of Skin Metabolome Changes in the Ultraviolet B-Induced Mice. *Biomol. Ther.* **2013**, *21* (6), 470–475. https://doi.org/10.4062/biomolther.2013.071.

(40) Morelato, M.; Beavis, A.; Kirkbride, P.; Roux, C. Forensic Applications of Desorption Electrospray Ionisation Mass Spectrometry (DESI-MS). *Forensic Sci. Int.* **2013**, *226* (1), 10–21. https://doi.org/10.1016/j.forsciint.2013.01.011.

(41) Harper, J. D.; Charipar, N. A.; Mulligan, C. C.; Zhang, X.; Cooks, R. G.; Ouyang, Z. Low-Temperature Plasma Probe for Ambient Desorption Ionization. *Anal. Chem.* **2008**, *80* (23), 9097–9104. https://doi.org/10.1021/ac801641a.

(42) Fussell, R. J.; Chan, D.; Sharman, M. An Assessment of Atmospheric-Pressure Solids-Analysis Probes for the Detection of Chemicals in Food. *TrAC Trends Anal. Chem.* **2010**, *29* (11), 1326–1335. https://doi.org/10.1016/j.trac.2010.08.004.

(43) Bruns, E. A.; Perraud, V.; Greaves, J.; Finlayson-Pitts, B. J. Atmospheric Solids Analysis Probe Mass Spectrometry: A New Approach for Airborne Particle Analysis. *Anal. Chem.* **2010**, *82* (14), 5922–5927. https://doi.org/10.1021/ac101028j.

(44) Petucci, C.; Diffendal, J. Atmospheric Solids Analysis Probe: A Rapid Ionization Technique for Small Molecule Drugs. *J. Mass Spectrom.* **2008**, *43* (11), 1565–1568. https://doi.org/10.1002/jms.1424.

(45) Smith, M. J. P.; Cameron, N. R.; Mosely, J. A. Evaluating Atmospheric Pressure Solids Analysis Probe (ASAP) Mass Spectrometry for the Analysis of Low Molecular Weight Synthetic Polymers. *Analyst* **2012**, *137* (19), 4524–4530. https://doi.org/10.1039/C2AN35556F.

(46) Twohig, M.; Shockcor, J. P.; Wilson, I. D.; Nicholson, J. K.; Plumb, R. S. Use of an Atmospheric Solids Analysis Probe (ASAP) for High Throughput Screening of Biological Fluids: Preliminary Applications on Urine and Bile. *J. Proteome Res.* **2010**, *9* (7), 3590–3597. https://doi.org/10.1021/pr100120g.

(47) Rapid Screening of Anabolic Steroids in Urine by Reactive Desorption Electrospray Ionization | Analytical Chemistry https://pubs-acs-org.libproxy.txstate.edu/doi/10.1021/ac0711079 (accessed Mar 22, 2020).

(48) McEwen, C. N.; McKay, R. G.; Larsen, B. S. Analysis of Solids, Liquids, and Biological Tissues Using Solids Probe Introduction at Atmospheric Pressure on Commercial LC/MS Instruments. *Anal. Chem.* **2005**, *77* (23), 7826–7831. https://doi.org/10.1021/ac051470k.

(49) Takáts, Z.; Wiseman, J. M.; Gologan, B.; Cooks, R. G. Mass Spectrometry Sampling Under Ambient Conditions with Desorption Electrospray Ionization. *Science* **2004**, *306* (5695), 471–473. https://doi.org/10.1126/science.1104404.

(50) Ifa, D. R.; Manicke, N. E.; Dill, A. L.; Cooks, R. G. Latent Fingerprint Chemical Imaging by Mass Spectrometry. *Science* **2008**, *321* (5890), 805–805. https://doi.org/10.1126/science.1157199.

(51) Comi, T. J.; Ryu, S. W.; Perry, R. H. Synchronized Desorption Electrospray Ionization Mass Spectrometry Imaging. *Anal. Chem.* **2016**, *88* (2), 1169–1175. https://doi.org/10.1021/acs.analchem.5b03010.

(52) Fernández, F. M.; Cody, R. B.; Green, M. D.; Hampton, C. Y.; McGready, R.; Sengaloundeth, S.; White, N. J.; Newton, P. N. Characterization of Solid Counterfeit Drug Samples by Desorption Electrospray Ionization and Direct-Analysis-in-Real-Time Coupled to Time-of-Flight Mass Spectrometry. *ChemMedChem* **2006**, *1* (7), 702–705. https://doi.org/10.1002/cmdc.200600041.

(53) Fernandez, F. M.; Green, M. D.; Newton, P. N. Prevalence and Detection of Counterfeit Pharmaceuticals: A Mini Review. *Ind. Eng. Chem. Res.* **2008**, *47* (3), 585–590. https://doi.org/10.1021/ie0703787.

(54) Cody, R. B.; Laramée, J. A.; Durst, H. D. Versatile New Ion Source for the Analysis of Materials in Open Air under Ambient Conditions. *Anal. Chem.* **2005**, *77*, 2297–2302. https://doi.org/10.1021/ac050162j.

(55) Cody, R. B. Observation of Molecular Ions and Analysis of Nonpolar Compounds with the Direct Analysis in Real Time Ion Source. *Anal. Chem.* **2009**, *81*, 1101–1107. https://doi.org/10.1021/ac8022108.

(56) Grange, A. H.; Sovocool, G. W. Detection of Illicit Drugs on Surfaces Using Direct Analysis in Real Time (DART) Time-of-Flight Mass Spectrometry. *Rapid Commun. Mass Spectrom.* **2011**, *25* (9), 1271–1281. https://doi.org/10.1002/rcm.5009.

(57) Duvivier, W. F.; van Beek, T. A.; Pennings, E. J. M.; Nielen, M. W. F. Rapid Analysis of Δ-9-Tetrahydrocannabinol in Hair Using Direct Analysis in Real Time Ambient Ionization Orbitrap Mass Spectrometry. *Rapid Commun. Mass Spectrom.* **2014**, *28* (7), 682–690. https://doi.org/10.1002/rcm.6831.

(58) Chen, T.-H.; Hsu, H.-Y.; Wu, S.-P. The Detection of Multiple Illicit Street Drugs in Liquid Samples by Direct Analysis in Real Time (DART) Coupled to Q-Orbitrap Tandem Mass Spectrometry. *Forensic Sci. Int.* **2016**, *267*, 1–6. https://doi.org/10.1016/j.forsciint.2016.07.025.

(59) Steiner, R. R. Use of DART-TOF-MS for Screening Drugs of Abuse. In *Analysis of Drugs of Abuse*; Musah, R. A., Ed.; Methods in Molecular Biology; Springer New York: New York, NY, 2018; pp 59–68. https://doi.org/10.1007/978-1-4939-8579-1_5.

(60) Nilles, J. M.; Connell, T. R.; Stokes, S. T.; Dupont Durst, H. Explosives Detection Using Direct Analysis in Real Time (DART) Mass Spectrometry. *Propellants Explos. Pyrotech.* **2010**, *35* (5), 446–451. https://doi.org/10.1002/prep.200900084.

(61) Forbes, T. P.; Sisco, E.; Staymates, M.; Gillen, G. DART-MS Analysis of Inorganic Explosives Using High Temperature Thermal Desorption. *Anal. Methods* **2017**, *9* (34), 4988–4996. https://doi.org/10.1039/C7AY00867H.

(62) Frey, W. H.; DeSota-Johnson, D.; Hoffman, C.; McCall, J. T. Effect of Stimulus on the Chemical Composition of Human Tears. *Am. J. Ophthalmol.* **1981**, *92* (4), 559–567. https://doi.org/10.1016/0002-9394(81)90651-6.

(63) Plotnikoff, N. P.; Miller, G. C. Enkephalins as Immunomodulators. *Int. J. Immunopharmacol.* **1983**, *5* (5), 437–441. https://doi.org/10.1016/0192-0561(83)90020-6.

(64) Blaukat, A. Structure and Signalling Pathways of Kinin Receptors. *Andrologia* **2003**, *35* (1), 17–23. https://doi.org/10.1046/j.1439-0272.2003.00533.x.

(65) Adeghate, E.; Ponery, A. S. The Role of Leucine-Enkephalin on Insulin and Glucagon Secretion from Pancreatic Tissue Fragments of Normal and Diabetic Rats. *Arch. Physiol. Biochem.* **2001**, *109* (3), 223–229. https://doi.org/10.1076/apab.109.3.223.11586.

(66) Golias, C.; Charalabopoulos, A.; Stagikas, D.; Charalabopoulos, K.; Batistatou, A. The Kinin System - Bradykinin: Biological Effects and Clinical Implications. Multiple Role of the Kinin System - Bradykinin. *Hippokratia* **2007**, *11* (3), 124–128.

(67) Johnson, M. B.; Young, A. D.; Marriott, I. The Therapeutic Potential of Targeting Substance P/NK-1R Interactions in Inflammatory CNS Disorders. *Front. Cell. Neurosci.* **2017**, *10*. https://doi.org/10.3389/fncel.2016.00296.

(68) Manicke, N. E.; Abu-Rabie, P.; Spooner, N.; Ouyang, Z.; Cooks, R. G. Quantitative Analysis of Therapeutic Drugs in Dried Blood Spot Samples by Paper Spray Mass Spectrometry: An Avenue to Therapeutic Drug Monitoring. *J. Am. Soc. Mass Spectrom.* **2011**, *22* (9), 1501–1507. https://doi.org/10.1007/s13361-011-0177-x.

(69) Damon, D. E.; Davis, K. M.; Moreira, C. R.; Capone, P.; Cruttenden, R.; Badu-Tawiah, A. K. Direct Biofluid Analysis Using Hydrophobic Paper Spray Mass Spectrometry. *Anal. Chem.* **2016**, *88* (3), 1878–1884. https://doi.org/10.1021/acs.analchem.5b04278.

(70) Liu, J.; Wang, H.; Manicke, N. E.; Lin, J.-M.; Cooks, R. G.; Ouyang, Z. Development, Characterization, and Application of Paper Spray Ionization. *Anal. Chem.* **2010**, *82* (6), 2463–2471. https://doi.org/10.1021/ac902854g.

(71) Chu, Z.; Seeger, S. Superamphiphobic Surfaces. *Chem Soc Rev* **2014**, *43* (8), 2784–2798. https://doi.org/10.1039/C3CS60415B.

(72) Ashurst, W. R.; Carraro, C.; Maboudian, R. Vapor Phase Anti-Stiction Coatings for MEMS. *IEEE Trans. Device Mater. Reliab.* **2003**, *3* (4), 173–178. https://doi.org/10.1109/TDMR.2003.821540.

(73) Wang, L.; McCarthy, T. J. Covalently Attached Liquids: Instant Omniphobic Surfaces with Unprecedented Repellency. *Angew. Chem. Int. Ed.* **2016**, *55* (1), 244–248. https://doi.org/10.1002/anie.201509385.

(74) Bagheri, H.; Aliofkhazraei, M.; Forooshani, H. M.; Rouhaghdam, A. S. Electrodeposition of the Hierarchical Dual Structured (HDS) Nanocrystalline Ni Surface with High Water Repellency and Self-Cleaning Properties. *J. Taiwan Inst. Chem. Eng.* **2017**, *80*, 883–893. https://doi.org/10.1016/j.jtice.2017.07.023.

(75) Miljkovic, N.; Preston, D. J.; Enright, R.; Wang, E. N. Electric-Field-Enhanced Condensation on Superhydrophobic Nanostructured Surfaces. *ACS Nano* **2013**, *7* (12), 11043–11054. https://doi.org/10.1021/nn404707j.

(76) Barati Darband, Gh.; Aliofkhazraei, M.; Khorsand, S.; Sokhanvar, S.; Kaboli, A. Science and Engineering of Superhydrophobic Surfaces: Review of Corrosion Resistance, Chemical and Mechanical Stability. *Arab. J. Chem.* **2018**. https://doi.org/10.1016/j.arabjc.2018.01.013.

(77) Yang, J.; Zhang, Z.; Men, X.; Xu, X.; Zhu, X. A Simple Approach to Fabricate Superoleophobic Coatings. *New J Chem* **2011**, *35* (3), 576–580. https://doi.org/10.1039/C0NJ00826E.

(78) Maboudian, R.; Ashurst, W. R.; Carraro, C. Tribological Challenges in Micromechanical Systems. *Tribol. Lett.* **2002**, *12* (2), 95–100. https://doi.org/10.1023/A:1014044207344.

(79) Boban, M.; Golovin, K.; Tobelmann, B.; Gupte, O.; Mabry, J. M.; Tuteja, A. Smooth, All-Solid, Low-Hysteresis, Omniphobic Surfaces with Enhanced Mechanical Durability. *ACS Appl. Mater. Interfaces* **2018**, *10* (14), 11406–11413. https://doi.org/10.1021/acsami.8b00521.

(80) Golias, C.; Charalabopoulos, A.; Stagikas, D.; Charalabopoulos, K.; Batistatou, A. The Kinin System - Bradykinin: Biological Effects and Clinical Implications. Multiple Role of the Kinin System - Bradykinin. *Hippokratia* **2007**, *11* (3), 124–128.

(81) Wong, M. Y.-M.; Tang, H.-W.; Man, S.-H.; Lam, C.-W.; Che, C.-M.; Ng, K.-M. Electrospray Ionization on Porous Spraying Tips for Direct Sample Analysis by Mass Spectrometry: Enhanced Detection Sensitivity and Selectivity Using Hydrophobic/Hydrophilic Materials as Spraying Tips. *Rapid Commun. Mass Spectrom.* **2013**, *27* (6), 713–721. https://doi.org/10.1002/rcm.6497.

(82) Tuteja, A.; Choi, W.; Mabry, J.; Mckinley, G.; E Cohen, R. Robust Omniphobic Surfaces. *Proc. Natl. Acad. Sci. U. S. A.* **2008**, *105*, 18200–18205. https://doi.org/10.1073/pnas.0804872105.

(83) Milionis, A.; Bayer, I. S.; Loth, E. Recent Advances in Oil-Repellent Surfaces. *Int. Mater. Rev.* **2016**, *61* (2), 101–126. https://doi.org/10.1080/09506608.2015.1116492.

(84) Zeng, J.; Wang, B.; Zhang, Y.; Zhu, H.; Guo, Z. Strong Amphiphobic Porous Films with Oily-Self-Cleaning Property beyond Nature. *Chem. Lett.* **2014**, *43* (10), 1566–1568. https://doi.org/10.1246/cl.140600.

(85) Zhou, H.; Wang, H.; Niu, H.; Gestos, A.; Lin, T. Robust, Self-Healing Superamphiphobic Fabrics Prepared by Two-Step Coating of Fluoro-Containing Polymer, Fluoroalkyl Silane, and Modified Silica Nanoparticles. *Adv. Funct. Mater.* **2013**, *23* (13), 1664–1670. https://doi.org/10.1002/adfm.201202030.

(86) Wang, X.; Liu, X.; Zhou, F.; Liu, W. Self-Healing Superamphiphobicity. *Chem. Commun.* **2011**, *47* (8), 2324–2326. https://doi.org/10.1039/C0CC04066E.

(87) Wang, H.; Zhou, H.; Gestos, A.; Fang, J.; Lin, T. Robust, Superamphiphobic Fabric with Multiple Self-Healing Ability against Both Physical and Chemical Damages. *ACS Appl. Mater. Interfaces* **2013**, *5* (20), 10221–10226. https://doi.org/10.1021/am4029679.

(88) Wang, H.; Zhou, H.; Gestos, A.; Fang, J.; Niu, H.; Ding, J.; Lin, T. Robust, Electro-Conductive, Self-Healing Superamphiphobic Fabric Prepared by One-Step Vapour-Phase Polymerisation of Poly(3,4-Ethylenedioxythiophene) in the Presence of Fluorinated Decyl Polyhedral Oligomeric Silsesquioxane and Fluorinated Alkyl Silane. *Soft Matter* **2012**, *9* (1), 277–282. https://doi.org/10.1039/C2SM26871J.

(89) Yuan, Z.; Xiao, J.; Wang, C.; Zeng, J.; Xing, S.; Liu, J. Preparation of a Superamphiphobic Surface on a Common Cast Iron Substrate. *J. Coat. Technol. Res.* **2011**, *8* (6), 773. https://doi.org/10.1007/s11998-011-9365-7.

(90) Zhu, X.; Zhang, Z.; Xu, X.; Men, X.; Yang, J.; Zhou, X.; Xue, Q. Facile Fabrication of a Superamphiphobic Surface on the Copper Substrate. *J. Colloid Interface Sci.* **2012**, *367* (1), 443–449. https://doi.org/10.1016/j.jcis.2011.10.008.

(91) Rangel, T. C.; Michels, A. F.; Horowitz, F.; Weibel, D. E. Superomniphobic and Easily Repairable Coatings on Copper Substrates Based on Simple Immersion or Spray Processes. *Langmuir* **2015**, *31* (11), 3465–3472. https://doi.org/10.1021/acs.langmuir.5b00193.

(92) Ge, B.; Zhang, Z.; Men, X.; Zhu, X.; Zhou, X. Sprayed Superamphiphobic Coatings on Copper Substrate with Enhanced Corrosive Resistance. *Appl. Surf. Sci.* **2014**, *293*, 271–274. https://doi.org/10.1016/j.apsusc.2013.12.148.

(93) Zhu, P.; Kong, T.; Tang, X.; Wang, L. Well-Defined Porous Membranes for Robust Omniphobic Surfaces via Microfluidic Emulsion Templating. *Nat. Commun.* **2017**, *8*, 15823. https://doi.org/10.1038/ncomms15823.

(94) Mazumder, P.; Jiang, Y.; Baker, D.; Carrilero, A.; Tulli, D.; Infante, D.; Hunt, A. T.; Pruneri, V. Superomniphobic, Transparent, and Antireflection Surfaces Based on Hierarchical Nanostructures. *Nano Lett.* **2014**, *14* (8), 4677–4681. https://doi.org/10.1021/nl501767j.

(95) Li, J.; Yan, L.; Ouyang, Q.; Zha, F.; Jing, Z.; Li, X.; Lei, Z. Facile Fabrication of Translucent Superamphiphobic Coating on Paper to Prevent Liquid Pollution. *Chem. Eng. J.* **2014**, *246*, 238–243. https://doi.org/10.1016/j.cej.2014.02.062.

(96) Zhu, X.; Zhang, Z.; Ren, G.; Men, X.; Ge, B.; Zhou, X. Designing Transparent Superamphiphobic Coatings Directed by Carbon Nanotubes. *J. Colloid Interface Sci.* **2014**, *421*, 141–145. https://doi.org/10.1016/j.jcis.2014.01.026.

(97) He, Z.; Ma, M.; Lan, X.; Chen, F.; Wang, K.; Deng, H.; Zhang, Q.; Fu, Q. Fabrication of a Transparent Superamphiphobic Coating with Improved Stability. *Soft Matter* **2011**, *7* (14), 6435–6443. https://doi.org/10.1039/C1SM05574G.

(98) Lee, S. G.; Ham, D. S.; Lee, D. Y.; Bong, H.; Cho, K. Transparent Superhydrophobic/Translucent Superamphiphobic Coatings Based on Silica–Fluoropolymer Hybrid Nanoparticles. *Langmuir* **2013**, *29* (48), 15051–15057. https://doi.org/10.1021/la404005b.

(99) Golovin, K.; Lee, D. H.; Mabry, J. M.; Tuteja, A. Transparent, Flexible, Superomniphobic Surfaces with Ultra-Low Contact Angle Hysteresis. *Angew. Chem. Int. Ed.* **2013**, *52* (49), 13007–13011. https://doi.org/10.1002/anie.201307222.

(100) Wong, T.-S.; Kang, S. H.; Tang, S. K. Y.; Smythe, E. J.; Hatton, B. D.; Grinthal, A.; Aizenberg, J. Bioinspired Self-Repairing Slippery Surfaces with Pressure-Stable Omniphobicity. *Nature* **2011**, *477* (7365), 443–447. https://doi.org/10.1038/nature10447.

(101) Love, J. C.; Estroff, L. A.; Kriebel, J. K.; Nuzzo, R. G.; Whitesides, G. M. Self-Assembled Monolayers of Thiolates on Metals as a Form of Nanotechnology. *Chem. Rev.* **2005**, *105* (4), 1103–1170. https://doi.org/10.1021/cr0300789.

(102) Pensa, E.; Cortés, E.; Corthey, G.; Carro, P.; Vericat, C.; Fonticelli, M. H.; Benítez, G.; Rubert, A. A.; Salvarezza, R. C. The Chemistry of the Sulfur–Gold Interface: In Search of a Unified Model. *Acc. Chem. Res.* **2012**, *45* (8), 1183–1192. https://doi.org/10.1021/ar200260p.

(103) Gold - Element information, properties and uses | Periodic Table https://www.rsc.org/periodic-table/element/79/gold (accessed Mar 25, 2020).

(104) Dykman, L. A.; Khlebtsov, N. G. Gold Nanoparticles in Biology and Medicine: Recent Advances and Prospects. *Acta Naturae* **2011**, *3* (2), 34–55.

(105) Fischer, D.; Curioni, A.; Andreoni, W. Decanethiols on Gold: The Structure of Self-Assembled Monolayers Unraveled with Computer Simulations. *Langmuir* **2003**, *19* (9), 3567–3571. https://doi.org/10.1021/la034013c.

(106) Wang, L.; McCarthy, T. J. Covalently Attached Liquids: Instant Omniphobic Surfaces with Unprecedented Repellency. *Angew. Chem. Int. Ed.* **2016**, *55* (1), 244–248. https://doi.org/10.1002/anie.201509385.

(107) Grate, J. W.; Dehoff, K. J.; Warner, M. G.; Pittman, J. W.; Wietsma, T. W.; Zhang, C.; Oostrom, M. Correlation of Oil–Water and Air–Water Contact Angles of Diverse Silanized Surfaces and Relationship to Fluid Interfacial Tensions. *Langmuir* **2012**, *28* (18), 7182–7188. https://doi.org/10.1021/la204322k.

(108) Andre, C. M.; Hausman, J.-F.; Guerriero, G. Cannabis Sativa: The Plant of the Thousand and One Molecules. *Front. Plant Sci.* **2016**, *7*. https://doi.org/10.3389/fpls.2016.00019.

(109) Vandevenne, M.; Vandenbussche, H.; Verstraete, A. Detection Time of Drugs of Abuse in Urine. *Acta Clin. Belg.* **2000**, *55* (6), 323–333. https://doi.org/10.1080/17843286.2000.11754319.

(110) M.M. Srinivas Bharath; Pratima Murthy; Priyamvada Sharma. Chemistry, Metabolism, and Toxicology of Cannabis: Clinical Implications. *Iran. J. Psychiatry* **2012**, No. 4, 149.

(111) Lean, M. E. J.; Hankey, C. R. Aspartame and Its Effects on Health. *BMJ* **2004**, *329* (7469), 755–756.

(112) Artificial Sweeteners - SHP - Nutrition Trends | UAB https://www.uab.edu/shp/nutritiontrends/recipes-food-facts/food-facts/artificial-sweeteners (accessed Oct 23, 2019).

(113) 3 Final Report on the Safety Assessment of Methylparaben, Ethylparaben, Propylparaben, and Butylparaben. *J. Am. Coll. Toxicol.* **1984**, *3* (5), 147–209. https://doi.org/10.3109/10915818409021274.

(114) Oishi, S. Effects of Propyl Paraben on the Male Reproductive System. *Food Chem. Toxicol.* **2002**, *40* (12), 1807–1813. https://doi.org/10.1016/S0278-6915(02)00204-1.

(115) Sánchez-Borzone, M. E.; Delgado Marin, L.; Asmed García, D. Effects of Insecticidal Ketones Present in Mint Plants on GABAA Receptor from Mammalian Neurons. *Pharmacogn. Mag.* **2017**, *13* (49), 114–117.

(116) Public Statement on the Use of Herbal Medicinal Products1 Containing Pulegone and Menthofuran. 24.

(117) Anderson, I. B.; Mullen, W. H.; Meeker, J. E.; Khojasteh-BakhtSC; Oishi, S.; Nelson, S. D.; Blanc, P. D. Pennyroyal Toxicity: Measurement of Toxic Metabolite Levels in Two Cases and Review of the Literature. *Ann. Intern. Med.* **1996**, *124* (8), 726–734.

(118) Chakrabarty, S.; Shelver, W. L.; Hakk, H.; Smith, D. J. Atmospheric Solid Analysis Probe and Modified Desorption Electrospray Ionization Mass Spectrometry for Rapid Screening and Semi-Quantification of Zilpaterol in Urine and Tissues of Sheep. *J. Agric. Food Chem.* **2018**, *66* (41), 10871–10880. https://doi.org/10.1021/acs.jafc.8b03925.

(119) McEwen, C.; Gutteridge, S. Analysis of the Inhibition of the Ergosterol Pathway in Fungi Using the Atmospheric Solids Analysis Probe (ASAP) Method. *J. Am. Soc. Mass Spectrom.* **2007**, *18* (7), 1274–1278. https://doi.org/10.1016/j.jasms.2007.03.032.

(120) Xiao, X.; Miller, L. L.; Parchert, K. J.; Hayes, D.; Hochrein, J. M. Atmospheric Solids Analysis Probe Mass Spectrometry for the Rapid Identification of Pollens and Semi-Quantification of Flavonoid Fingerprints. *Rapid Commun. Mass Spectrom.* **2016**, *30* (13), 1639–1646. https://doi.org/10.1002/rcm.7601.

(121) Tose, L. V.; Murgu, M.; Vaz, B. G.; Romão, W. Application of Atmospheric Solids Analysis Probe Mass Spectrometry (ASAP-MS) in Petroleomics: Analysis of Condensed Aromatics Standards, Crude Oil, and Paraffinic Fraction. *J. Am. Soc. Mass Spectrom.* **2017**, *28* (11), 2401–2407. https://doi.org/10.1007/s13361-017-1764-2.

(122) Leghissa, A. Method Development for Qualification and Quantification of Cannabinoids and Terpenes in Extracts by Gas Chromatography-Mass Spectrometry; 2016.

(123) Russo, E. B.; Jiang, H.-E.; Li, X.; Sutton, A.; Carboni, A.; del Bianco, F.; Mandolino, G.; Potter, D. J.; Zhao, Y.-X.; Bera, S.; Zhang, Y.-B.; Lü, E.-G.; Ferguson, D. K.; Hueber, F.; Zhao, L.-C.; Liu, C.-J.; Wang, Y.-F.; Li, C.-S. Phytochemical and Genetic Analyses of Ancient Cannabis from Central Asia. *J. Exp. Bot.* **2008**, *59* (15), 4171–4182. https://doi.org/10.1093/jxb/ern260.

(124) Hanuš, L. O. Pharmacological and Therapeutic Secrets of Plant and Brain (Endo)Cannabinoids. *Med. Res. Rev.* **2009**, *29* (2), 213–271. https://doi.org/10.1002/med.20135.

(125) Skoglund, G.; Nockert, M.; Holst, B. Viking and Early Middle Ages Northern Scandinavian Textiles Proven to Be Made with Hemp. *Sci. Rep.* **2013**, *3*, 2686. https://doi.org/10.1038/srep02686.

(126) Winder, M. Medicine in China. A History of Pharmaceutics. *Med. Hist.* **1988**, *32* (3), 345.

(127) Baron, E. P. Medicinal Properties of Cannabinoids, Terpenes, and Flavonoids in Cannabis, and Benefits in Migraine, Headache, and Pain: An Update on Current Evidence and Cannabis Science. *Headache J. Head Face Pain* **2018**, *58* (7), 1139–1186. https://doi.org/10.1111/head.13345.

(128) Bogdanović, V.; Mrdjanović, J.; Borišev, I. A Review of the Therapeutic Antitumor Potential of Cannabinoids. *J. Altern. Complement. Med.* **2017**, *23* (11), 831–836. https://doi.org/10.1089/acm.2017.0016.

(129) State Marijuana Laws in 2019 Map https://www.governing.com/gov-data/safety-justice/state-marijuana-laws-map-medical-recreational.html (accessed Jul 2, 2019).

(130) Farrer, D. G. OREGON HEALTH AUTHORITY'S PROCESS TO DETERMINE WHICH TYPES OF CONTAMINANTS TO TEST FOR IN CANNABIS PRODUCTS, AND LEVELS FOR ACTION. 18.

(131) Geesaman, J. Code of Colorado Regulations. 210.

(132) WAC 314-55-102: https://apps.leg.wa.gov/wac/default.aspx?cite=314-55-102 (accessed Jul 1, 2019).

(133) Leghissa, A.; Hildenbrand, Z. L.; Schug, K. A. A Review of Methods for the Chemical Characterization of Cannabis Natural Products. *J. Sep. Sci.* **2018**, *41* (1), 398–415. https://doi.org/10.1002/jssc.201701003.

(134) Jikomes, N.; Zoorob, M. The Cannabinoid Content of Legal Cannabis in Washington State Varies Systematically Across Testing Facilities and Popular Consumer Products. *Sci. Rep.* **2018**, *8* (1), 4519. https://doi.org/10.1038/s41598-018-22755-2.

(135) Hazekamp, A. The Trouble with CBD Oil. *Med. Cannabis Cannabinoids* **2018**, *1* (1), 65–72. https://doi.org/10.1159/000489287.

(136) Industrial Hemp | National Institute of Food and Agriculture https://nifa.usda.gov/industrial-hemp (accessed Jul 1, 2019).

(137) The 2018 Farm Bill: What This Means for Hemp https://www.analyticalcannabis.com/news/the-2018-farm-bill-what-this-means-for-hemp-311394 (accessed Jul 1, 2019).

(138) Cardenia, V.; Gallina Toschi, T.; Scappini, S.; Rubino, R. C.; Rodriguez-Estrada, M. T. Development and Validation of a Fast Gas Chromatography/Mass Spectrometry Method for the Determination of Cannabinoids in Cannabis Sativa L. *J. Food Drug Anal.* **2018**, *26* (4), 1283–1292. https://doi.org/10.1016/j.jfda.2018.06.001.

(139) Pan, M.; Xiang, P.; Yu, Z.; Zhao, Y.; Yan, H. Development of a High-Throughput Screening Analysis for 288 Drugs and Poisons in Human Blood Using Orbitrap Technology with Gas Chromatography-High Resolution Accurate Mass Spectrometry. *J. Chromatogr. A* **2019**, *1587*, 209–226. https://doi.org/10.1016/j.chroma.2018.12.022.

(140) Schwope, D. M.; Scheidweiler, K. B.; Huestis, M. A. Direct Quantification of Cannabinoids and Cannabinoid Glucuronides in Whole Blood by Liquid Chromatography-Tandem Mass Spectrometry. *Anal. Bioanal. Chem.* **2011**, *401* (4), 1273–1283. https://doi.org/10.1007/s00216-011-5197-7.

(141) Meng, Q.; Buchanan, B.; Zuccolo, J.; Poulin, M.-M.; Gabriele, J.; Baranowski, D. C. A Reliable and Validated LC-MS/MS Method for the Simultaneous Quantification of 4 Cannabinoids in 40 Consumer Products. *PLoS ONE* **2018**, *13* (5). https://doi.org/10.1371/journal.pone.0196396.

(142) Wilkins, D.; Haughey, H.; Cone, E.; Huestis, M.; Foltz, R.; Rollins, D. Quantitative Analysis of THC, 11-OH-THC, and THCCOOH in Human Hair by Negative Ion Chemical Ionization Mass Spectrometry. *J. Anal. Toxicol.* **1995**, *19* (6), 483–491. https://doi.org/10.1093/jat/19.6.483.

(143) Broecker, S.; Pragst, F. Isomerization of Cannabidiol and Δ9-Tetrahydrocannabinol during Positive Electrospray Ionization. In-Source Hydrogen/Deuterium Exchange Experiments by Flow Injection Hybrid Quadrupole-Time-of-Flight Mass Spectrometry. *Rapid Commun. Mass Spectrom.* **2012**, *26* (12), 1407–1414. https://doi.org/10.1002/rcm.6244.

(144) Broecker, S.; Herre, S.; Wüst, B.; Zweigenbaum, J.; Pragst, F. Development and Practical Application of a Library of CID Accurate Mass Spectra of More than 2,500 Toxic Compounds for Systematic Toxicological Analysis by LC–QTOF-MS with Data-Dependent Acquisition. *Anal. Bioanal. Chem.* **2011**, *400* (1), 101–117. https://doi.org/10.1007/s00216-010-4450-9.

(145) Brook, K.; Bennett, J.; Desai, S. P. The Chemical History of Morphine: An 8000-Year Journey, from Resin to de-Novo Synthesis. *J. Anesth. Hist.* **2017**, *3* (2), 50–55. https://doi.org/10.1016/j.janh.2017.02.001.

(146) Mahler, D. L.; Forrest, W. H. Relative Analgesic Potencies of Morphine and Hydromorphone in Postoperative Pain. *Anesthesiol. J. Am. Soc. Anesthesiol.* **1975**, *42* (5), 602–607.

(147) Murray, A.; Hagen, N. A. Hydromorphone. *J. Pain Symptom Manage.* **2005**, *29* (5), 57–66. https://doi.org/10.1016/j.jpainsymman.2005.01.007.

(148) CDC Advises Against Misapplication of the Guideline for Prescribing Opioids for Chronic Pain | CDC Online Newsroom | CDC https://www.cdc.gov/media/releases/2019/s0424-advises-misapplication-guideline-prescribing-opioids.html (accessed Mar 27, 2020).

(149) The Promotion and Marketing of OxyContin: Commercial Triumph, Public Health...: “Start Your Research” http://eds.b.ebscohost.com.libproxy.txstate.edu/eds/detail/detail?vid=3&sid=f1a7dcb0-7c5d-4cc3-8105-cbdf29b170d4%40pdc-v-sessmgr02&bdata=JnNpdGU9ZWRzLWxpdmUmc2NvcGU9c2l0ZQ%3d%3d#AN=000262795100007&db=edswsc (accessed Mar 27, 2020).

(150) Rosenblum, A.; Marsch, L. A.; Joseph, H.; Portenoy, R. K. Opioids and the Treatment of Chronic Pain: Controversies, Current Status, and Future Directions. *Exp. Clin. Psychopharmacol.* **2008**, *16* (5), 405–416. https://doi.org/10.1037/a0013628.